8-9-2006

Geomorphologic Evaluation of the Gulf of Mexico, Northwest Garden Banks, and Supra/Inter/Subsalt Architectural Influences on Possible Reservoir Characterization from the Miocene to Pleistocene Epochs

Sheri Sullivan
University of New Orleans

GEOMORPHOLOGIC EVALUATION OF THE GULF OF MEXICO, NORTHWEST GARDEN BANKS, AND SUPRA/INTER/SUBSALT ARCHITECTURAL INFLUENCES ON POSSIBLE RESERVOIR CHARACTERIZATION FROM THE MIOCENE TO PLEISTOCENE EPOCHS

A Thesis

Submitted to the Graduate Faculty of
the University of New Orleans in partial fulfillment of
the requirements for the degree of

Master of Science
in
Geology/Geophysics

By

Sheri Sullivan

B.S. Louisiana State University, 2003
M.S. University of New Orleans, 2006

August, 2006

ACKNOWLEDGEMENTS

I would like to give special thanks to the people at Murphy Exploration and Production Company who supported me throughout this process with the use of their data and the knowledge and expertise they possess. Thank you to my advisor Dr. Mostofa Sarwar, and my committee members Dr. Juliette Ioup and Dr. George Ioup. Also, thanks to Dr. Laura Serpa and Dr. Terry Pavlis who helped me in any way they could throughout this process. I would also like to thank my family and friends for helping and supporting me over the years.

TABLE OF CONTENTS

List of Figures

Abstract

This study describes the geomorphology and characterizes the sequence stratigraphy of deep-water depositional elements and salt interactions in the northwest Garden Banks region with a focus on the Miocene epoch. The use of 2D and 3D data for the analysis of sediment feeders, shelf-margin location, timing of salt diapirism, faulting, and fluid migration can lend useful clues to the spatial patterns of plays. The 3D data focus mainly on blocks 236, 237, 191, 192, and 193. The 2D seismic data, while less precise, are used in conjunction with 3D seismics for an overview of the surrounding area. Some logs are used in conjunction with the seismics for upper Miocene to Pleistocene control. This geologic re-evaluation of the Gulf of Mexico, Garden Banks field 236 and a one to three block periphery of approximately 21 by 18 square miles will examine possible reservoir characterization in the Miocene to Pleistocene time period.

CHAPTER 1: INTRODUCTION

1.1: Study Area

The Garden Banks 236 Field contains six 3 by 3 mile blocks and lies within the Gulf Coast Basin. It is between the Texas-Louisiana upper slope and the Texas-Louisiana outer shelf. The area is located 257 km (160miles) southwest of Lafayette, Louisiana and at a water depth of around 214 – 400 meters (700 – 1300 feet). A one (north, east, and west) to three (south) block radius has also been examined, and a general geomorphological description has been given to an even broader, surrounding area. This includes blocks 147, 148, 149,150, 190, 191, 192, 193, 194, 235, 236, 237, 238, 279, 280, 281, 282, 323, 324, 325, 326, 367, 368, and 369. Water depth ranges from 700 to 900 feet and up to 1,200 feet to the southern most regions, near block 367. Figure 1.1 highlights the entire Garden Banks region and the salt canopy that intersects it. This layer of salt, formally referred to as the Louann salt, began forming during the Jurassic some 150 million ago. The Louann salt extends southward to a great wall of salt, the Sigsbee Escarpment, located 100 miles off the present shoreline. The Louann salt bed is miles beneath the surface, and it is available to us through salt domes, extrusions of salt that extend to or near the surface. Figure 1.2 shows the region of focus.

Figure 1.1: Garden Banks area and salt canopy. Taken from Chevron - Tahiti Project Development Team

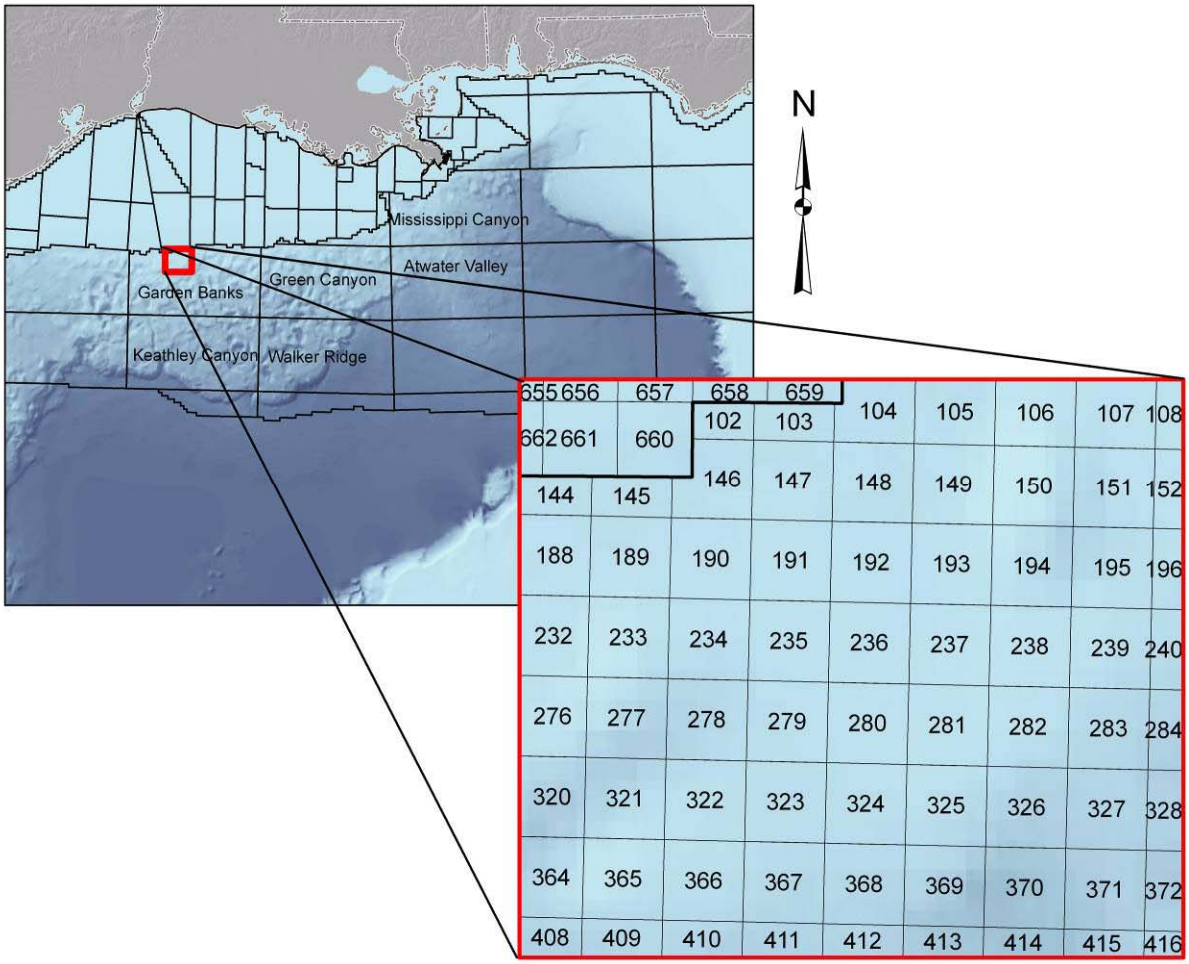

Figure 1.2: Study area

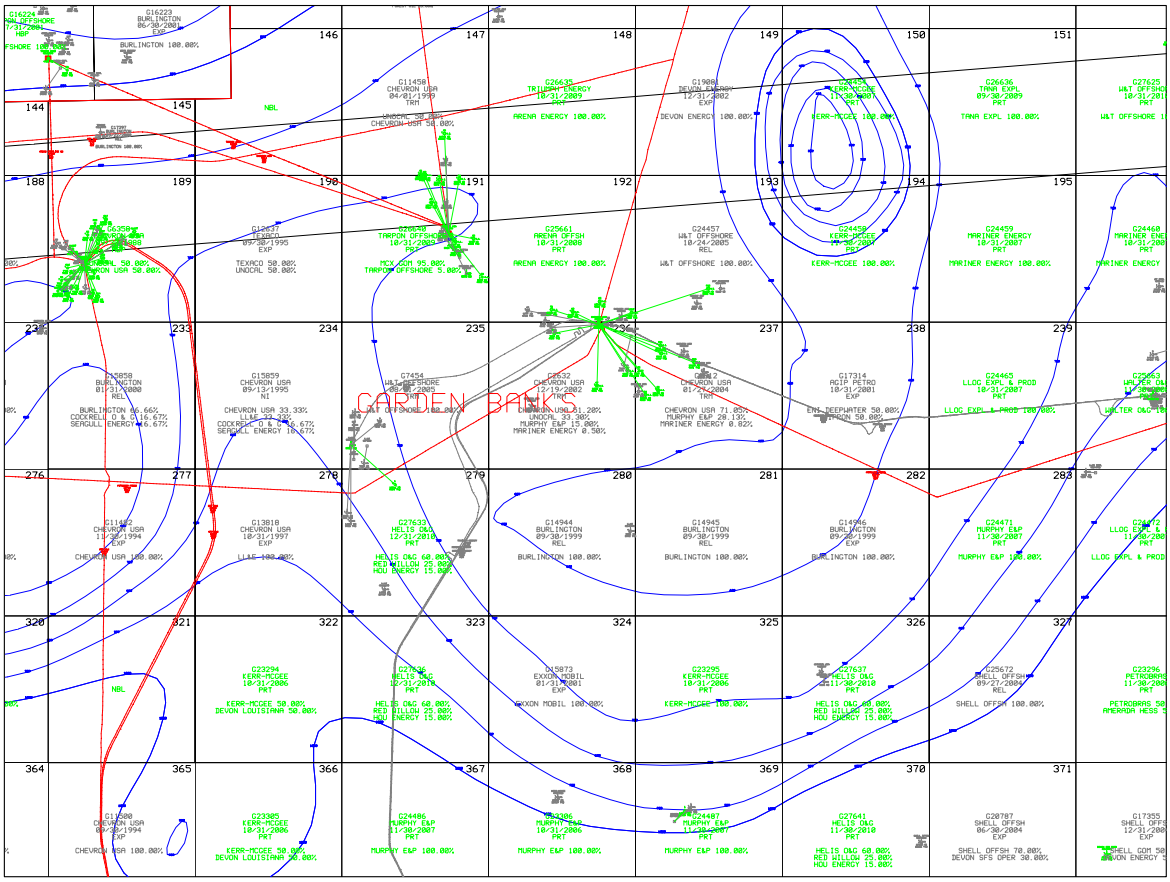

Figure 1.3: Lexco map. Well locations.

Blue – water depth contours
Red pipelines – gas

1.2: Objective

The objective of the study is to describe the geologic structure and stratigraphy in the Gulf of Mexico (GOM), northwest Garden Banks area, determine what controls the geology has on hydrocarbon formation, and to use seismic attributes to determine if any hydrocarbons exist in the study area. The area is located 257 km (160miles) southwest of Lafayette, Louisiana, at a water depth of approximately 214 – 275 meters (700 – 900 feet). Focus will be on the Miocene deposition. This study will provide a better understanding of hydrocarbon formation, distribution, and the underlying geology responsible for gas migration and accumulation. It will also yield increased structural knowledge of a region/time that has received little geologic study.

1.3: Significance of Thesis

There are significant untapped lower Pliocene and upper to middle Miocene hydrocarbon resources remaining in various stratigraphic and structural producing associations. These deeper prospects in the GOM are intrinsically tied to salt and the difficulties it creates. The types of subsalt complexes, discussed later in more detail, are related to the probability for a potential trap. These structures are highly variable. Therefore, a comprehensive characterization and analysis of subsalt trap structure is needed.

Previous papers that I will refer to in Chapters two and five have not included an overview of the northwest Garden Banks area at Pliocene to Miocene depths. This time period has, however, been mapped in most surrounding fields. Previous studies such as Paul Lawless and Richard Fillon's (1999) "Lower Miocene - Early Pliocene Deposystems in the Gulf of Mexico" have stated that deeper water Miocene plays only spanned the Mississippi Canyon, Ewing Bank, Atwater Valley, and eastern portions of Green Canyon and Walker Ridge where upper, middle and sometimes lower Miocene sections are economically drillable. Therefore, by inferring the processes of deposition of the Miocene sands we can construct a reasonable new evaluation of the present geologic situation of the Gulf of Mexico's Garden Banks area. Also, taking into account previous studies, an examination of possible deeper production capabilities will be

developed using seismic and log interpretations incorporating subsalt architectural influences on possible reservoir characterization.

Given the ever-increasing demand for hydrocarbons, this project will take another look at new, deeper possibilities in an area that has received little attention lately. It will elucidate the present geologic situation of Garden Banks field 236 and surrounding areas. It will also take into account previous studies on the area, but with deeper prospects in mind. The centralized area has been examined previously in depths ranging primarily to around 4500 feet, with a few up to 15,000 feet. In this study the depths will be roughly 9000 to 20,000 feet. Reaching a more comprehensive understanding of the geologic situation, with the aid of more advanced, technological capabilities, may allow re-focusing on the area's still relevant production prospects.

1.4: Field Acquisition Parameters

The 3D data used were initially shot by Shell in 1994 and reprocessed by Diamond in 1997. There are discrepancies in the amplitude scale in the two sets (gb237 and gb192). Amplitude scale changes at around 3500ms. The field data acquisition parameters of the 191, 192, 193, 236 and 237 blocks 3-D seismic data are:

- Line direction: N-S
- Trace direction: E-W

Positions are noted in X,Y coordinates.

The acquisition parameters of the 2-D seismic data of the expanded, surrounding area are lines shot in NE/SW and NW/SE directions.

Chapter 2: Geology of the Area

2.1: Introduction

The geologic evaluation of the Gulf of Mexico Garden Banks Field 236 and surrounding area of approximately 21 by 18 square miles will examines possible deeper production capabilities using seismic data and log interpretation and incorporating subsalt architectural influences on possible reservoir characterization in the Miocene to Pleistocene time period. The 2D and 3D data are the most useful in yielding a better geologic understanding of the Garden Banks area. The 3D data focus mainly on Blocks 235, 236, 237, 191, 192, and 193. The 2D data, while less precise, are used in conjunction with 3D for an overview of the surrounding area.

The focus of this study is to explain the geomorphology and characterize the sequence stratigraphy of deep-water depositional elements and salt interference in the northwest Garden Banks region. Because of the mobility of salt under pressure, the salt has risen in diapirs and sheets, disrupting the sediment column in the northwestern GOM. These structures have formed faults that cut through deep hydrocarbon reservoirs, allowing the migration of hydrocarbons. They have also created sea-floor structures of domes and basins as salt diapirs and withdrawal basins formed. The utilization of 3D seismic data, the analysis of sediment feeders, shelf-margin location, timing of salt diapirism, faulting, and fluid migration can lend useful clues to the spatial location patterns of plays. A re-evaluation of the geology of Gulf of Mexico Garden Banks area will lead to possible deeper production capabilities.

2.2: History/Tectonic Setting

The Gulf basin formed in upper Jurassic time when the Yucatan block pulled away from North America. Rifting resulted in passive margins flanking a small area of oceanic crust in the deep, central part of the basin. Structures on passive margins include growth faults, salt-withdrawal basins and salt domes that were produced by remobilization of Jurassic salt from sediment loading. High angle faults are parallel to the coast. Source rocks include late Jurassic and Neogene marine shales. Jurassic

evaporites provide effective seals for deeper offshore hydrocarbons related to the earlier rift history. These are now being tested by deepwater drilling. There are two Mesozoic hydrocarbon plays observed in the GOM (Diegel et al., 2001).

In the southern Gulf of Mexico, a stable Late Jurassic tectonic setting developed following a period of extensional tectonics that began in the Late Triassic. This period of tectonism involved three general phases: (1) Late Triassic to middle Jurassic continental rifting, (2) middle Jurassic to early late Jurassic opening of the Gulf of Mexico Basin, and (3) late Jurassic regional subsidence (Salvador, 1991). Several large grabens developed, along with Middle Jurassic salt deposits, the latter of which are widespread in the Gulf of Mexico. The cessation of extensive salt deposition coincided with the opening of the Gulf of Mexico Basin, which resulted in a greater influx and deepening of marine waters. This tectonic setting remained stable from late Jurassic through the Tertiary (Peterson, 1983). A marine transgression in late Jurassic time resulted in the deposition of a major source rock (Guzman-Vega and Mello, 1999). In general, the upper Jurassic strata are dark-gray to black limestone, argillaceous limestone, calcareous shale, and dark shale that originated in various shelf, ramp, and basin settings (Salvador, 1991). These depositional settings continued into the early Cretaceous but by mid- Cretaceous, the important carbonate buildups of the Tuxpan and the Yucatan platforms were well developed (McFarlan and Menes, 1991). The Yucatan platform and extensions to the west continued to be a site of carbonate platform and slope sedimentation through the late Cretaceous (Sohl et al., 1991), and similar carbonate sedimentation continued into the Paleocene along the Yucatan platform (Galloway et al., 1991).

The Cretaceous and Paleocene carbonates that were deposited in various platform margin, ramp, and basinal settings are the principal reservoir rocks in the Gulf of Mexico Basin provinces (Enos, 1977, 1985). The remainder of the Tertiary sedimentary sequence provided the overburden necessary to generate and mobilize the petroleum that charged these reservoirs (Guzman-Vega and Mello, 1999). High volumes of clastic deposition prograded into the deep basin throughout the Cenozoic. Cretaceous intervals and salt

tectonism started around this time. The diapirism causes mostly normal and some reverse faulting. They, in turn, develop into growth faults with thick sediments on downthrown sides. Salt also withdraws and causes minibasins. On the east side of the southern Gulf of Mexico, salt movement formed traps; whereas on the western side, traps formed on carbonate reefs and in debris flows (Enos, 1977, 1985). It is also important to note the Chicxulub impact on the Yucatan Penninsula, which occurred at the beginning of the Cenozoic, and the effect it could have had on the general stratigraphy and salt tectonics. The impact marker is buried beneath ~1km of Tertiary carbonate sediments. The proximity to this impact could have caused more volatile salt movement and promoted major slumping in the area.

In summary, the 100 million years of tectonic and depositional stability between the late Jurassic and the Paleocene in this region led to development of the excellent source and reservoir rocks, whereas the Tertiary sedimentation that followed provided the overburden rock to create salt movement that formed traps and matured the underlying source rock. This overburden is where nearly all the past hydrocarbon targets have been found.

2.3: Previous Work

2.3.1: Regional Exploration in Garden Banks, Gulf of Mexico

Productions in the Garden Banks area are mostly suprasalt sands ranging from shallow Pliocene to upper Miocene. In the past decade, industry's push to explore greater depths and subsalt prospects in the deepwater Gulf of Mexico has advanced depth imaging technology, and changed the typical project size and the workflow of exploration and appraisal. Kerr-McGee has been using regional (several hundred OCS blocks) 3D pre-stack depth migration data for exploration in Northeast Garden Banks. They imaged the steep-dipping sediment truncations against bases of salt (one of the major traps) in the area. It was discovered that horizontal salt sheets seep oil and gas along the edges and on the crests of salt sheets over known sub-salt discoveries (Pan et al., 2006).

2.3.2: General Sequence Stratigraphy of the Miocene (Not GB):

The Miocene is a pivotal interval in the history of the Cenozoic. Within its nearly 19 million years, profound oceanographic and climatic changes occurred. These include the transition from globally more uniform environments of the Paleogene, to the modern world where extreme climatic and oceanographic contrasts are the norm. Important Miocene climatic changes are reflected by the increasing importance of higher frequency cycles of deposition in the Gulf of Mexico.

Gas resources are broadly distributed in reservoirs ranging in age from Jurassic to upper Pleistocene, unlike oil reserves which are mainly found in the upper Miocene to lower Pleistocene. A switch from progradational plays to submarine-fan plays is the result of the shift in exploration focus from the maturely explored shelf to deep-water tracts seaward of the shelf margin. The deeper tracts are where submarine fans are the primary depositional environment containing reservoir-quality sandstones (Seni et al., 1995).

Paul Lawless and Richard Fillon's paper titled "Lower Miocene - Early Pliocene Deposystems in the Gulf of Mexico: Regional Sequence Relationships" showed extensive analysis of the lower, mid and upper Miocene. Major differences have been recognized between submarine fan sections in third and fourth-order sequences deposited on a second-order relative fall of sea level, as opposed to submarine fan sections deposited on a second-order rise. Advances in biostratigraphy in the past two decades have greatly improved zonations and have allowed sequence stratigraphy to develop as an effective exploration tool. Modern computer technology has breathed new life into old exploratory field techniques such as gravity. Computer generated second-vertical derivative (SVD) gravity maps can now contrast low density salt with higher density sediment-filled minibasins, providing a high-resolution virtual image of shelf and slope structures.

Lawless et al., 2000, examines deep water Miocene deposystems but does not include the Garden Banks study area. He states that the plays span Mississippi Canyon, Ewing Bank, Atwater Valley Lund, and eastern portions of Green Canyon and Walker ridge and contains upper, middle and sometimes lower Miocene sections that are

economically drillable. This play has evolved from drilling structural highs in the early 1980s to seeking amplitude-associated pay trapped in ponded turbidite facies in supra-salt and intra-salt mini-basins of the uppermost continental shelf in the late 1980s. Larger prospects in this area drilled in the 1990s have targeted salt overhangs and sub-salt structures. The recent billion barrel "Thunder Horse" discovery in southern Mississippi Canyon proved that large amounts of nonamplitude pay exist.

2.3.3: Tectonic and Structural Characterization of Salt

Diegel et al., 2001 also described the Cenozoic structural evolution of the northern Gulf of Mexico Basin. It is controlled by progradation over deforming, largely allochthonous salt structures derived from an underlying autochthonous Jurassic salt. The wide variety of structural styles is due to a combination of (1) original distribution of Jurassic and Mesozoic salt structures, (2) different slope depositional environments during the Cenozoic, and (3) varying degrees of salt withdrawal from allochthonous salt sheets. Tectono-stratigraphic provinces describe regions of contrasting structural styles and ages and are described later in chapter 5. The key provinces include (1) a contractional foldbelt province, (2) a tabular salt-minibasin province, (3) a Pliocene-Pleistocene detachment province, (4) a salt dome-minibasin province, (5) an Oligocene-Miocene detachment province. Only numbers 2 and 3 span the Garden Banks area.

Within several tectono-stratigraphic provinces, shale-based detachment systems (dominated by lateral extension) and allochthonous salt-based detachment systems (dominated by subsidence) can be distinguished by geometry, palinspastic reconstructions, and subsidence analysis. Many shale-based detachments are linked downdip to deeper salt-based detachments. Large extensions above detachments are typically balanced by salt withdrawal.

Salt-withdrawal minibasins with flanking salt bodies occur as both isolated structural systems and components of salt-based detachment systems. During progradation, progressive salt withdrawal from tabular salt bodies on the slope formed salt-bounded minibasins which, on the shelf, evolved into minibasins bounded by arcuate

growth faults and remnant salt bodies. Associated secondary salt bodies above allochthonous salt evolved from pillows, ridges, and massifs to leaning domes and steep-sided stocks.

Many researchers along with Shinol et al., 2000, have studied the salt structures in the GOM. These include the works of Rowan, Fillon and Hart mentioned throughout this paper. This research topic has evolved due to advancements in technology which allow them to search for structures below the salt in waters thousands of feet deep. There are 4 major provinces outlined by John Shinol (2000) in the deep water subsalt play based on geological, geophysical, and associated petroleum system attributes.

- The Primary Basins.
- The Eastern Sigsbee Salt Canopy.
- The Central Sigsbee Salt Canopy.
- Isolated Salt tablets

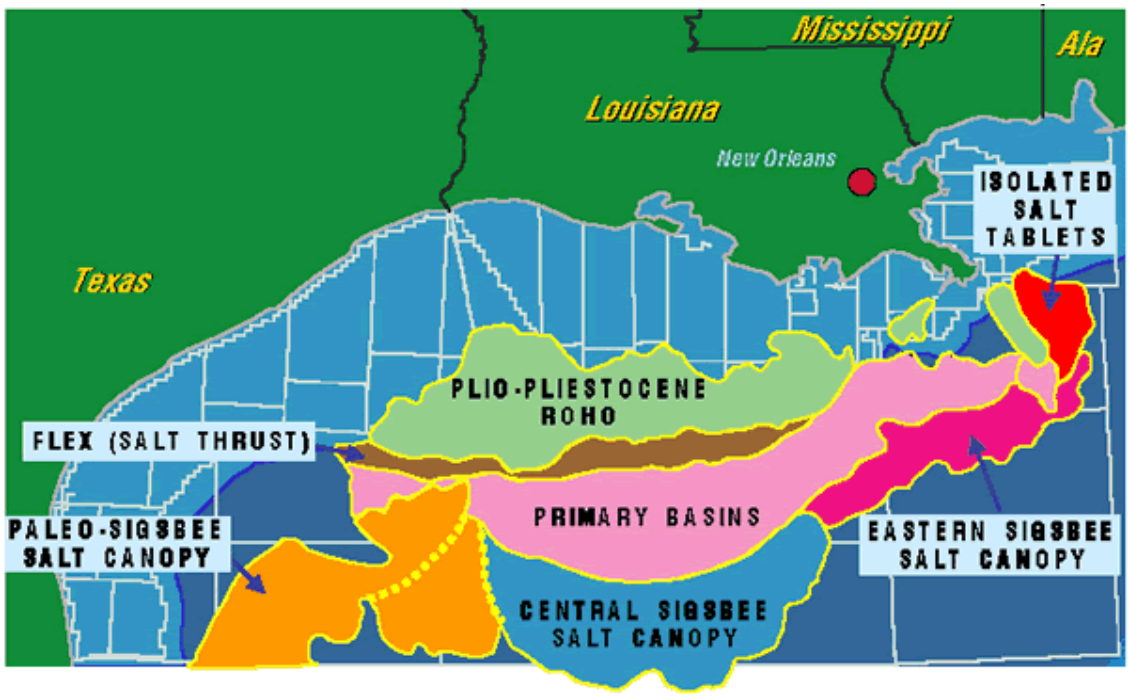

Figure 2.1: Gulf of Mexico subsalt plays.

For our purposes we will focus on the ones relevant to the Garden Banks area. These include: the salt thrust flex, the primary basin and a small portion of the Plio-Pleistocene Roho.

Much of the deep water portion of the northwest Gulf of Mexico (Shinol 2000) is covered by shallow allochthonous salt with deep-rooted feeders. There are extensional Oligocene-Pleistocene faults and detachments updip with an arc of salt-cored compressional folds downdip that help accommodate the updip extension. In addition, there are several major transform faults running northwest to southeast that accommodated the original opening of the Gulf of Mexico in Late Triassic and Early Jurassic, he added. Rifts on the abyssal plain are related to these transform faults, which may have had controls on salt thicknesses when it was originally deposited.

Shinol says there are basically four different types of salt prospects in these provinces:

- Low relief salt-cored pillow folds.
- Thrusted folds.
- Higher relief folds.
- Inverted sediment thicks called turtle structures, found predominately updip to the other three.

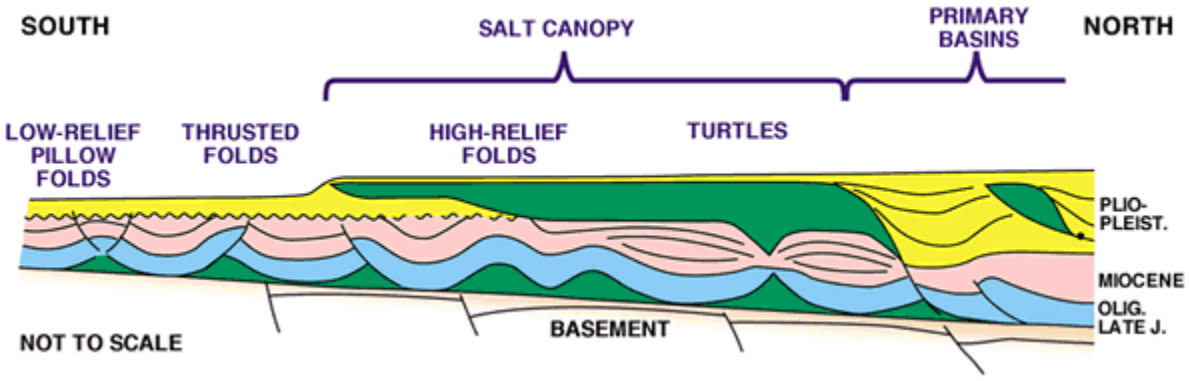

Figure 2.2: Salt prospect types.

2.3.4: Turtles and Primary Basins

One deep water subsalt province is the Primary Basins. This is the region where most of the supra-salt deep water discoveries were made early in deep water exploration. This province covers the eastern East Breaks, Garden Banks, Green Canyon and Mississippi Canyon areas. There are basically two subsalt plays in this region. Companies tend to look for localized younger Miocene through Pleistocene confined turbidite sections associated with salt overhangs.

It is important to search for fault/salt closures beneath small salt tablets and overhangs. "There is potential for these targets under the salt overhangs, but the problem is they can be relatively difficult to image," (Shinol 2000). "There have been several dry holes drilled in this play - however, if you find one (target), the sands are very thick, very clean and have great production parameters. It is difficult to see through the salt because the rate of deposition moved the salt relatively quickly in some areas. The further east you go the better behaved the salt is, but in the Garden Banks and Green Canyon regions it's difficult to image the targets."

The Primary Basin's subsalt play is centered in the province's eastern side and is targeting deeper, larger four-way closure turtle structures. These structures are expected to be productive from the early and middle Miocene section at about 23,000-28,000 feet, with reserve potential greater than 300 million barrels of oil equivalent. Deeper turtle structures are difficult to image on 3-D seismic data. There are no diagnostic hydrocarbon indicating amplitudes related to this play, so companies are targeting structures. Geologically, turtle structures can have some complications. "These structures were synclines at one time and were receiving sediments," Shinol said. "Then the structure inverted due to salt withdrawal - so what was a low is now a high. That in itself implies there may be a complex relationship between timing of trap formation, hydrocarbon charge and migration." One must ask, "Was there trap formation during the hydrocarbon migration phase?" "Also, there can be crestal faulting on these structures that can degrade the top seal of the traps," he said, "(but) the size of the potential discoveries makes the risk worthwhile." "In the Central Sigbee Escarpment, there are salt-cored pillow folds as well as large turtle structures, generally updip of the pillow folds.

Chapter 3 Methods:

3.1: Introduction

The software companies in this project include Geographix, NeuraSection and Landmark. The seismic data companies who were involved in the attainment of the seismics used were Murphy Exploration and Production Company, Diamond Geophysical, Western and Shell. The data used were initially shot by Shell in 1994, and reprocessed by Diamond in 1997. There are discrepancies in the two data sets (gb237 and gb192): 32 and 8 bit data vary; amplitude scaling (histogram) changes at around 3500ms. High amplitude events to distinguish gas reservoirs is the most obvious method to be used. These bright spots are zero phase. The data in the gas areas are significantly clipped, meaning there are more contrasting colors at the ends of the color bar.

Biostratigraphic data were taken from PaleoData, and logs were analyzed in NeuraSection. Landmark's seisworks 2D, 3D depth and time software, Earthcube and some well log correlation using mainly gamma and resistivity logs were used for this project. In Seisworks, relevant horizons were picked and tracked throughout the area. Integration of well interpretations and time slice variations were also used. The 236 Field area contains more extensive 3D data. This collection of closely-spaced seismic lines over an area permits three-dimensional processing of the data as a volume. It is also necessary to observe the high amplitudes in order to distinguish gas reservoirs.

3.2: Horizons

3.2.1: Seismic Wavelet Behavior

The seismic wavelet is the link between seismic data (traces) on which interpretations are based and the geology (reflection coefficients) that is being interpreted, and it must be known to interpret the geology correctly. However, it is typically unknown, and assumed to be both broad band and zero phase. Providing this broad band, zero phase wavelet is the processing goal of deconvolution. Unfortunately, this goal is rarely met and the typical wavelet that remains in fully processed seismic data

is mixed-phase. Differences in mixed-phase wavelets result in mis-ties and often incorrect interpretations. Significant improvements in seismic data quality and, correspondingly, their interpretations of those data are easily obtainable by converting from mixed-phase to zero phase wavelets (Henry 2001).

Lithologic boundaries define a Reflection Coefficient series. When convolved (*) with the field wavelet, a simulated raw field trace is the result. Figure 3.1 shows that interpreting the highest amplitude event (2.5 seconds) as the reservoir sand would be wrong. This mixed phase wavelet provides a distorted image of the actual geology (Figure 3.1). When the field wavelet is known, deterministic deconvolution is able to produce a processed trace that contains the desired broad band-zero phase wavelet. Note, the highest amplitude in the processed trace is now associated with the largest Reflection Coefficient at the top sand (Figure 3.2) (Henry, 2001).

A zero-phase wavelet is symmetrical with the majority of the energy being concentrated in the central lobe. This wavelet shape minimizes ambiguity in associating oversized waveforms with subsurface interfaces. A horizon track drawn at the center of the wavelet coincides in time with the two way travel time to the subsurface interface causing the reflection. The maximum amplitude occurs at the center of the waveform and thus coincides with the time horizon and the resolution is better than for other wavelets with the same frequency content (Brown 2004).

The common assumption that seismic data contain a broad band zero phase wavelet is nearly always wrong. The majority of mis-tie problems between seismic and synthetics, seismic to seismic of different vintages and many of the misinterpretations based on modeling (lithology prediction, trace attributes, AVO, etc.) are the result of mixed phased wavelets remaining in fully processed seismic data. Significant improvements in seismic data quality and their interpretations based on these data are easily obtainable by converting from mixed-phase to zero phase wavelets (Henry 2001).

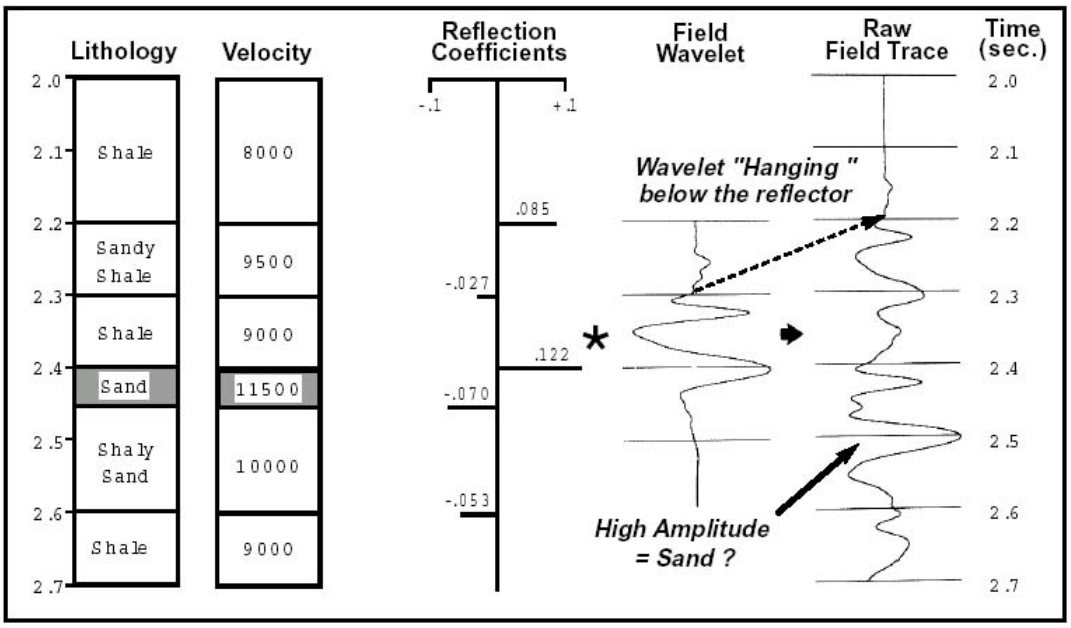

Figure 3.1: Using highest amplitude as the reservoir gives an incorrect interpretation (Henry, 2001).

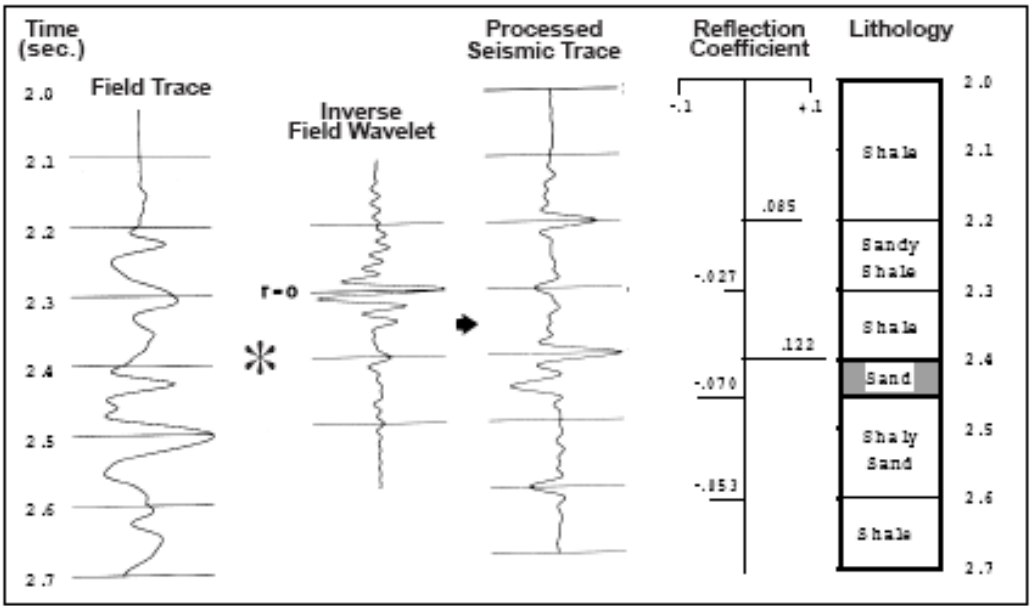

Figure 3.2: Processed trace that contains the desired broad band-zero phase wavelet (Henry, 1997).

3.2.2: Mapped Horizons

The sands in Garden Banks blocks 147, 191, 192, 193, 236 and 237 lie in the northwest corner of the Garden Banks area. This area will be described more thoroughly than the surrounding blocks simply because data is unavailable. This area is also where

most drilling has been focused. Only a few 2D seismic lines were run across the expanded area. Thus far, there have been two basic pay possibilities examined in these blocks. The first, and most studied and drilled, is the 4500 foot sand. This is a relatively shallow sand, especially by today's standards. The second, and more areally limited, is the 8500-ft, thought only to be significant in the 191 block. In this study, an attempt is made to identify a third possible pay zone. There seems to be another sand around 15,000 feet deep. It is hoped to further explore the productive possibilities in this sand. This horizon is followed out to a one to three block radius in the surrounding blocks. Three horizons have therefore been mapped. The 4500-ft sand is, of course, better displayed than other less prevalent and less studied sands. The 8500-ft, while not productive everywhere, was mapped, and shows some consistency across the area. The third is a generically termed "deep sand." This sand occurs at a time of 3500 to 5000 milliseconds. There is such a wide depth range because of the salt tectonics. There was no paleontology documented at this depth. For the data available, the deepest paleontology recorded was in Block 237, Well 3, at 12,527 feet, which is equivalent to around 3700 milliseconds. This was upper Pliocene (Gelasian) *Discoaster pentaradiatus*. Also, there was not very much of the deep sand in Block 237. The horizon was traced from 192 down to 236 where it encounters major salt. Block 237 Well 3 was drilled at 13557 feet on the other side of this salt diapir, but with no pay results. Paleontology of the main wells drilled with pay results is listed in chart 1.

When a horizon is tracked, the extreme amplitude as well as its time is stored in the digital database. Mapping of the times produces a structure map. Mapping the amplitudes produces a horizon slice. More commonly, only the time is stored as a result of horizon tracking and later the amplitudes are extracted from the data (Brown, 1999). The time slice of the 4500-ft sand was performed with a typical seismic interpretation workstation displaying the seismic data in vertical, horizontal and arbitrary crossing planes as images. The horizontal section is called a "time slice". In the process of seismic interpretation the geophysicist uses the seismic workstation to map seismic anomalies correlating them with geological settings in the subsurface. The seismic interpretation

carried out on workstation is materialized in attribute anomaly maps of predicted oil and gas reservoirs in the subsurface. These images are shown in Chapter 8.

3.3: Paleontology of blocks 147, 191, 192, 193, 235, 236, and 237

The gas reserves sought after in this project are Pliocene and Miocene in age and have been trapped due to progradation. Deeper Miocene sands may be delta fan systems. The upper Pleistocene submarine fan sandstone is correlated with the Hyalinea B/Trimosina B and Trimosina A biozones. Below is the paleontology that has been documented in this area. It only covers the Plio-Pleistocene sands that have been drilled in the past. The depths are designated as mean depths (MD) and total vertical depths (TVD).

Chart (1)

	Trim A	4500ft sand	Trim B	8500ft sand	Gas (MCF)
	MD TVD (ft)	MD TVD (ft)	MD TVD (ft)	MD TVD (ft)	
GB 147 A3				11402 8815	
				11554 8930	
GB 147 A8		7484 4428		15600 9177	4,913,769/1,696,820
GB 191 A1	5160 4794		14400 11743	11108 8884	
GB 191 A4	8600 6161	4657 3728		11620 8894	
				11986 9260	
GB 191 A5		5772 5174			16,869,350
		5930 5292			
GB 191 A6		5157 4895			24,900,484
		5634 5372			
GB 191 A9		7960 4453			
		8402 4460			
GB 192 A1	5890 4055	6569 4436	5040 5039		19,134,543
	3480 3479	6855 4599	7480 7478		
GB 192 A3	4550 4123	5004 4489			39,887,326

GB 192 A5	8030 3978	9198 4430			13,526,901
A5ST	7920 3998	9198 4452			
GB 192 A8	4260 4133				10,572,720
A8ST	4520 4122	5990 4638			
GB 193 1	5240 5219	Shaled out	8160 8160		
GB 193 A12	12,420 4335	13,496 4733			
235 3		Pay	Globigerina nepenthes		
		9732 7665	9850 7720		
			Sphenolithus heteromorphus		
			9820 7706		
GB 236 A7	6270 3682	7665 4234			14,224,671
GB 236 A9	6270 3682	7723 4451			19,488,579
GB 236 A10	5750 3918				
GB 236 A14		6668 4208			10,917,400
GB 237 A2	6800 3800	8710 4327	11960 4327		23,441,146
GB 237 A4	9950 3627	10,914 3881			38,010,459
GB 237 A6	6900 3900	8860 4584			
GB 237 A11	7880 4185	8769 4602			16,066,689
GB 237 A13	9850 4049	11,136 4399			

SYSTEM	SERIES	ATLAS CHRONO-ZONE	CHRONO-ZONES	BIOCHRONOZONES
QUATERNARY	Pleistocene	UPL	UPL-4	Sangamon fauna
			UPL-3	*Trimosina* A 1st
			UPL-2	*Trimosina* A 2nd
			UPL-1	*Hyalinea* B/*Trimosina* B
		MPL	MPL-2	*Angulogerina* B 1st
			MPL-1	*Angulogerina* B 2nd
		LPL	LPL-2	*Lenticulina* 1
			LPL-1	*Valvulineria* H
TERTIARY	Plio-cene	UP	UP	*Buliminella* 1
		LP	LP	*Textularia* X
	Miocene	UM3	UM-3	*Robulus* E/*Bigenerina* A
			UM-2	*Cristellaria* K
		UM1	UM-1	*Discorbis* 12
		MM9	MM-9	*Bigenerina* 2
			MM-8	*Textularia* W
		MM7	MM-7	*Bigenerina humblei*
			MM-6	*Cristellaria* I
			MM-5	*Cibicides opima*
		MM4	MM-4	*Amphistegina* B
			MM-3	*Robulus* 43
			MM-2	*Cristellaria* 54/*Eponides* 14
			MM-1	*Gyroidina* K
		LM4	LM-4	*Discorbis* B
			LM-3	*Marginulina ascensionensis*
		LM2	LM-2	*Siphonina davisi*
		LM1	LM-1	*Lenticulina hanseni*
	Olig-ocene	OL1	Oligocene Frio–Anahuac	*Bolivina perca*
CRE-TACEOUS		LK		
JURASSIC		JUR		

Figure 3.3: Chronostratigraphic subdivisions and biostratigraphic zones used for the Gulf of Mexico. Modified from Reed et al., 1987.

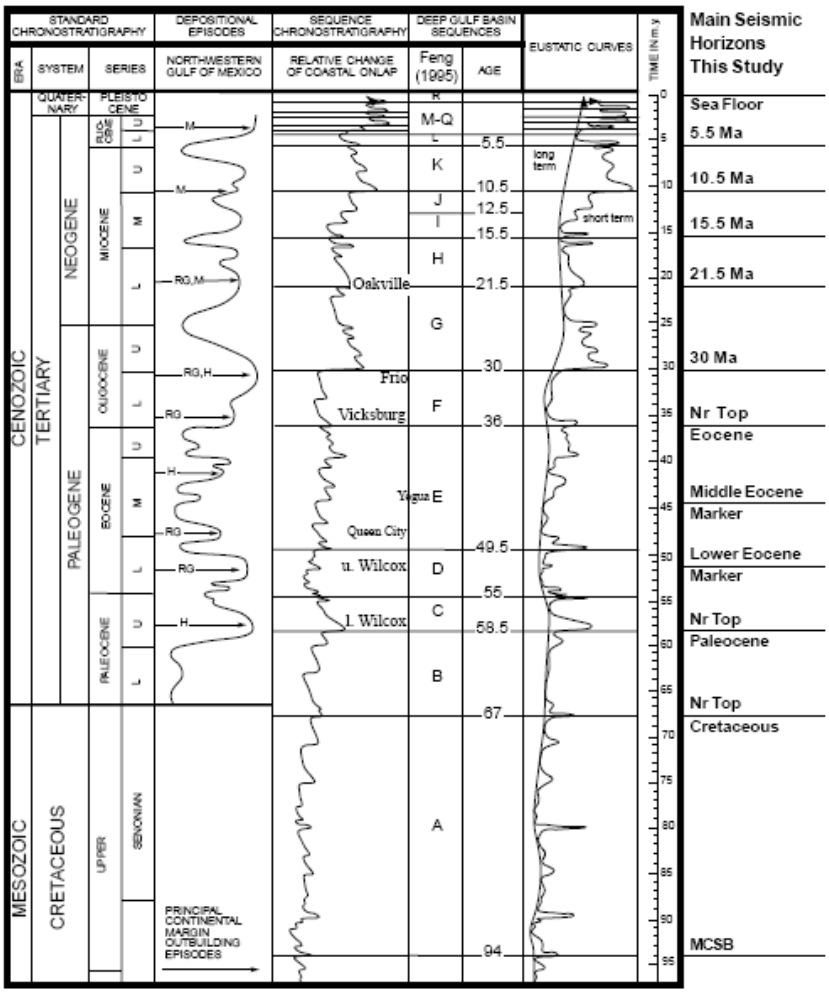

Figure 4— Chronostratigraphic correlation chart for deep Gulf of Mexico seismic sequences, middle Cretaceous through Cenozoic (adapted from Feng, 1995). Coastal onlap and eustatic sea level curves from Haq et al. (1987), and major transgressions and regressions (depositional episodes) from Galloway (1989). RG = Rio Grande Embayment, H = Houston Embayment, M = Mississippi Embayment. See Figure 12 for locations of depocenters.

Figure 3.4: Chronostratigraphic correlation chart for the Gulf of Mexico.

The Garden Banks 236 Field has been examined over the years in many areas. There have been problems in doing this in the past because of salt issues. The salt distorts seismic data and logs alike. However, advances in seismic imaging have improved this. Some of the data used in this area are quite outdated. Therefore, using the very few logs provided from depths greater than 10,000 feet, I have chosen to look to gamma and SP, which is not significantly affected by salt, and resistivity, although salt may cause resistivity to read very low.

Chapter 4: Sequence Stratigraphy and Salt Structures in Garden Banks

4.1: Introduction

Deeper prospects in the GOM are intrinsically tied to salt. The type of subsalt complex is related to the possibilities of a potential trap. These structures are highly variable. Therefore, a comprehensive characterization of subsalt trap structure is needed. By recognizing influences of deformation modes on prospectivity, attention can then be focused on discerning which attributes of the underlying salt system most directly dictate the deformation styles and therefore trap value.

4.2: Salt Structure Types

One type of salt structure trap is narrow, three-way ribbon truncation closures and steep stratal dips. These pose generic exploration risks, while trap prospectivity may be greatly improved where subsalt strata have been counter-rotated, inverted and downwardly flexed (Hart et. al., 2001). Ribbon truncation closures occur where stratal horizons terminate at nearly uniform depth along a salt face. The concept of vertical linkage describes the systematic relationship between deep salt movement and the magnitude of the subsalt trap deformation (Hart et al., 2001). Three kinematically distinct subsalt root types are recognized: autochthonous, fore-ramping allochthonous, and back-ramping allochthonous. Autochthonous implies that the salt is located where it formed. These will show a root. Allochthonous implies it has moved from its original position. Most of the subsalt traps in the Garden Banks area are sutured, meaning they are covered.

The two images below in Figure 4.1 show an interdomal saddle located in Blocks 236 to 237. The layers are truncated on either side of the allochthonous salt. It appears that some portioned rotation has occurred. This can lead to large hydrocarbon traps. However, the well to the far right was drilled with no success. The high amplitude spot on the right could contain a hydrocarbon trap because the strata is less synclinal, and therefore could hold a better reservoir.

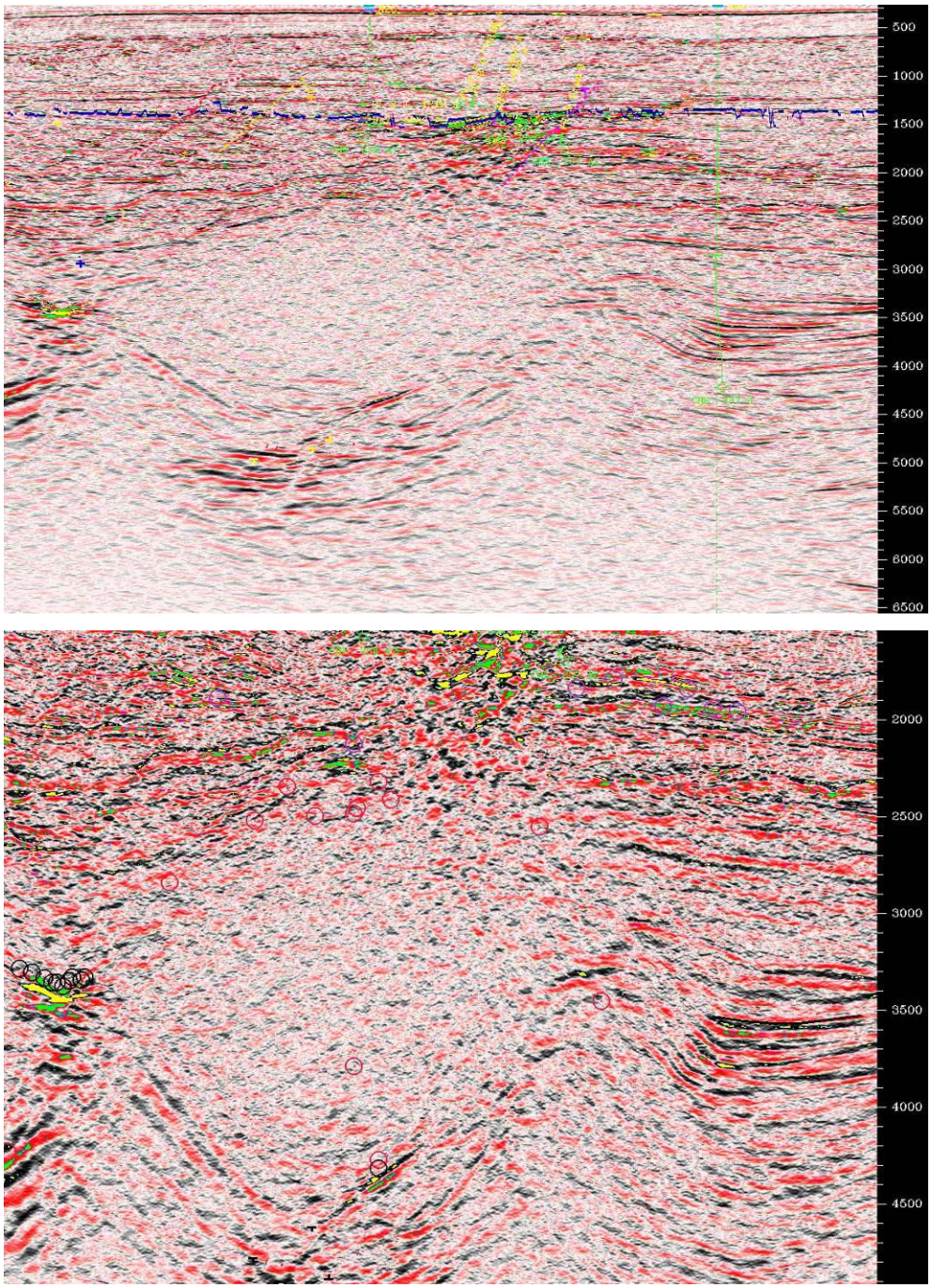

Figure 4.1: Allochthonous salt body: first image is further right and has different a time setting, the second image is to the left and has greater clipping (see footnote at end of Chapter).

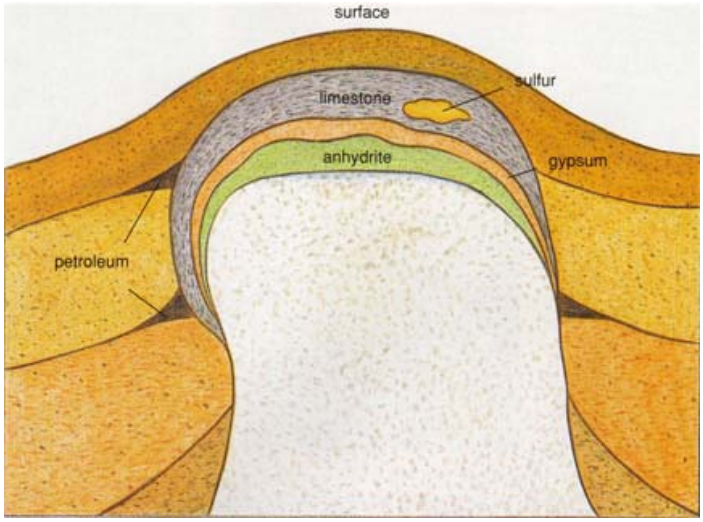

Figure 4.2: Typical salt trap occurrence (Martinez, 1991).

4.2.1: Salt Dynamics

The effects of salt on surrounding strata vary from a simple reduction in stratal dips against the salt face to dramatic downward stratal flexures. Previously rotated strata collapse below their horizontal position and become inverted. These inversions could be caused by counter-rotational collapse of adjacent diapirs and deflation of a feeder stem. Emplacement of the overlying allochthonous salt followed by a counter-rotation can influence sediment facies distributions, with inboard rim synclines which have good reservoir potential (Hart et al., 2001). The way the strata surrounding the salt flexes is connected to how dependable the trap may be. An upward flex of strata (synclinal) is less reliable than a downward/anticlinal shape. These close against allochthonous salt stems and overhangs. They are usually caused by counter-rotational collapse of a neighboring diaper. Unfortunately, most of the deeper possible traps in the Garden Banks 236 Field are synclinal. The 4500 foot sand most commonly drilled lies mostly atop an autochthonous root.

Because of the mobility of salt under pressure, it has risen in diapirs and sheets, disrupting the sediment column in the northern and western GOM. The flanks of the diapirs are steeply dipping. These structures have formed faults that cut through deep hydrocarbon reservoirs, allowing for the migration of hydrocarbons to the seafloor. They have also created sea-floor structures of domes and basins as salt diapirs and withdrawal

basins form. Tabular salts are often limited to the southern deeper water portion. In between salt bodies, mini sedimentary basins show significant difference in velocity variation both vertically and laterally. Overhangs and multiple stacks of salt bodies are common in this area. There is little resemblance of the sediment packages among the mini basins in the Garden Banks area (Pan et al., 2006).

Salt-controlled bathymetric relief provides accommodation for the deposition of reservoir sands in slope minibasins of the northern Gulf of Mexico. It is important to determine whether minibasin-flank relief is controlled more by underlying salt withdrawal or surrounding salt inflation. And in the case of withdrawal, is it primarily from allochthonous or autochthonous salt?

Salt inflation is the main cause of shallow suprasalt traps in the GOM. The most obvious, but by no means unique, example is the Sigsbee Escarpment, where there can be over 1 km of relief that is entirely due to inflation of allochthonous salt. Inflation of shallow salt is caused not just by vertical loading of the source layer, but also by lateral loading of the shallow salt itself during shortening. Salt inflation is most common above the basinward portions of linked allochthonous detachment systems, where contraction is a dominant process Rowan et al., 2003).

The majority of slope minibasins west of Mississippi Canyon have traditionally been interpreted as forming due to evacuation of allochthonous salt, but a model by (Hall, 2000) suggests instead that autochthonous salt deflation is largely responsible for thick accumulations of upper Miocene to Pleistocene sediments in areas such as eastern Garden Banks. While early inflation and late deflation of the Louann salt are certainly common processes, they may not be so wide-spread. Many of the minibasins interpreted as primary are in fact floored by allochthonous welds, and subsalt geometries show that the minibasins formed by withdrawal of allochthonous, not autochthonous, salt (Rowan et al., 2003).

4.3: Salt Effects on Sequence Stratigraphy

The northern Gulf of Mexico Basin can be divided into various tectonic provinces that parallel the shelf/slope break (Diegel et al., 1995; Karlo and Shoup, 1999). Salt-withdrawal minibasins on the continental slope, such as those in the Green Canyon and Garden Banks areas, are bounded by salt walls and filled with the ponded turbidite sands that provide reservoirs for most of the earlier deep-water Gulf of Mexico discoveries. The middle to lower continental slope contains fold/thrust belts with large prospective geological structures that are the focus of current deep-water drilling and include several recent discoveries (Peel, 1999; Rowan et al., 2000).

Domes of coastal Louisiana and of the Texas/Louisiana inner/mid-shelf tend to be more complex, often representing second-generation diapirs that have evolved from deeper allochthonous salt bodies. The shape and extent of salt overhangs can vary significantly, both across the trend and along the flanks of individual diapirs. Diapir complexity further increases in the outer-shelf to mid-slope trends, where allochthonous salt may occur as multi-tiered sheets that are interconnected vertically and horizontally. Below in Figure 4.3 is a 2D seismic profile of chaotic salt diapirism. These salt diapirs, along with the natural down slope system, can give way to turbidity flows. Some areas in the Outer Continental Shelf (OCS) setting simply occur as sheet sands. Leveed channels' sizes can range from 3 km to 200m and in sinuosity (the ratio of channel-axis length to channel-belt length) between 1.2 and 2.2. Leveed channels can also be associated with overbank sediment waves, frontal splays and crevasse splays (organized as distributary-channel complexes).

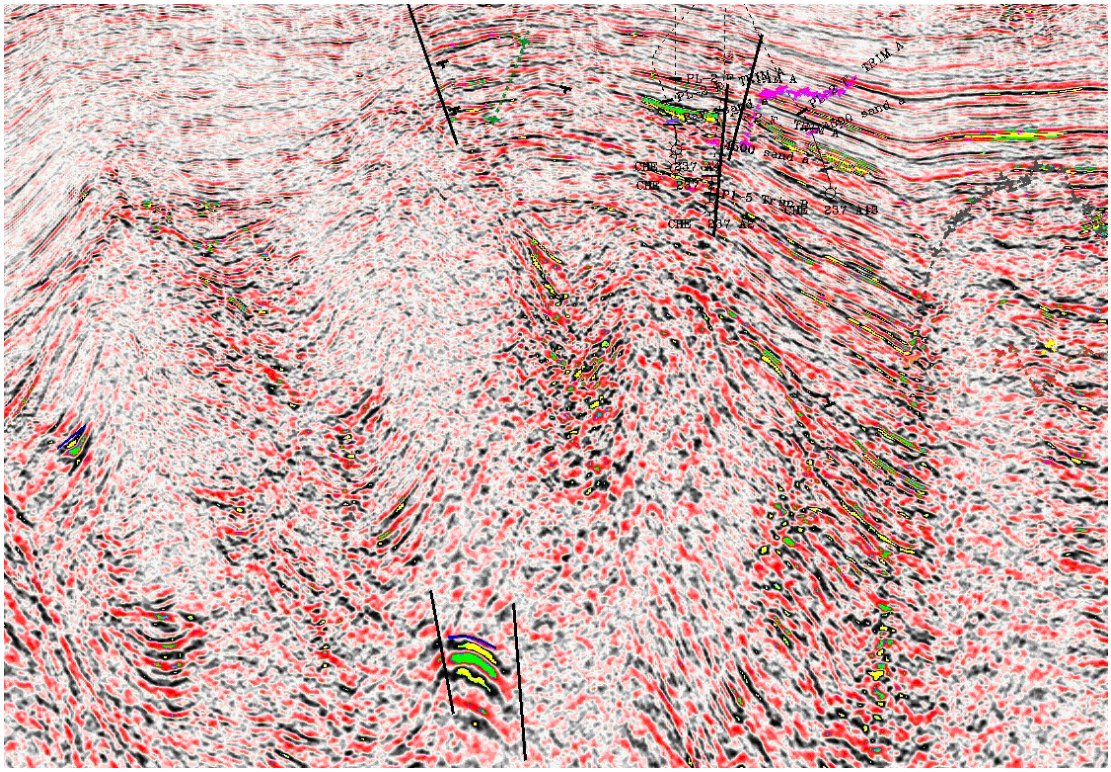

Figure 4.3: 2D view. Downwardly flexed, possible trap. Highly distorted traps intermixed with salt (see footnote at end of Chapter).

4.4: Biostratigraphic Observations Related to Salt Canopies and Salt Welds in the Deep-Water Gulf of Mexico

Richard H. Fillon (1999) briefly describes the biostratigraphic relation to salt canopies and welds. He states that when salt canopies inflate, they create bathymetric highs that divert sediment-carrying bottom currents at their flanks while creating sediment-starved habitats at their crests. Conversely, when canopies deflate beneath prograding slope sediments, displacement of the mobile salt accommodates large volumes of sediment in growth-faulted intraslope basins. These contrasting roles are biostratigraphically manifested both regionally and locally. Regionally, they occur as large sequential changes in patterns of mapped accumulation rates, i.e., abnormally low rates succeeded by abnormally high rates. Locally, they occur in individual wells, as changes from "stacked" or super-condensed section to expanded section. The latter is indicated in biostratigraphic data by unusual occurrences of index taxa, such as: (1) Miocene to Eocene taxa in younger sections; (2) close succession of index taxa in high

abundance zones within super-condensed sections, especially overlying younger expanded sections; (3) reoccurrence of short-ranging (younger) taxa beneath older markers; (4) substantial reversals in total assemblage age, e.g., middle Miocene section overlying Plio-Pleistocene; (5) mixed, "jumbled" occurrences of index taxa; (6) intercalated stratigraphic "slices," out-of-order, but internally consistent. These various observations are consistent with: (1) age limits of fossils from in-salt inclusions; (2) salt-rafted suprasalt super-condensed sections; (3) the tendency of displaced salt to override intraslope basin-fills; (4) minor age inversions related to repeat section associated with high-angle reverse faulting; and, (5) multiple or major age inversions, associated with imbricate thrust sheets and horizontal salt welds associated with extensive low-angle overthrusts (Fillon et al., 1999).

4.5: Overpressured Sands in Deep Water

In most areas of the world, pressure-related drilling problems are the leading cause for abandoning a deep-water well or else requiring expensive remedial changes in the drilling and casing programs to reach the targeted reservoir depths. Therefore, some discussion of this issue is needed. These geological controls and trends include: geopressure in the deep-water Gulf of Mexico, shallow water flow from overpressured sands in the top-hole section, and other pressure-related problems unique to deep water. Pore-pressure prediction has become a subject of intense current interest with several joint industry projects and predictive models now available for government and company participation (Smith et al., 2002).

As exploration moves into deeper water in the Gulf of Mexico, pore-pressure prediction and the correct anticipation of overpressured sands becomes more and more critical to the effective evaluation of federal outer continental shelf (OCS) lease blocks. The thermal gradient in the eastern study area is lower than that of deep-water areas to the west, generally about 1.05^{o}F/100 ft (0.58^{o}C/30.5 m). The thermal gradient falls from an average of 1.25^{o}F/100 ft (0.69^{o}C/30.5 m) in East Breaks to about 1.0^{o}F/100 ft (0.555^{o}C/30.5 m) in Garden Banks, and in Green Canyon the temperature gradient appears to decrease from 1.3 to 0.8^{o}F/100 ft (from 0.72 to 0.44^{o}C/30.5 m) to the southeast

with greater water depths. These observations suggest that lower thermal gradients may correspond to a deeper top of geopressure. Throughout the deep-water Gulf of Mexico, as shown in Figure 4.4, it appears that older and more compacted strata have a deeper top of geopressure than occurs in younger strata. (Smith et al., 2002).

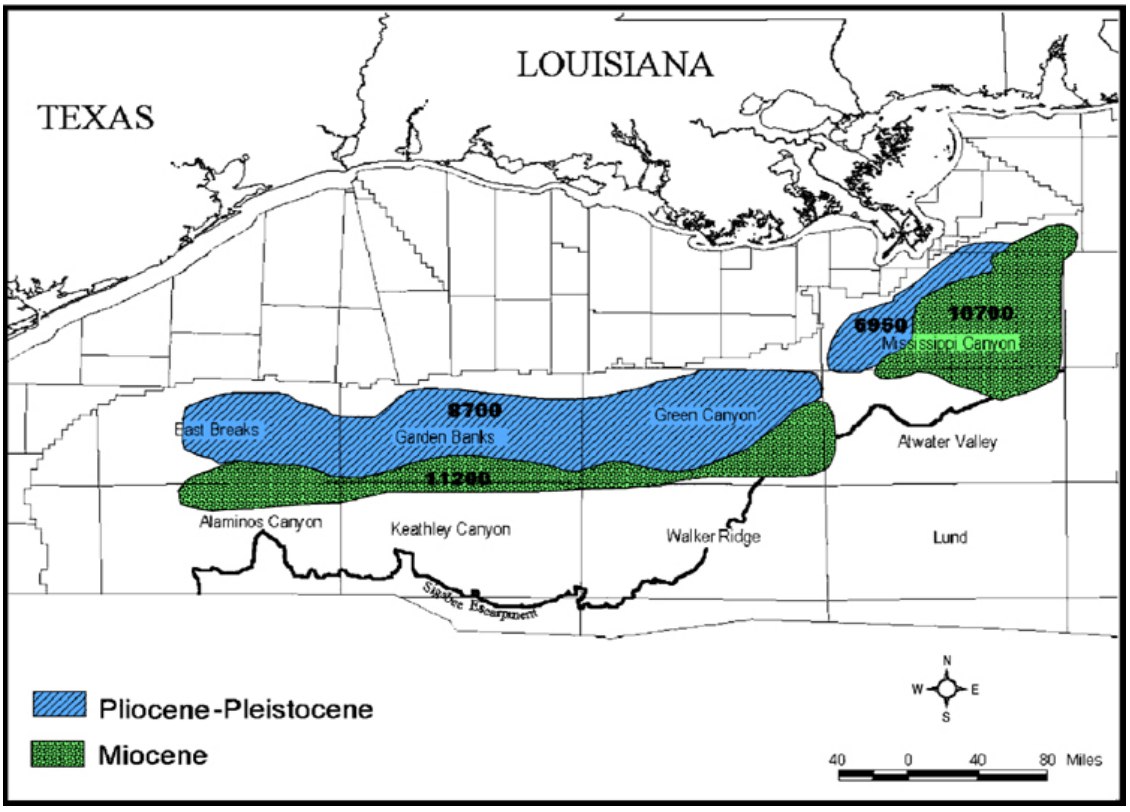

Figure 4.4: Average depth and stratigraphic interval for the occurrence of moderate overpressures (12.5 ppg pore pressure), deep-water Gulf of Mexico (Smith et al., 2002).

In the centroid concept, pore pressure in a reservoir sand at the crest of a high-relief overpressured structure can exceed pore pressure in the bounding shale. Deep-water areas with extensive shallow faulting are particularly vulnerable to low-margin drilling conditions that require extra casing strings. The top of a large, high-relief fold or anticlinal structure at various depths in an exploratory well may contain fluid pressures that approach the fracture gradient in adjacent shale (Traugott, 1997).

In deeper water, the average top of geopressure occurs in the Miocene at about 10,700 ft (3261 m) bml (below mud line). In the younger Pliocene-Pleistocene section to

the west in Garden Banks, the average top of geopressure occurs at about 8700 ft (2652 m) bml. In the deeper water sections in Garden Banks to the south and southeast, however, the top of geopressure occurs in the Miocene at an average depth of about 11,200 ft (3414 m) bml. Throughout the deep-water Gulf of Mexico, as shown in Figure 4.4, it appears that older and more compacted strata have a deeper top of geopressure than occurs in younger strata (Smith et al., 2002).

Porosities over 30 percent and permeabilities greater than one darcy in deepwater turbidite reservoirs have been commonly cited. Compaction and diagenesis of deepwater reservoir sands are minimal because of relatively recent and rapid sedimentation. Sands at almost 20,000 feet in the Auger Field (Garden Banks 426) still retain a porosity of 26% and a permeability of almost 350 md (Smith et al., 2002).

Chapter 5: The Miocene

5.1 Introduction

The Miocene sands range in age from 5.3 to 23 My. The equivalent depth begins at around 10,000 to over 25,000 feet. They contain around 39% of the recoverable in-place hydrocarbons in the Federal Outer Continental Shelf (OCS). The progradational style plays are dominant in the middle Miocene to the Plio-Pleistocene. However, this is due to the fact that the maturely explored shelf has contained progradational plays, while the deeper, less explored reservoir targets on the shelf and beyond are submarine fans.

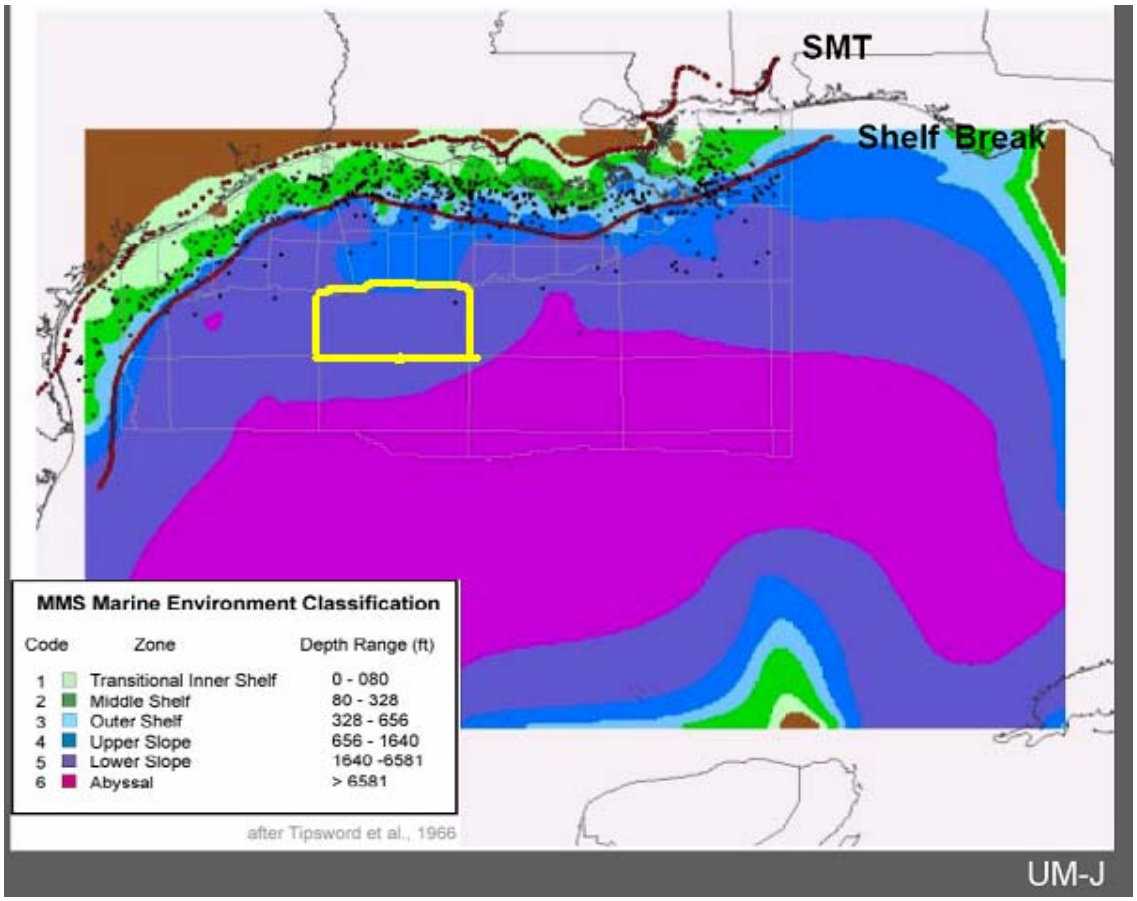

Figure 5.1: 2D Paleobathemetry of Upper Miocene lower slope area (Sylvia et al., 2003).

It has been previously referenced that Miocene stratigraphy and deeper water Miocene plays have been mostly examined in areas spanning Mississippi Canyon, Ewing Bank, Atwater Valley, Lund, and eastern portions of Green Canyon and Walker Ridge

where upper, middle and sometimes lower Miocene sections are economically drillable. This play has evolved over time and has the potential to continue to do so. An important factor in accomplishing this is the examination of salt overhangs and sub-salt structures and possible nonamplitude pay existing.

5.2: Sequence Stratigraphy

One of the earliest hydrocarbon plays on the outer continental shelf (OCS) is of lower Miocene age and occurs in a localized area near the Texas-Louisiana border. In the Federal OCS, lower Miocene and older reservoirs generally occur below 3,050 m (10,000ft) of water. Deposition was restricted to the western portion of the present-day Louisiana shelf. Only progradational and submarine fan facies are observed during the lower Miocene (Hunt et al., 1995). The ancestral Mississippi River depocenter began migrating to the west during the upper Miocene. Deposition extends significantly basinward across the Louisiana OCS, especially during late upper Miocene (Hunt et al., 1995). Isolated submarine fan facies with associated hydrocarbons extend across the Garden Banks area. During the Pliocene, productive facies extend farther basinward than in the upper Miocene. The submarine fan hydrocarbon play expands in Garden Banks.

The reservoir is a combination structural and stratigraphic trap with deep-water turbidite sands draped across a structural nose. The upper Miocene reservoir is a deep-water turbidite system that scoured and filled an upper/middle slope, low-relief canyon with an aggradational channel/overbank system. The channels are highly amalgamated resulting in stacked reservoirs with vertical and lateral communication. There are localized overbank deposits within the channel (Pulham et al., 1991).

The Upper Miocene (Late Middle to Early Late Miocene) depositional episode (UM episode), defined by two widespread, transgressive deposits associated with biostratigraphic top Textularia W (12.0 Ma) and Robulus E (6.2 Ma), records long-lived sediment dispersal systems that persisted for nearly 6 m.y. with little modification. In the east-central Gulf of Mexico, this episode records extensive margin offlap, primarily centered on the ancestral Tennessee River and Mississippi River dispersal axes. The deepwater depositional style consists of abundant sediment supply which has prograded

along the northern and northwestern basin margin 150 to 180 mi (240 to 290 km) from its inherited Cretaceous position. Margin outbuilding has been locally and briefly interrupted by hyper-subsidence due to salt withdrawal and mass wasting. Three depositional systems tracts characterize Cenozoic genetic sequences: (1) fluvial -> delta -> delta-fed apron, (2) coastal plain -> shore zone -> shelf -> shelf-fed apron, and (3) delta flank -> submarine fan. One or more examples of the fluvial -> delta -> delta-fed apron systems tract occur in each of the major genetic sequences. Immense volumes of sand have bypassed the shelf margin to be deposited in slope and base-of-slope systems, primarily within fluvial -> delta -> delta-fed apron system tracts, during all major Paleogene and Neogene depositional episodes. Deposition and preservation of volumetrically significant coastal plain -> shore zone -> shelf -> shelf-fed apron tracts is typical of Paleogene through Miocene depositional episodes only. Fan system origin was commonly associated with major continental margin failures, but large submarine canyons occur mainly in Pleistocene sequences. Thick, potential reservoir sand bodies occur in offlapping delta-fed slope and subjacent basin floor aprons, in autochthonous slope aprons and related infills of slide scars and canyon cuts, and in submarine fans (Xinxia et al. 2004).

The Gulf Basin Depositional Synthesis Project's interpretive GIS database (Galloway et al., 2000) has been combined with the published MMS paleodata (planktonic marine markers) and reconstructed paleoshorelines to produce a suite of 2-D and 3-D images that relate major depocenter evolution to the paleostructure and paleobathymetry of the northern Gulf of Mexico (GOM). Paleobathymetric surfaces were constructed for thirteen time steps during the Cenozoic. The reconstructions illustrate how 3-D visualization can be used to assess the effects that eustatic and continental climate change as well as tectonics have on the sedimentation history of the GOM basin. Bathymetric surfaces were modeled for each of the major Oligocene and younger depositional episodes. Doppler maps that illustrate depositional pattern change also were constructed. Three-dimensional visualization takes advantage of the natural human ability to see patterns in pictures and helps uncover hidden trends in the data. The constructs can be navigated in 3-D space and time to understand better the depositional history and

focus the petroleum explorationist's attention on those geographic areas and stratigraphic intervals with the greatest reservoir potential (Fig. 5.2).

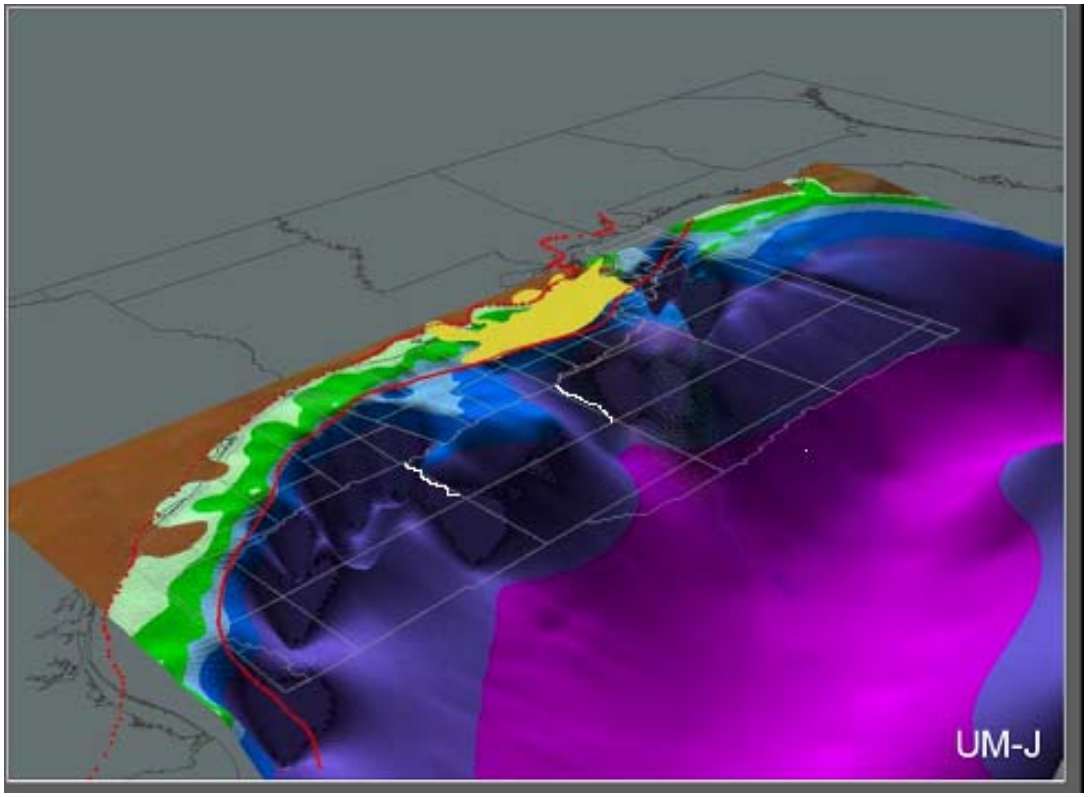

Figure 5.2: Upper Miocene: Data courtesy of sponsors of The University of Texas at Austin Gulf Basin Depositional Synthesis: EnCana, ENI Petroleum, Amerada Hess, Anadarko, ConocoPhillips, ExxonMobil, JNOC, Kerr-McGee, Marathon, Nexen, Norsk Hydro, ChevronTexaco, Total, Unocal, and Woodside Energy.

If we examine the sequence stratigraphy from the figure above, there appears to be a sea level fall until middle early Miocene, a slight transgressive tract, another fall until the middle Miocene, and then a rise until the upper Miocene and then a final fall. If this is the case, it would make sense to assume the early Miocene sands were deposited, then salt canopies began to rise as isostatic pressure was decreased. A point of equilibrium was reached, and water level fell again as another middle Miocene sand was deposited. Following this, sea level rose and there is a slight shale layer covering the sands. Yet another sea level drop occurs and this shale layer is broken apart by another salt upwelling event. Therefore, there are three different levels of Miocene sands that

have been pushed upward by salt, some remaining at their original depth as the salt moved above and around these sands.

The Middle Miocene constitutes a prolific hydrocarbon-producing interval in the Gulf of Mexico. However, regional synthesis of the evolution of the middle Miocene is needed. The depositional episode is bounded by regional-marine transgressive deposits and flooding surfaces associated with the faunal tops *Amphistegina* B (15.5 Ma) *Textularia* W (12 Ma) (Morton et al., 1988; Galloway et al., 2000; Combellas-Bigott et al., 2006). The evolution of the depositional episode in the east-central Gulf of Mexico is recorded in four genetic cycles (each around 1 to 2 m.y.) bounded by regional maximum flooding surfaces and distal condensed sections in the basin margin and by three equivalent seismic sequences punctuated by condensed sections in the slope and basin floor. Distribution of depositional systems during the middle Miocene depositional episode was controlled by the high rate of sediment supply, low to moderate wave energy influx, high-frequency sea level changes, and salt tectonics (Combellas-Bigott et al., 2006).

5.3: General Stratigraphic Work on Surrounding Area

This description is included to give the reader a feel for what was happening as the present day salt structures began to form. To begin, the offlapping shelf margin systems were punctuated by a large-scale slope failure. This was known as the Harang collapse system, associated with massive salt-withdrawal and retreat of delta systems. A large volume of sediment, funneled by the Harang collapse system, bypassed the slope, initiating a long-lived submarine fan system. The fan formed in a minibasin corridor and unconfined abyssal plain, approximately 240 miles (384 km) from the active shelf margins. The fan system evolved from a structurally-controlled, elongate, sand-rich fan to a mixed sand/mud fan to a large, radial, mixed sand/mud fan. Significant untapped middle Miocene hydrocarbon resources remain in the deep Harang collapse system and sand-rich ponded facies assemblages of the fan system (Combellas-Bigott et al., 2006).

The Middle Miocene also covers three seismic sequences bounded by widespread condensed sections which recorded the evolution of the fan. Decreasing percentage of

sand and structural control, increasing development of turbidite channel fills, and general westward shift of the sediment dispersal system are characteristic of the MCAVLU Fan. Three seismic sequences bounded by condensed sections recorded the evolution of the MCAVLU Fan. Each seismic sequence is affected by salt tectonism in the slope. Dormant salt ridges and plateaus, shallow salt sheets, salt welds, and basement faults composed the mosaic of relic structures that controlled the deposition of the MCAVLU Fan. Seismic Sequence 1 shows the greatest influence of the relic salt structures. Sequence 1 is mostly composed by sandy mounded and sheet like turbidites that followed a tortuous NNW-SSE corridor of connected minibasins down the slope (Combellas-Bigot et al., 2006).

Deposits of the second seismic sequence migrated westward and are dominated by turbidite channel fills in the slope and abyssal plain, and vertically stacked, multi-lobe turbidites in the abyssal plain. In the final stage, Seismic Sequence 3, two major depositional axes are present. The western axis is characterized by turbidite channel fills in the slope and sand-rich amalgamated lobes in the abyssal plain. Dominant progradational to aggradational delta-lobe facies of the ancestral Mississippi delta extended above the prodelta shelf facies and fed the delta apron systems in the constructional shelf margin. The mud-dominated, delta-fed apron is traversed by prominent submarine-channel fills or channel-levee complexes, overlain by more progradation mud. The MCAVLU fan system continued to grow. Bypass facies assemblages characterize the fan system (Combellas-Bigott et al., 2006).

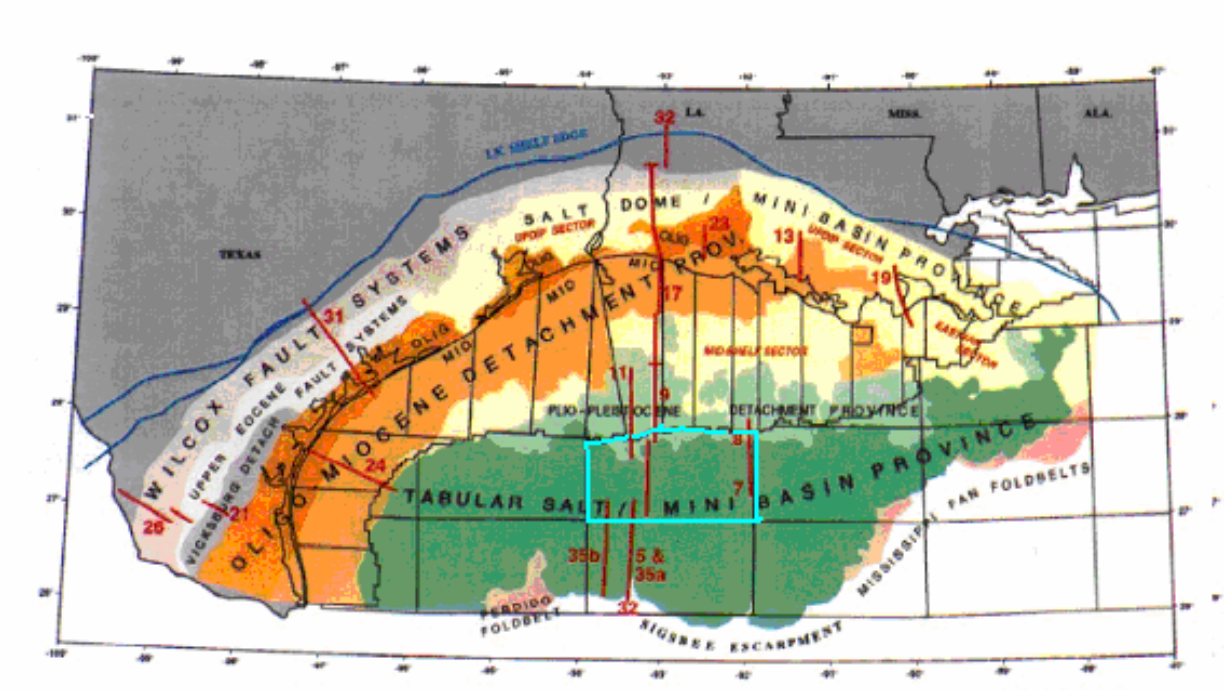

Figure 5.3: Tectono-stratigraphic province map.

The tectono-stratigraphic province map (Figure 5.3) illustrats eight distinct regions defined by contiguous areas of similar structural style. The ones of importance here include a tabular salt-minibasin province on the slope and the Pliocene–Pleistocene detachment province on the outer shelf. The tabular salt–minibasin province is characterized by extensive salt sheets with intervening deep-water sediment-filled minibasins. Most of these minibasins form bathymetric lows today. The Pliocene–Pleistocene detachment province includes areas of evacuated allochthonous salt along detachments for listric growth faults as well as remnant allochthonous or "secondary" salt domes and wings in the area of the Pliocene–Pleistocene shelf margin depocenters (Diegel et al., 1995). Emphasis on the key salt dynamic stages that reflect main events of the basin evolution. The Oligocene-Miocene detachment province is characterized by listric down-to-the-basin growths faults that sole in the Paleogene. The western linked system is characterized by an early phase of massive salt inflation during the Paleogene (Diegel et al., 1995; Peel et al., 1995). Salt extrusion and spreading extended to within 15 mi (24 km) of the Sigsbee Escarpment (Peel et al., 1995). Some believe early Miocene clastic progradation onto this allochthonous nappe triggered massive salt evacuation that continued during the middle Miocene (Diegel et al., 1995). However, I think salt

evacuation is more dependant on plate movement and faulting relieving pressure rather than deposition.

Most of the lower−middle Miocene minibasins grew above the allochthonous Paleogene salt canopy. However, deflation of autochthonous salt and formation of primary minibasin during the Neogene was locally important (Rowan, 2002). In general, there is a gradual transition from isolated minibasins surrounded by contiguous salt in the lower slope to isolated salt bodies surrounded by interconnected fault-bounded minibasins near the shelf margin. This transition reflects progressive deformation during progradation of the margin across allochthonous salt. The middle slope shows an early stage of sedimentation above allochthonous salt. The perched basin is beginning to subside into the salt, whereas faults with seafloor expression indicate a contemporaneous sliding downslope. Normal faults occur at the northern end, and reverse faults occur at the southern end.

In this province, deposits of the middle Miocene depositional episode reached almost 8500 ft (2590 m) in thickness. Roller fault families detached from the Paleogene canopy, forming a roho-salt system. Subvertical south-leaning feeders are clearly imaged on seismic data, showing the allochthonous origin of the detachment surface. The roller fault system consists of a series of nested, arcuate, listric faults rooted at depth on the evacuated Paleogene canopy. The roller fault system formed above an elongate and relatively thin Paleogene salt canopy and was accommodated both by partial withdrawal of salt and by major basinward translation of the overburden. The major deltaic depocenter of the middle Miocene is located within the central linked system, accommodated by lateral extension and gravity spreading, which drove salt inflation (Diegel et al., 1995).

From 10.5 to 5.5 m.y., a relatively uniform southward progradation occurred and the movement of depocenters was toward the south. At ~5.5 m.y., successive sequence depocenters began to migrate eastward. The rate of southerly progradation in the west decreased, while that in the east increased. From around 3.1 to 4.9 my (Pliocene) a megaslide complex formed. One part was a progradational delta-fed apron and further

south was a shelf-fed apron. These changes may reflect a transition from sandier to muddier sediment. Sequence development was primarily governed by sea level, but changes in depositional patterns are related to local controls, i.e., changes in drainage patterns, sediment supply, subsidence history (including effects of salt tectonics) (Buffler et al., 2005).

5.4: Problems

There are some problems that may occur when exploring reservoirs in slope fans. One can drill too high on a levee where sand is missing, find a shale-filled channel, or mistake a slumped unit for a leveed channel. Leveed channels are elusive targets and are best used when three-dimensional seismic surveys are available (Brown, 1991). However, a large percentage of the deep-water sand production from the Gulf of Mexico is from these sands which show "bright spots" (Pacht et al., 1990).

Petroleum entrapment in the basin floor has certain risks such as a lack of hydrocarbon migration path from source to reservoir. In the Pliocene-Pleistocene strata of the Gulf of Mexico, faulting and vertical migration paths are commonly required to get migration from deeper mature source rocks to younger reservoirs. Also, there may be a lack of top seal if the slope fan sands rest directly on the basin floor fan. Most basin floor fans that produce in the Gulf of Mexico are associated with combination structural-stratigraphic traps (Mitchum et al., 1991).

Chapter 6: Pleistocene Complexes

6.1 Introduction

What is being called Pleistocene in this paper overlaps with what is being referred to as Pliocene, which overlaps Miocene. I separate it more so into upper Pliocene-Pleistocene and lower Pliocene-upper Miocene. The first, younger grouping has, for the most part, been previously analyzed for reservoir prospects. For deeper stratigraphic analysis there is little paleo-data available for the second time range, so it is hard to differentiate at what depths one begins and another ends. This chapter is simply stating what has been said about the events in this time and general area. This area has been studied and debated more than somewhat deeper Miocene events.

6.2: Partially Confined Depositional Systems, Magnolia Field, Garden Banks, Gulf of Mexico

The formation of fill and spill channel complexes is a complex balance between the creation of accommodation space and the local sedimentation rate. This dynamic balance controls the channel architecture that develops and changes systematically through deposition. The complex of Magnolia Field is one of several reservoirs deposited at the southern end of a salt bounded mini-basin in the Garden Banks protraction area. This complex was deposited in the transition from the ponded basin succession to the bypass facies succession indicating that the salt movement and its ability to create accommodation space was waning and subsidence was becoming the main space creating force (McGee et al., 2003).

Integrated analysis of sedimentological core description, dipmeter image logs and pressure data with detailed seismic facies analysis has lead to the interpretation that there is an amalgamated channel complex that became more intensely amalgamated as the system came to the southern margin of the mini-basin and felt the effects of the salt-induced topographic high. The system did not pond up against the salt ridge, but erosively amalgamated as the local gradient increased. The system then continued into the next basin to the south. The next interval corresponds to the overlying leveed channel complex that developed when the system evolved into a “bypass” system directing most

of the sediments down system and formed levees through overbank and flow-stripping processes (McGee et al., 2003).

6.3: Late Pleistocene Depositional Systems

Recent studies of sediment-gravity-flow systems of the northern Gulf of Mexico Basin suggest that large submarine fans become increasingly rare going back through time, particularly prior to the Pleistocene (Pulham, 1993; Prather et al., 1998; Winker and Booth, 2000). Detailed studies of the late Pleistocene depositional systems along the shelf margin and slope describe minibasin sediment-gravity-flow fills that appear to have been emplaced without the aid of large, mappable submarine canyons (Winker and Booth, 2000).

In general terms, Beaubouef and Friedman (2000) agree: "The southern limit of the Texas-Louisiana Shelf is rimmed by thick shelf margin deltas interpreted to have formed during the last Wisconsin glacial event. These fluvio-deltaic systems provided the source for large volumes of sediment transported to the deep basin." However, referring to the minibasins in front of the Trinity-Brazos shelf margin delta, they stated: "The presence of an older, buried canyon beneath the deltas can not be precluded, as that region of the subsurface is not imaged by the high-resolution seismic data." These authors emphasized the uncertainties that remain: "although the source of sediment delivered to these basins is well known, the exact mechanisms of sediment gravity flow initiation and transport to the slope is not known."

On the other hand, Morton and Suter (1996) emphasized that "No incised valleys or submarine canyons breach the paleoshelf margin, even though incised drainages were present updip," apparently implying that sediment gravity flows originated on shelf-margin-delta clinoforms, and then continued downslope into minibasins. The late Pleistocene Mississippi canyon that strongly eroded a narrow corridor of the shelf and shelf margin did not form until after the Mississippi deltas had reached the shelf margin (Coleman et al., 1983). Additional work is required to resolve the important issues raised by Beaubouef and Friedman (2000).

During relative sea-level fall, a high-sediment-supply delta will deposit a single coherent, integrated deposit that can be considered a regressive systems tract. There is no surface comparable to the sequence boundary of the sequence-stratigraphic model that separates this delta into updip highstand and downdip lowstand systems tracts. In order to honor the genetic integrity of the delta deposit, cycle boundaries should be placed at flooding surfaces. Reorganization of depocenters is more likely to occur across flooding surfaces rather than between flooding surfaces. Subsurface maps of regressive cycles bounded by flooding surfaces will clearly show the positions of incised valleys, using either net sand or log facies data in the depoflank areas, due to their contrast with adjacent facies. In the depocenters, the discrimination of incised valleys from distributary channels is often either not possible, or not desirable, for sound theoretical reasons (Hunt et al., 1995).

It is possible that some degree of "forcing," or sea-level fall, accompanied many Gulf Coast Tertiary high-frequency ("4th order") cycles. In this case, "valley" features, difficult to identify in depocenters, would be important targets for exploration in depoflanks, where their detection would require time-scale stratigraphic analysis applied on a regional scale.

Chapter 7: Results and Discussion

7.1: Salt Structures

7.1.1: Introduction

The basic principles used in this paper are somewhat limited in their ability to identify hydrocarbons. Reflections of gas reservoirs change from a peak to a trough across the fluid contact. This implies a significant change in acoustic properties (phase change or polarity reversal) between the gas sand above the hydrocarbon/water contact and the water sand beneath it. It is noted for the seismic images shown in this paper that high amplitude reflections, shown as green, are possible gas sands, whereas yellow is a low amplitude reflection, usually implying shale. This is a decrease in acoustic impedance. Therefore, for the gas to be contained, a shale seal on top and a possible salt seal on bottom is required. Usually, two shale seals were needed, but recent discoveries have shown a sufficient trap occurs from salt. This high amplitude zone is shown most entirely when the arbitrary line is drawn diagonally from NW to SE (Figure 7.2) of the deep horizon traced (shown in Chapter 8). This is the "deeper horizon" that is mentioned throughout the paper. In this image we see salt moving above and below this horizon pushing it upwards. This may make for a good hydrocarbon trap. In the image below (Figure 7.1) is a base map showing the positional relationship of the seismic images. Each block is 3 by 3 miles and 3 miles equal 4828 meters.

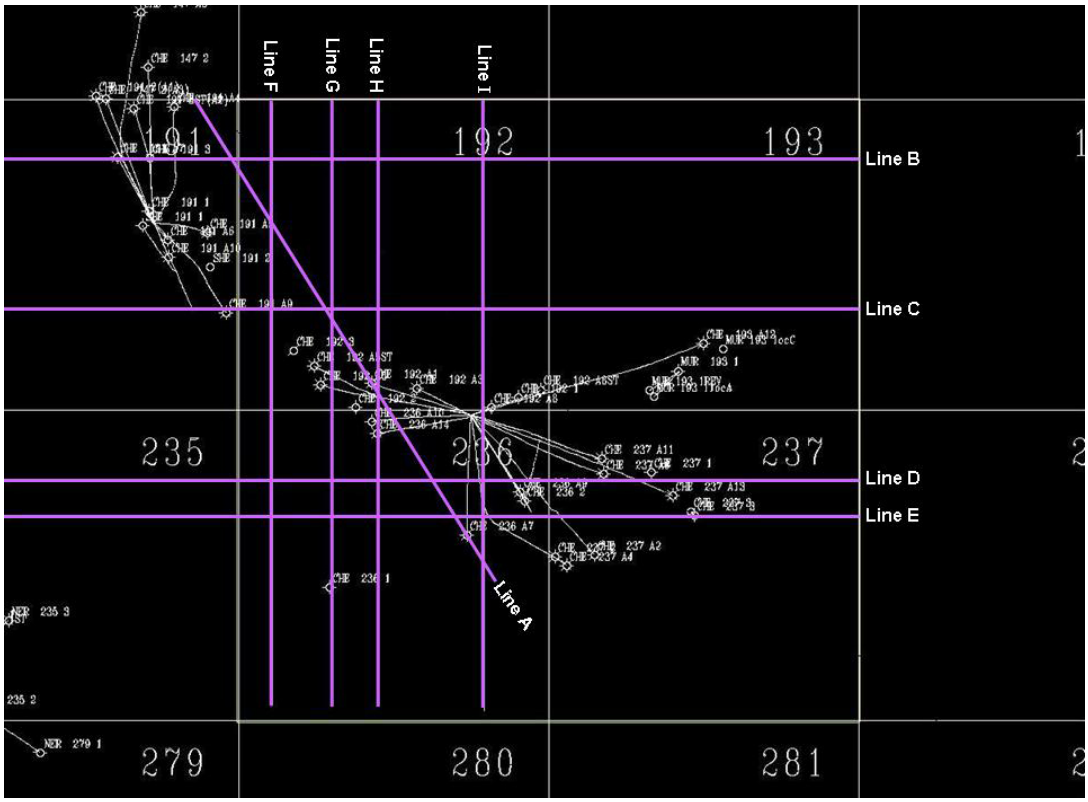

Figure 7.1: Base map showing position of seimic line images (12 x 9.6 km).

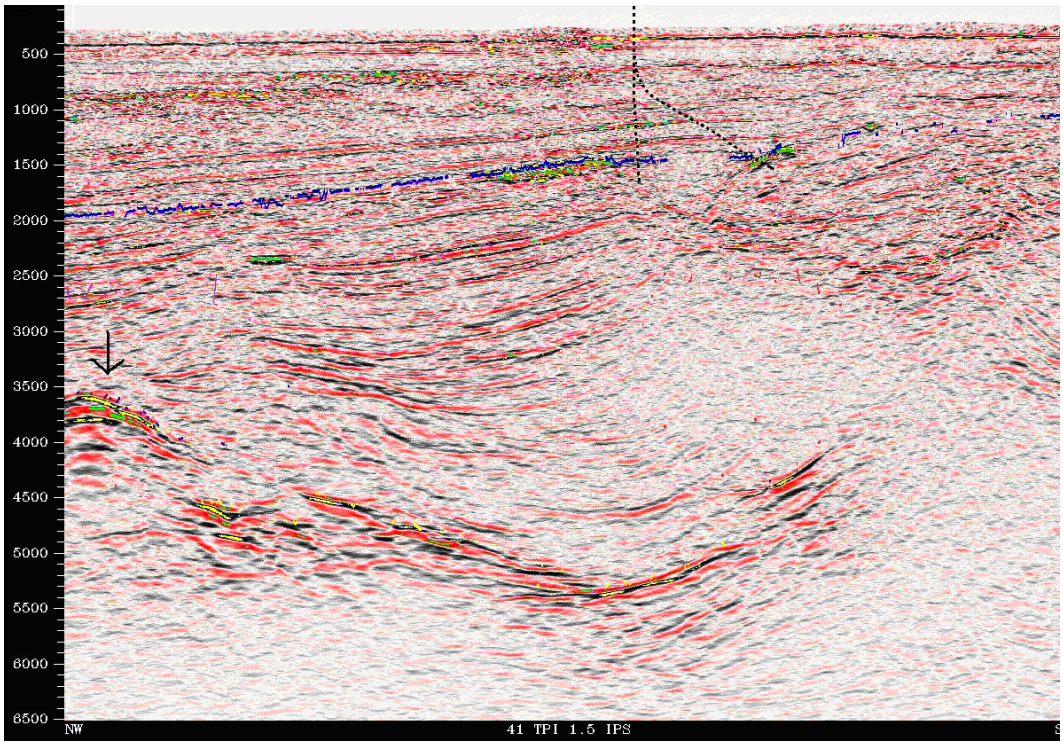

Figure 7.2: Line A from Figure 7.1.

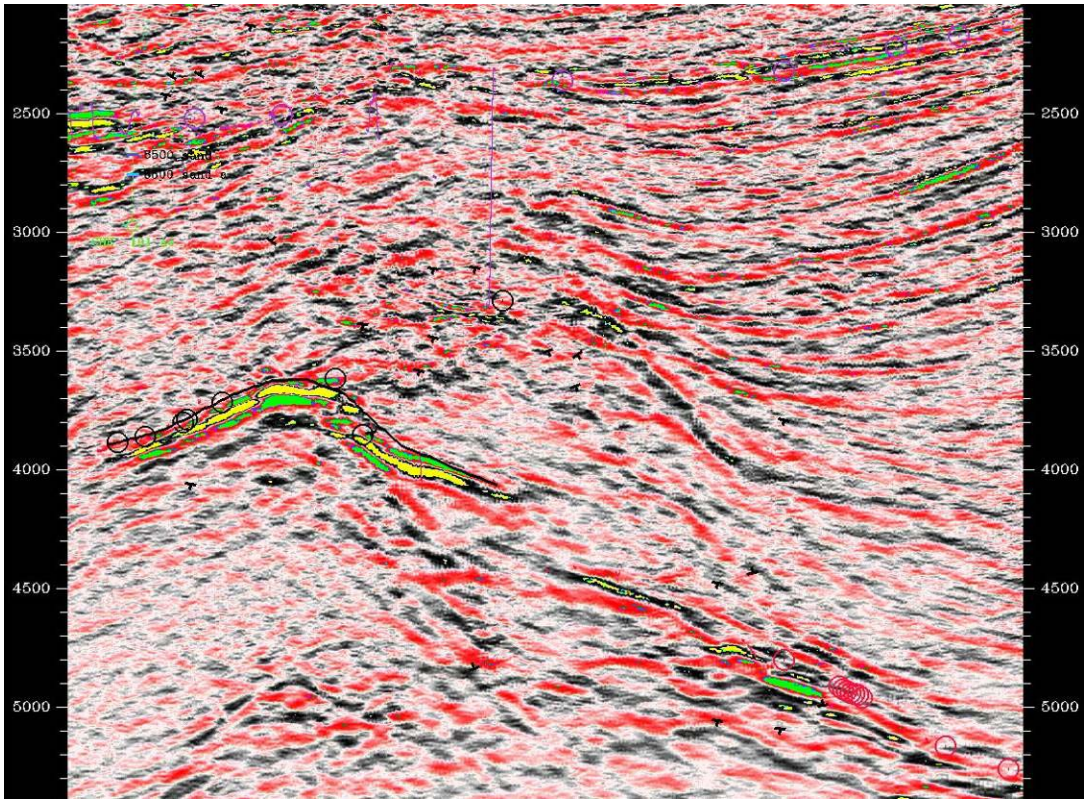

Figure 7.3: Line A from Figure 7.1: High amplitude zone drawn diagonally from NW to SE along new, deeper horizon. This is a magnified spot from Figure 7.2 (arrow) on the west end 3500ft sand.

7.1.2: Salt Weld Seals

Since time, not depth data are used and not depth, the salt structures inhibit some of the clarity of the surrounding strata. If depth data were used, we would see what is beneath the salt more clearly. Depth imaging was not used for most seismic perspectives because the depth data were processed only to around 9200 feet in depth. Time intervals went as far as 20,000 feet. Figure 7.4 is the intersection line for (Figure 7.5) in between Blocks 191 and 192. These two figures are the N/S, E/W slices through figure 7.3. The salt is along side of and in between the strata. This salt mass gets larger towards the south. It pushes the sand up and to the east, until it is not seen. This could mean that the sand's path is blocked.

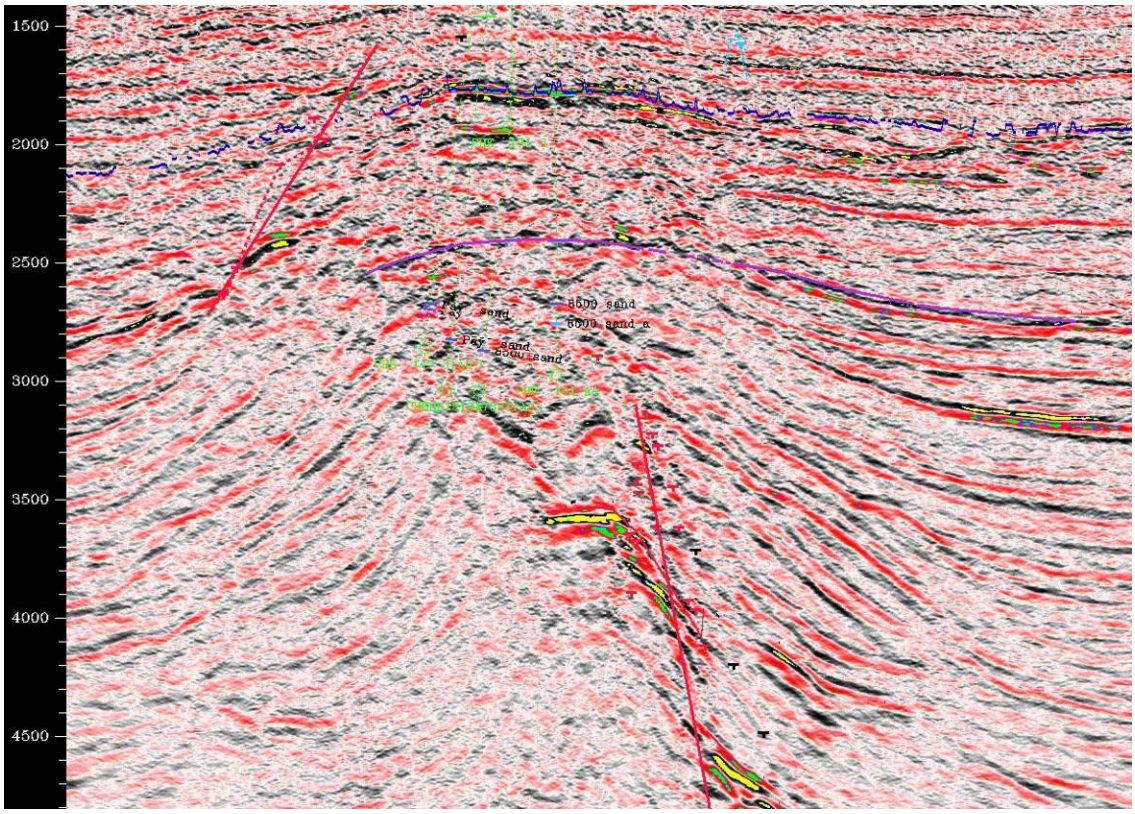

Figure 7.4: A little below line B from figure 7.1: Vertical line through Line A in Block 191. Also, N/S intersection of figure 7.5 along the fault**.**

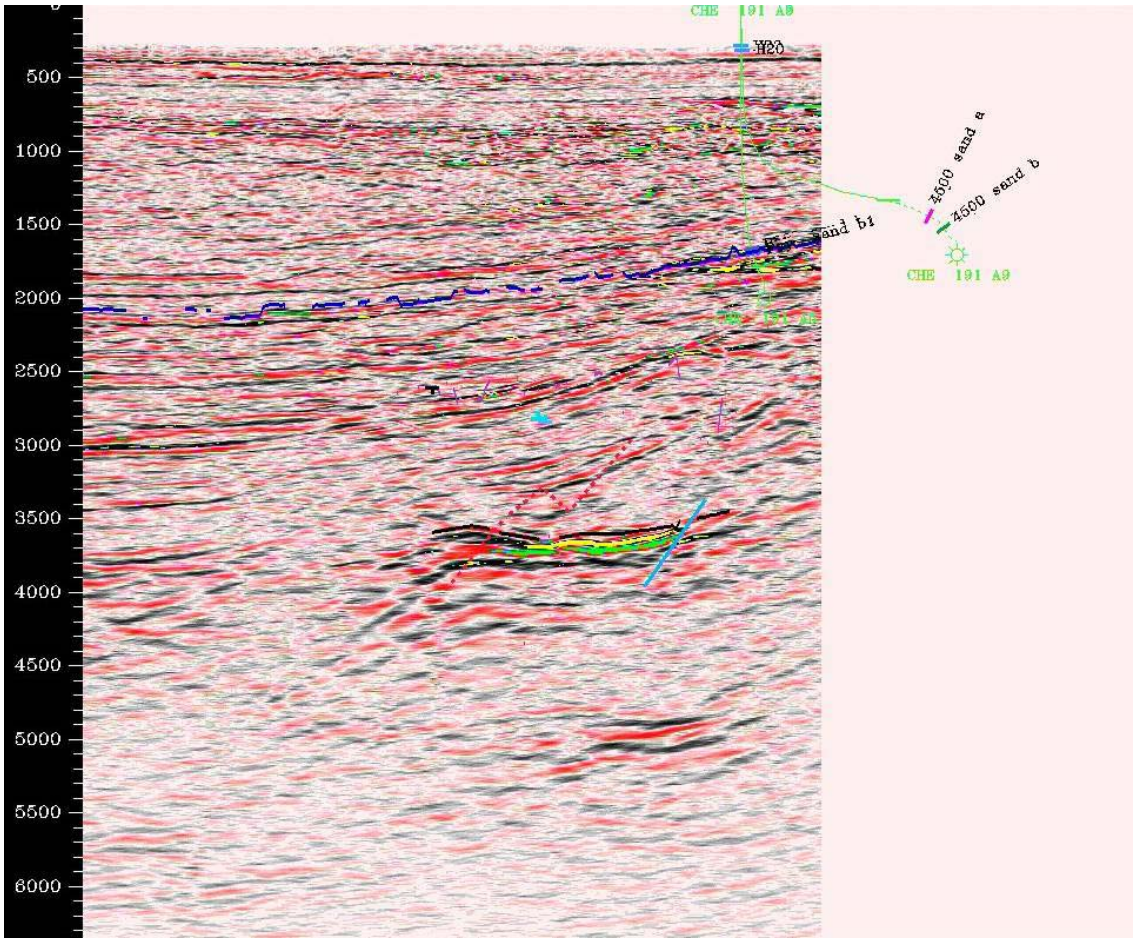

Figure 7.5: Block 191: East of Figure 7.6- prior to salt movement. Here with less detail.

Figures 7.4, 7.5 and 7.6 lie directly under well A4 in block 191. There seems to be a salt mass below the well which could have hindered reaching the deeper pay. Figure 7.4 lies further east than figure 7.6 and has different parameter settings. The salt has migrated and pushed its way on top of the pay zone more so in figure 7.6. In figure 7.5 the salt has not migrated between the strata as much.

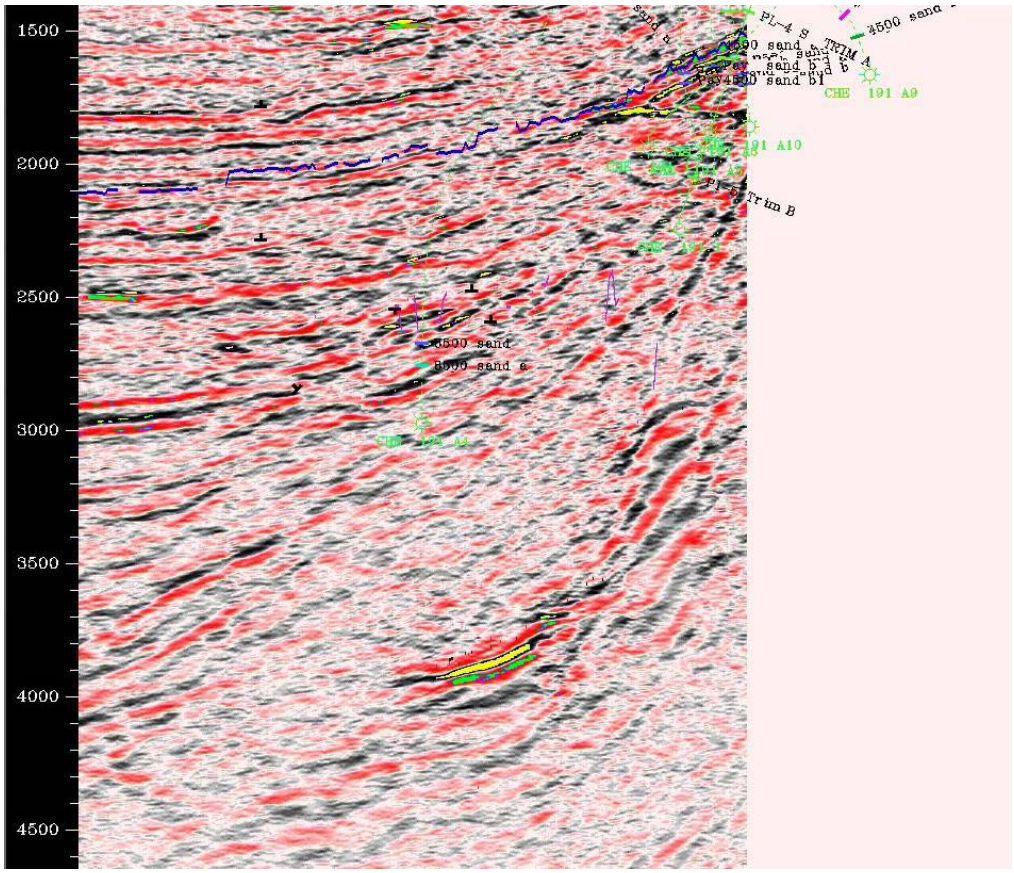

Figure 7.6: Block 191: Salt movement.

Figure 7.7-7.9 shows a sheet sand deposit that was leveed by salt. This usually occurs in the slope and basin-floor environments. It is possible that a deep water turbidity flow occurred from salt upwelling. In the seismic image below, the salt structures have compressed the syncline. It does not appear that a hydrocarbon trap is present.

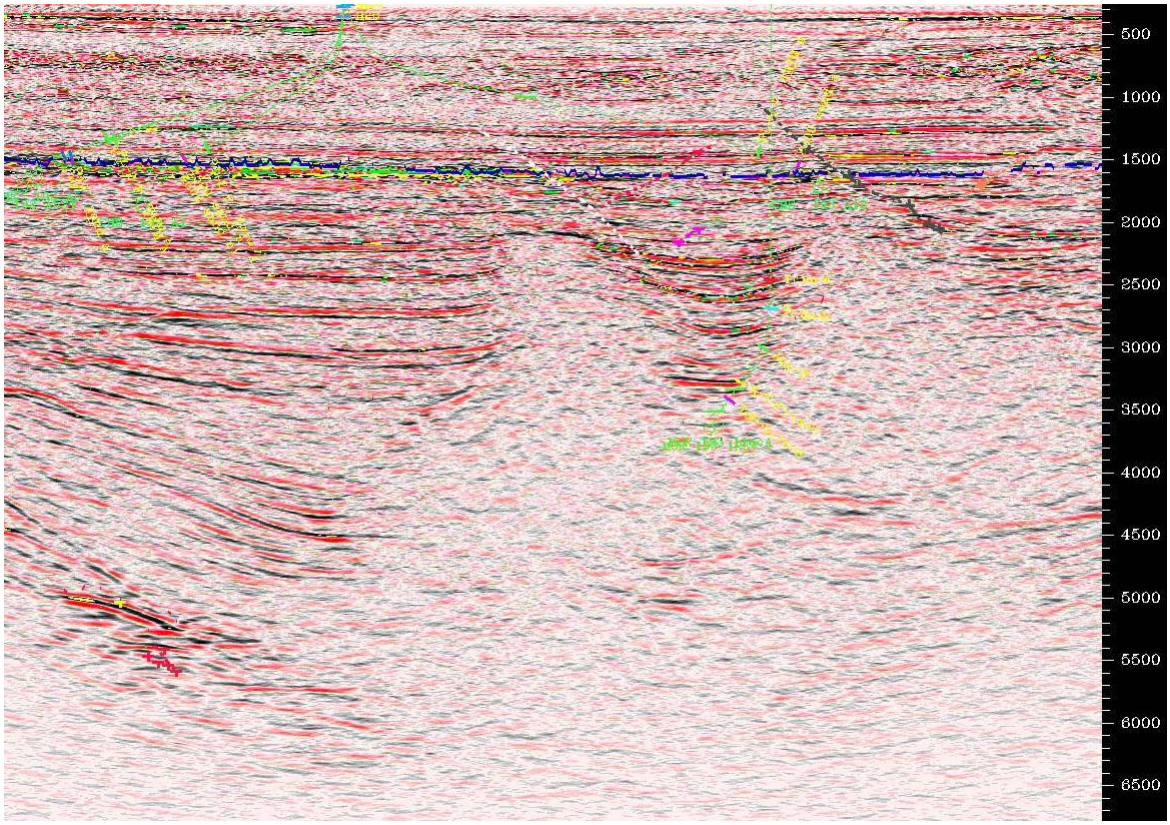

Fig. 7.7: Stratal truncation and salt below well 193 (1) which had no pay recovered. Possibly shaled out.

Figure 7.8, is further south than Figure 7.7 in Block 236 and 237. The blocks' boundary lies near where the strata truncates the salt dome. Interbedding these layers is an allochthonous salt body and linked weld. The weld is overlain by a transparent section which is probably a condensed mud; so, it is a good seal. The mud acts as a carapace over the canopy. If overlain by dipping sands and shales, the weld is probably a poor seal.

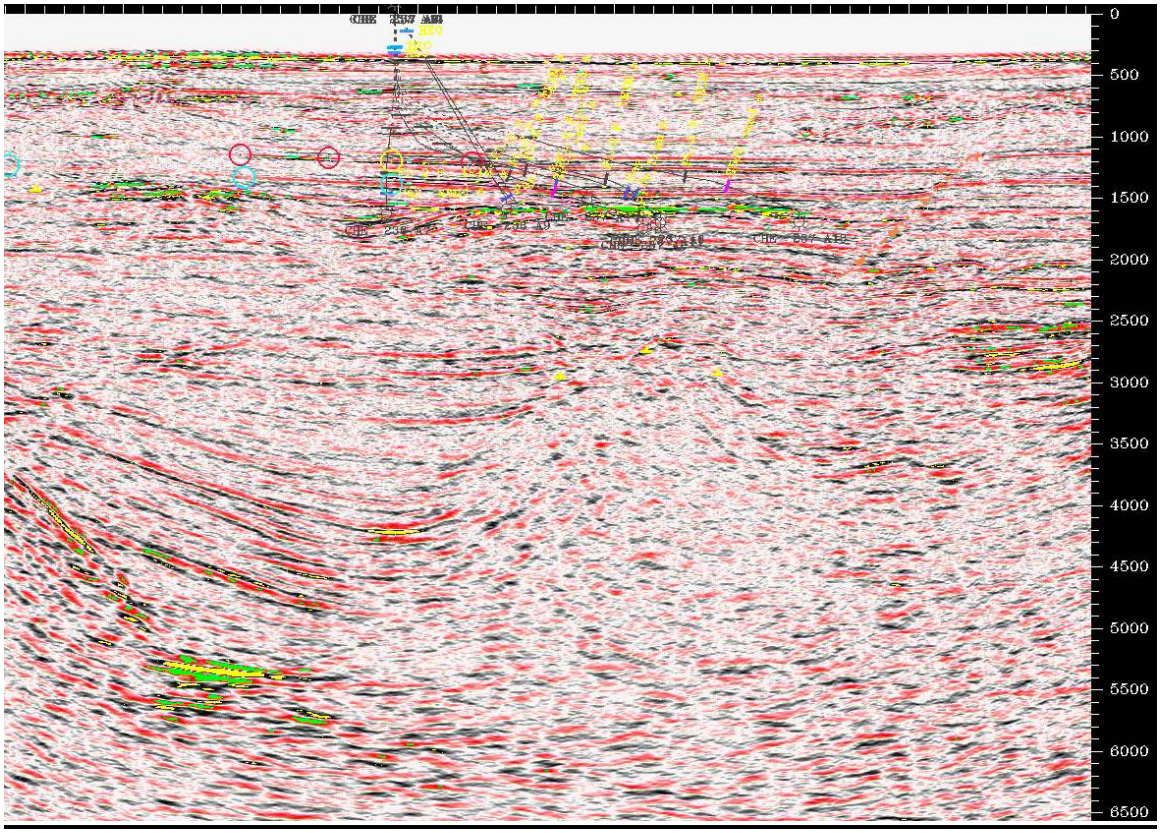

Fig. 7.8: Line D: South of figure 7.7-More salt infiltrating the sediments.

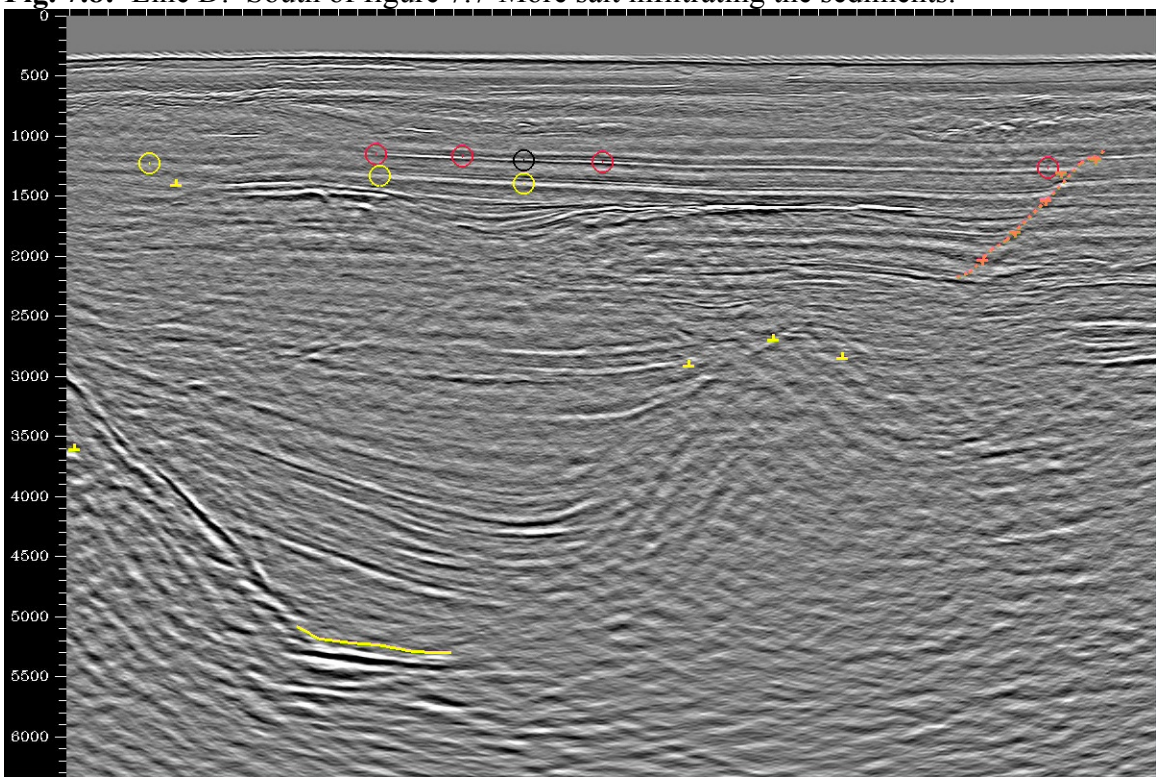

Figure 7.9: Same as figure 7.8 but with single gradational gray scale.

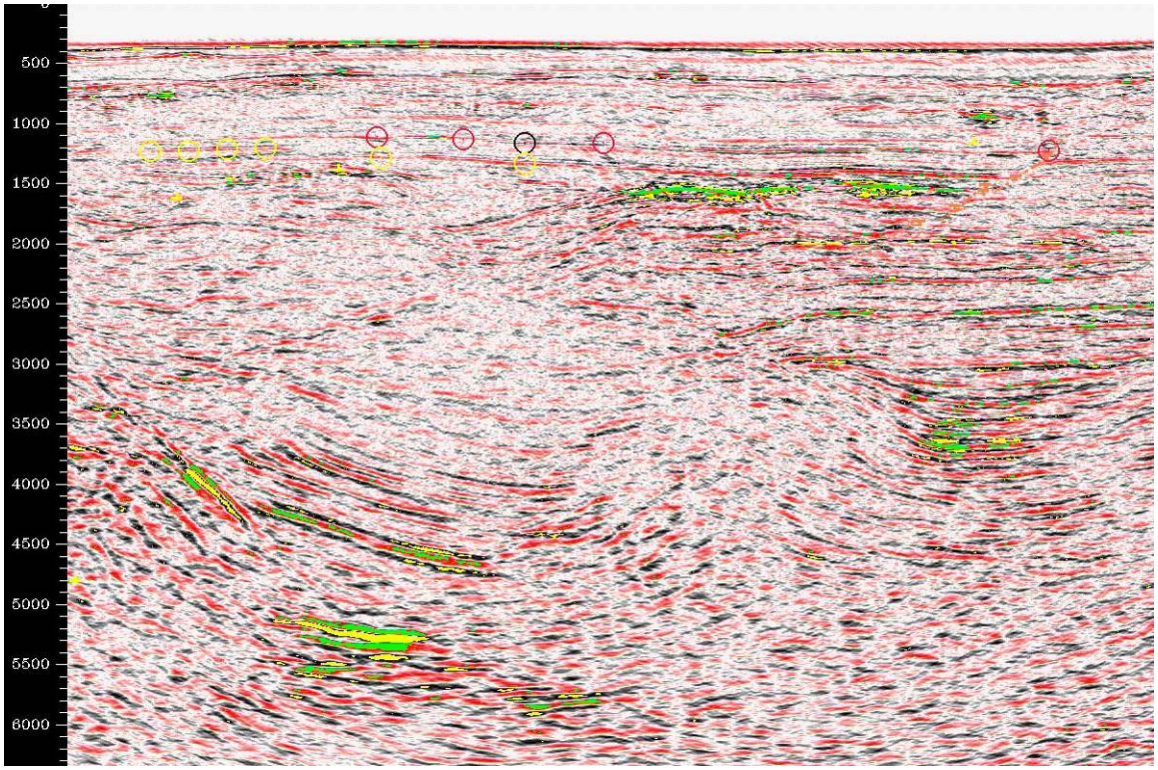

Figure 7.10: Same as figures 7.7-7.9, but moving even further south.

The possible pay sands shown above are rotated by the salt surrounding them. These sands would be considered intersalt plays. With clipping, the amplitude values are shown brighter and are more noticeable below the salt. This area lies in the far most western portion of Blocks 192 and 236. The high amplitude sands move deeper and are spread farther apart by salt as one move to the east. We also see another portion of the sand in 236 now in the top zone at 3300ms. There, it develops into three turbidite sand units. The salt has come in from the east and been isolated from the source by the third deposition to the upper right portion of the image. The first, and possibly second, deposition was blocked when it encountered this salt.

Many supra-weld traps throughout the world are charged with hydrocarbons from subweld source rocks, requiring migration through welds. However, not all welds are the same. We need to examine various factors that may influence the sealing capacity of salt welds. The probability of weld seal is enhanced by:

- the presence of remnant evaporite along the weld;
- relatively impermeable lithologies across the weld;

- subweld reservoirs that are encased in shales rather than in contact with the weld;
- the presence of clay gouge or smear generated during faulting; and
- an original base-salt geometry that creates divergent subsalt hydrocarbon migration pathways.

Another factor that must be considered is the timing of overburden deformation with respect to that of hydrocarbon generation and migration. Although weld seal is certainly a risk, traps that invoke weld seal should not be summarily discarded. Instead, each prospect should be evaluated separately in light of the factors presented here in order to derive a better assessment of the inherent risk. In addition, these ideas need to be tested with observations obtained from surface exposures and a combination of subsurface well and seismic data (Rowan et al., 2000).

7.1.3: Salt and Pressure

Salt domes and ridges that form the boundaries of salt-withdrawal minibasins cause increased pore pressure in the surrounding sediment. This fact results in anomalously high pore pressures in wells drilled on the flanks of a salt dome relative to wells drilled through equivalent strata toward the center of the basin. Pore-pressure ramps or steep increases also occur adjacent to salt masses, and some deep-water exploratory wells have had to be abandoned during attempts to drill through overpressured fractured shale associated with a salt diapir before the reservoir interval was reached. Below tabular salt sheets, formations can be overpressured because of an effective seal, and in some subsalt wells a pressure kick has been encountered in the rubble zone below salt. In general, however, the top of subsalt geopressure occurs at greater depths and deeper in the stratigraphic section than in wells without salt (Smith et al., 2002).

7.1.4: Downfalls

Liro et al., 2006 have stated some practical imitations of the interpretation of deepwater Gulf of Mexico subsalt seismic data. Exploration in the deepwater Gulf of

Mexico is hampered by shallow allochthonous salt. The high seismic velocity of salt, contrasting with relatively slow velocities of adjacent clastics, results in difficult seismic imaging. Inadequate seismic imaging in certain settings is commonly rationalized as "poor seismic." Liro et al., 2006 reviewed several common salt allochthon configurations where imaging is possible only under specific acquisition and processing workflows not typically found in "spec" data. Then, in consideration of their impact on geologic interpretation and risk evaluation, these points were noted: (1) Salt allochthon shape variations create irregular and often insufficient recovery of seismic signal. Resulting diminishment of the seismic image prevents adequate definition of the salt body, as well as subsalt structure, particularly 4-way closures. (2) Seismic processing algorithm difficulties of near-salt imaging result in poor definition of vertical and near-vertical salt feeder stock and weld systems. This effect is particularly detrimental to the definition of 3-way traps against or near vertical salt. (3) Inadequate and irregular recovery of seismic trace stack, coupled with typically low gas-saturation in encountered oils, leads to overall inability to use amplitude-versus-offset (AVO) and other direct hydrocarbon indicator (DHI) methods as an effective risk determiner. (4) Imperfect preservation of amplitudes prevents adequate stratigraphic (i.e., reservoir) interpretation. Each of these issues contributes to overall interpretational inadequacies, allowing only basic structural interpretation of subsalt. The difficulties of this exploration situation is that while the most sophisticated seismic tools and software are being utilized, only the most basic structural interpretation is possible.

There may also be some potential gas spots that do not have entirely flat amplitudinal appearances. They are due to gas velocity sag on a flat spot reflection. The trough dips and is depressed in time by the increased travel time through the low velocity, wedge-shaped gas sand. Flat spot dip caused in this way will always be in the opposite direction to structural dip (Brown, 1999).

Footnote:
Endnote: Seismic images used in this chapter were approved by PGS Data Management.

Chapter 8: Conclusions

8.1: Introduction

There have been significant hydrocarbon plays drilled in the Plio-Pleistocene depths of this study area. However, there are significant untapped lower Pliocene and upper to middle Miocene hydrocarbon resources remaining in the Garden Banks area. The various stratigraphic and structural environments are shown mainly with seismic data. Past studies of Fillon, Diegel, Combellas-Bigott, and Hunt, just to name a few, give hints to the present geologic situation of Garden Banks field 236 and surrounding areas. This study has built upon that basic understanding. The focus has been placed on new, deeper prospects in the region. The centralized area has been previously examined at depths ranging to 4500 feet, with a few up to 15,000 feet. In this study the range is roughly 9000 to 20,000 feet. Reaching a more comprehensive understanding of the geologic situation with the aid of more advanced, technological capabilities may allow re-focus on the area's still relevant production prospects. The most promising sands are Miocene-aged and deposited in turbidite-minibasin environments within an active salt province.

8.2: Pleistocene Geomorphology

The overall topography of the 236 area increases in elevation towards the south due to salt inflation. We see evidence for this in the pay sand horizons that have been mapped out. In seimic data and well log correlations it is seen that the pay sands of 4500 and 8500 feet get deeper as one proceeds north. There is a large syncline spanning 192 and 193. To the west, this syncline has been prevented from subsiding by salt, while subsidence occurred to the east due to sediment load. The deposition has definitely been disrupted by salt after the fact (Fig. 7.3, 7.4). As we move south, we see salt tongues slowly come into play where the syncline once spanned. At the 193/194 contact we see another salt diapir. This previous synclinal trap could have created a gas trap when it formed this anticlinal shape.

The area containing blocks 191, 192, 193, 236, shown in Figure 8.1, reveals the 4500ft horizon going from a low in the north to a high in the south. The normal fault lines are visible with down dip north of each fault block. Salt withdrawal and faulting causes these areas to be lower. Faults are striking north-east, and one is north-west. The hole in the center is due to salt which has penetrated to the 4500 foot sand. There are larger amounts of salt and at shallow depths in the 237 block. Most are allochthonous. There are fewer good pay areas in Block 237 than in the north block. This is mainly because the sands were deposited in the lower region and were stopped by the upwelling salt. There are some possible deep pay spots toward the south which most likely occurred before the salt mobilized.

Figure 8.1 shows the mapped horizon going from a low in the north to a high in the south. The normal fault lines are visible with down dip north of each fault block. Salt withdrawal and faulting causes this area to be lower. Three faults are striking north-east, and one is north-west. The hole in the center is due to salt which has penetrated to the 4500 foot sand. There are larger amounts of salt and at more shallow depths in the 237 block. Most of the salt bodies are allochthonous. There are fewer, good pay areas in the southern portion than the northern portion. This is mainly because the sands were deposited in the lower region and were stopped by the upwelling salt. However, this changes as we increase with depth. There are some possible deep pay spots toward the south which most likely occurred before and during the salt dynamics. The Zapped map of the shallow horizon results from a full-scale structural interpretation of the 3-D data. This is a horizon slice map of the 4500ft sand (Figure 8.2). ZAP! allows geoscientists to map a seismic reflection surface through an entire 3D volume in minutes or even seconds. This task could take weeks or months when done manually.

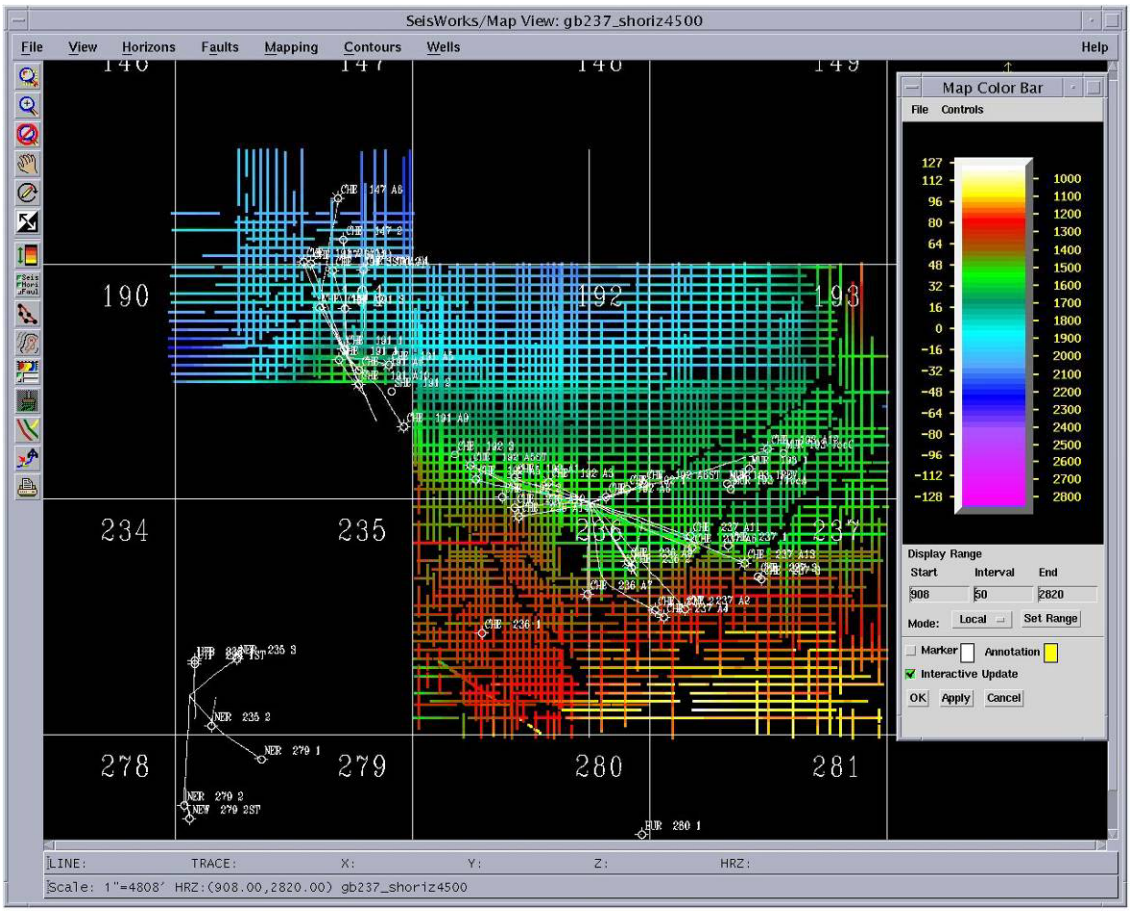

Fig. 8.1: 4500ft horizon ribbon map with faulting, Garden Banks 236 Field.

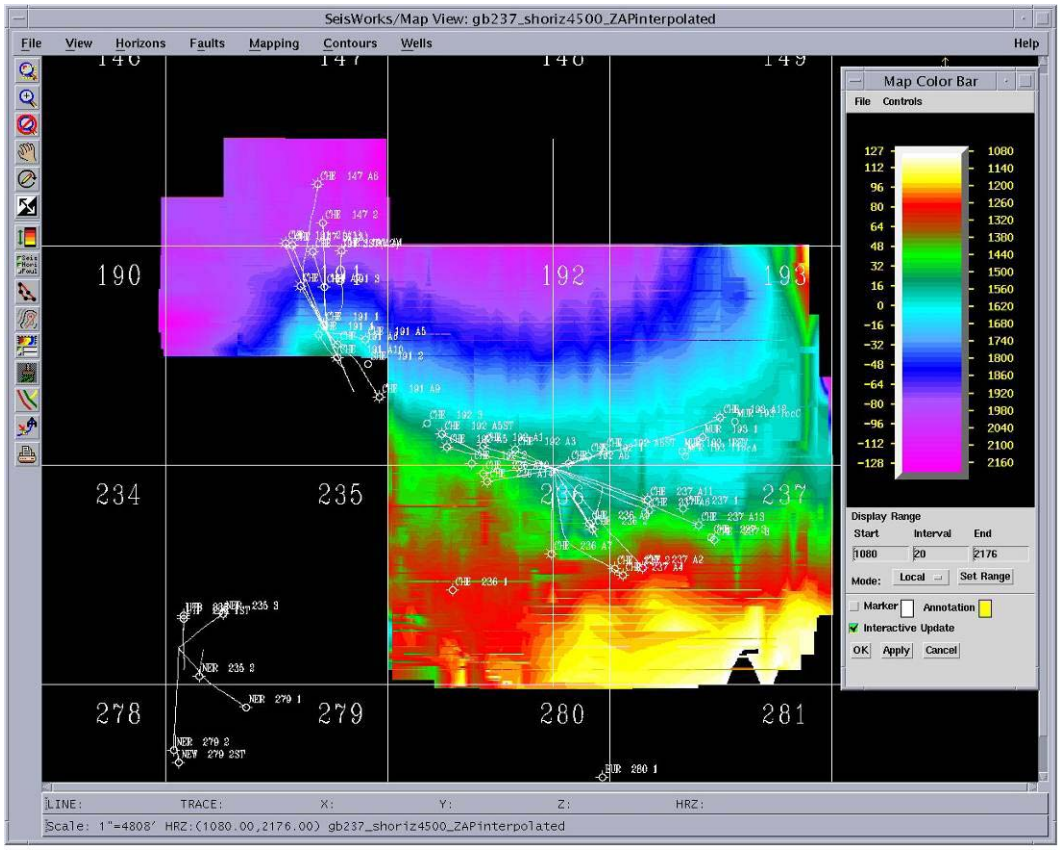

Figure 8.2: Zapped map of 4500 ft shallow horizon, Garden Banks 236 Field.

8.3: Sequence Stratigraphy

8.3.1: Introduction:

Previous studies on this area have been concentrated on Block 191, which contains both the 4500 and 8500 foot sands. Both of these are Pleistocene (Illionian) in age and are considered to be young by today's standards. It was hypothesized that they were formed by a sand-rich turbidity flow that was stopped in the southerly direction by salt diapirs and to the north by a strike-oriented shale ridge. This shale ridge extends east and curves slightly north in a bowl-like shape. As we look at the drill sites we can actually see this shape. However, these are all young pay sand discoveries. To find the deeper pays below previously drilled wells and perhaps beyond, we must take into account what happened before the turbidity flow and perhaps before and during the salt tectonics and diapirisms (Figure 8.3).

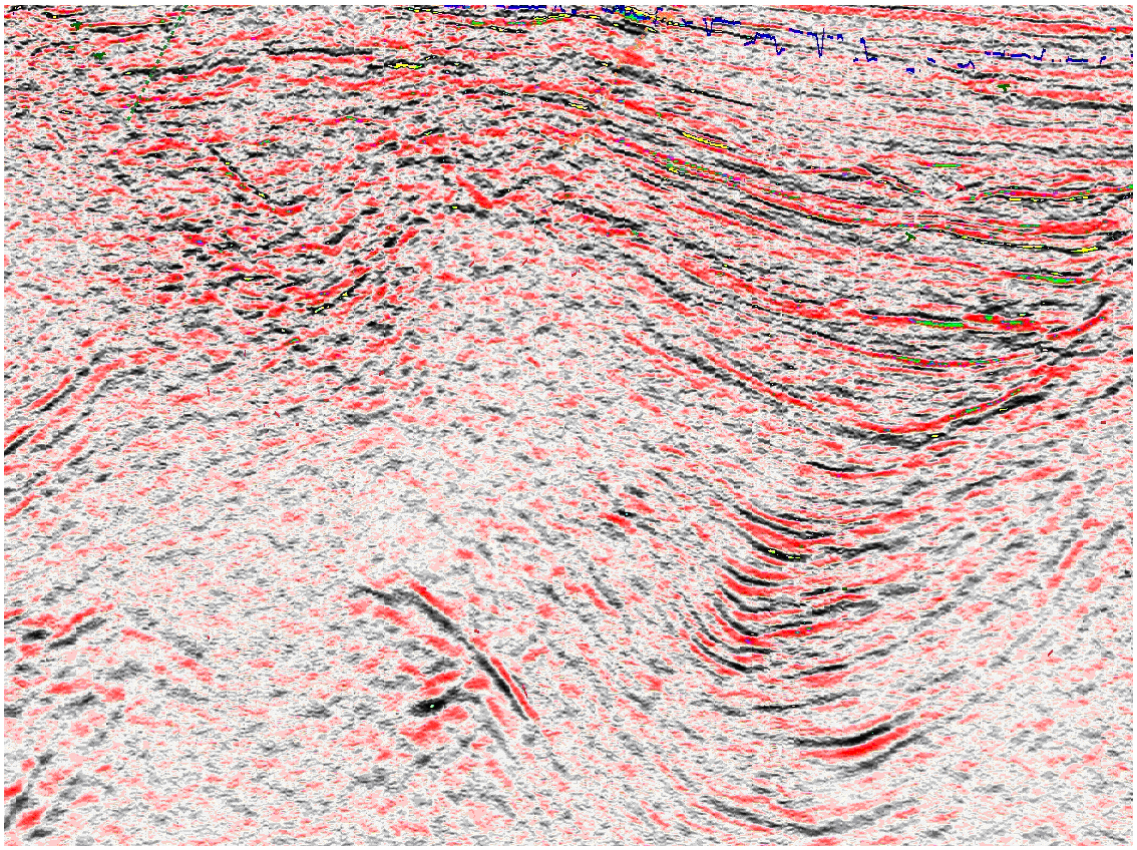

Figure 8.3: Two channel fill events across upper east 237 Block. The first (Miocene?) is surrounded by salt. At 3000 milliseconds a second sediment flow occurs in the Pliocene(?).

8.3.2: 4500 and 8500 foot sands

Focus has been placed on the 4500ft sand, the 8500ft sand, a deeper pay zone ranging from 12,000 to 21,000 feet (3500 – 5500 seconds), and the salt structures throughout this area and how they affect these horizons and their trap capabilities. . The blocky sand interval that we see in Block 191 from the 4500 and 8500 foot sands is indicative of a basin floor fan. The fan may rest on a sequence boundary which occurs above a clay-rich condensed section composed of basinal transgressive and highstand shale. One side of a salt/sediment contact may be clearer than the other side because of a less salt-related ray path distortion if it were under the overhung side (see Figures 8.7 and 8.8).

Initially, dip-oriented salt ridges funneled the sand-rich turbidite flows into the Garden Banks 236/191 area. The sand was then trapped on the north flank of the strike-oriented shale ridge at 236 and on the north flank of a salt diapir at 191. As the north flank mini-basin continued to subside due to continued loading and withdrawal, the 4500ft and 8500ft intervals were rotated and gas was trapped by the updip shale out of the sands to the south (Fugitt, 1999). The 4500 sand, however, did not stop at the salt. It was pushed upward and lies at around the 3750 to 3850 ft. depth in well A4, which is in the top most northern region (Figure 8.7 and 8.8). Also, the 8500 sand, being directly below this, was found deeper at 8900-9300 ft and lies along an outer ring encompassed by the diapir. Whereas Well A6 was located more south, the mid-east area was possibly brought deeper because it was along side the diapir as it rose (with part of the 4500 sand on top). Well A9, even further south, has two pay zones; the 4500 sand at 4453 and 4660 feet. The 4500 sand eventually shales out toward the north (Figure 8.7 and 8.8).

Figure 8.4 is a time slice based on the 4500 foot sand at 1560 ms. When a horizon is tracked, the extreme amplitude as well as its time is stored in the digital database. Mapping of the times produces a structure map; mapping of the amplitudes produces a horizon slice. This figure shows a bifurcating channel near a domal structure decreasing in elevation going north. The yellow colors represent a high velocity channel fill. The salt dome's semi-circular expression results from the intersection of the horizontal section with the dipping structural reflections adjacent to the dome. Away from dome the beds are close to flat-lying, so the horizontal section is sliced along the bedding plane. Because of this, the channel is almost completely visible. It is observed that the channel is deeper on the south-eastern part and is therefore dipping away from the dome. This was most likely induced by the movement of salt. We also notice that almost all of the wells drilled in this area are targeting the channel fill.

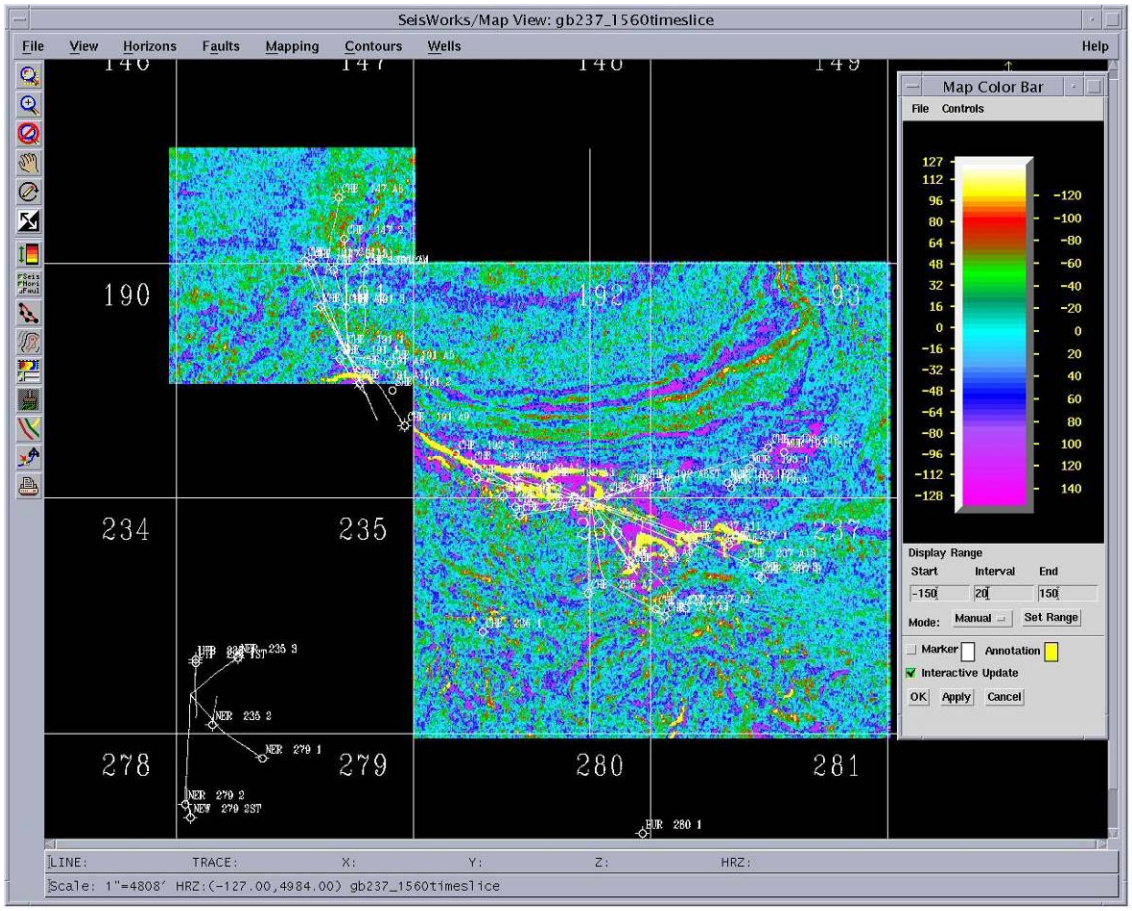

Figure 8.4: Time slice of 4500 foot sand.

The 4500 sand is prevalent across the area of focus. It seems to shale out towards the north. Block 147 has 8500 sand pay but no 4500 foot sand pay. Also, the 8500 foot sand may rise and merge with the 4500, but it is not pay sand in the same area. It has been previously stated that the 8500 foot sand is restricted to block 191. However, it could possibly be in Block 236 at a greater depth. In 191 the gas was trapped by the undip shaleout of the sands to the south. The 8500 sand is approximately 900ft thick and consists of a fining-upward channel succession that was deposited in a slope mini-basin formed by salt withdrawal. The other 4 blocks have only been drilled successfully at the 4500 foot sand. There was only a partial seismic survey for Block 235.

8.3.3: New Horizons

Garden Banks has been drilled over the years in deeper water and greater depths than previously mentioned, but most of these areas were concentrated in the southeast region and consist of tabular, salt/mini-basin plays. In introducing the new horizons tracked, it is important to incorporate salt architecture and its effect on possible hydrocarbon traps. Exploration and development of new reserves in the deepwater GOM is often hampered by extensive salt canopies, sheets and other salt bodies which absorb or redirect seismic energy resulting in poor seismic imaging. Interpretation of base of salt and sub-salt structures can be extremely difficult. Factors affecting sub-salt imaging are steep dips of the top of salt, rugose top of salt, salt structures with embdedded sediments, multiples and velocity anisotropy (Rowan, 2002). Salt-flank deformation during passive diapirism is a consequence of near-surface drape folding and not drag folding in a shear zone around the diapirs. The various styles of deformation result from the interplay between salt geometry, salt inflation/deflation rates, sedimentation rates, and the associated bathymetric relief. Salt-rise rates and sedimentation rates control the degree of bed rotation, the width of the deformation halo, the severity of angular truncation, and the amount of stratal thinning (Rowan, 2002). Most of the lower−middle Miocene minibasins grew above the allochthonous Paleogene salt canopy. However, deflation of autochthonous salt and formation of primary minibasins during the Neogene was locally important (Rowan, 2002). Rowan's analysis of salt structures and stratal deformation, however, makes no conclusions about hydrocarbon traps. It mentions what is probable, but stops there. Sediment flow and subsidence rate are the main factors that affect the upward folding of strata and consequently entrapment. Heavier sediment flux will cause beds to bend vertically as diapirs slowly rise. If sediment load is low, the beds will stay somewhat horizontal against the diapir. It is typically better for hydrocarbon traps to form when these upturned beds are then sealed by shales, which usually follow the fast sedimentation with a slower rate. This is known as drape folding. It counters a previous idea that diapirism simply pushed up through overlain strata causing drag folding as it rotated.

The horizon amplitude for the new "deep sand" is shown in Figures 8.5 and 8.6. This pay sand ranges from around 4500 to 5500 milliseconds or around 15,000-18,000 feet. This horizon gets deeper in the southerly direction and possibly to the east unlike the 8500 and 4500 foot sands which get shallower towards the south of this area. These deeper prospective zones lie along the same area where previous wells have been drilled. This means that, like the shallower pay sand that were deposited down slope and ran into salt structures, the sands before them followed a similar path. However, it is possible that this occurred as the salt structures were first developing and changing shape. This makes the deeper sands much more inconsistent. They are not as continuous because the salt structures have moved and separated them. Some prospects exist downdip of discovered fields and in between these fields where drilling has not penetrated deeper. The traps are the result of salt diapirism, anticlines, growth faults, normal faults and shale ridges.

Beginning with the northern region of the blocks at our new horizon depths, we see a synclinal basin area from the west portion of 192 to three-fourths of 193 (Figures 8.7, 8.8). On either side are major salt bodies. The 191 domes are farther from the surface and underlying the 8500 ft sand. Moving eastward, there is a syncline until the 236/237 Block boundary where it hits two salt dome sections at around 3000 ms. Above these domes, especially in 237, seems to be possible 8500 sand. However, pay was not encountered due to the sand being wet. The horizons shown in Figures 8.5 and 8.6 are traced only where the horizon seemed to have potential pay sand.

Block 192 shows good, deeper potential. Continuing from the 8500 sand found in 191, there is another possible sand to the east of the salt diapir below the 8500 pay. This zone is around 3600-4000 ms or roughly 11,000 to 13,000 feet. It lies on the border of 191 and 192. The salt surrounds this prominent area which is an arbitrary line running NW/SE. The pay zone begins where salt begins to overtake the strata from both above and below and where the salt overtakes the sand from the west. The deeper horizon can be traced at two different depths because the salt has disrupted the sediments. From the images in Figures 8.5 and 8.6, we see it does not affect the general shape too greatly. The main difference is the bottom left horizon section. This implies that salt domes during

the first episode were coming in from the west (Figure 8.6), then stopped and another came on the opposite side, pushing the sediments west (Figure 8.5).

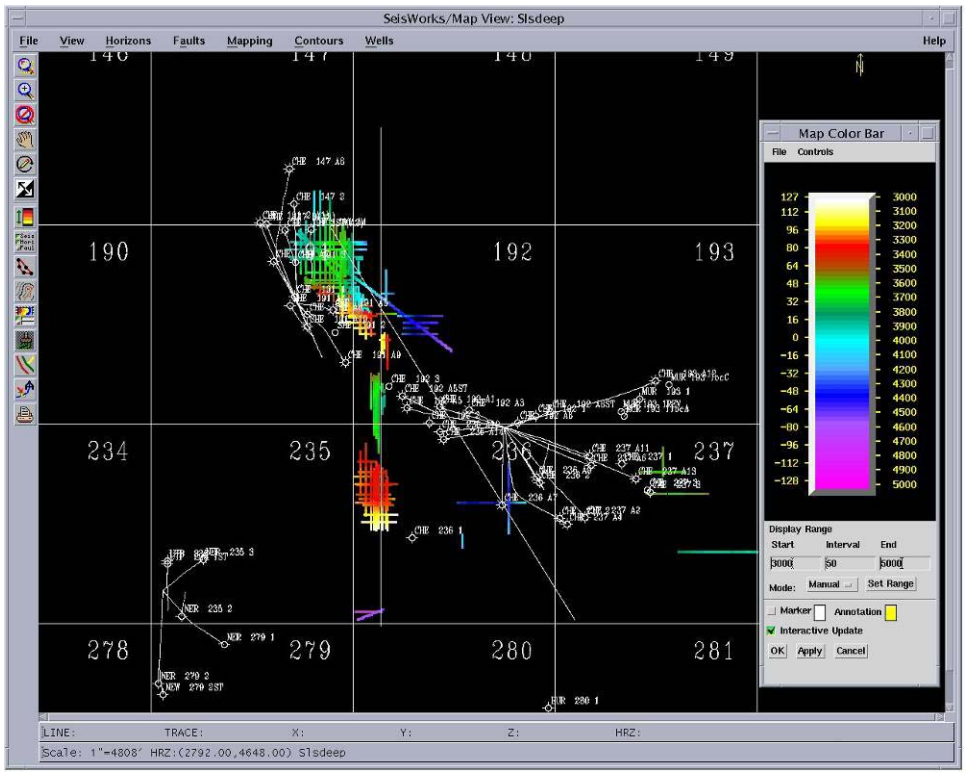

Figure 8.5: Shallower "deep sand" at around 3000-4000 milliseconds (11,000-13,000ft).

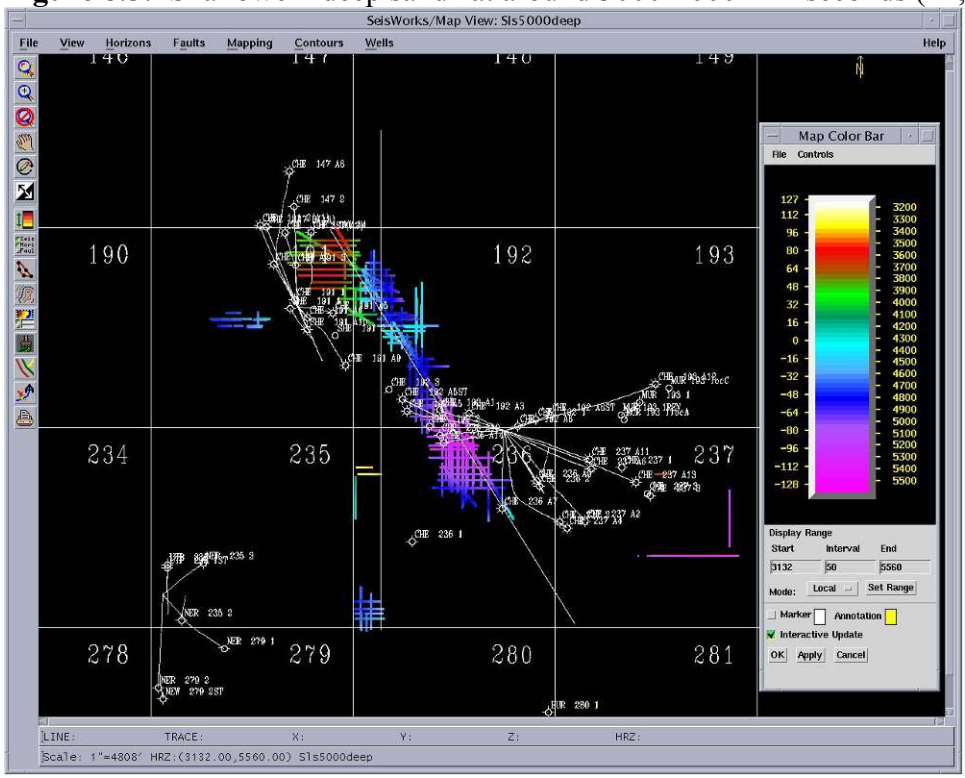

Figure 8.6: Possibly same horizon as Figure 8.5 but a deeper region.

There is a likely relationship that these deeper pay zones lie along the same drilled shallow regions. This means that, like the shallower pay sands that were deposited down slope and ran into salt structures, the sands before them followed a similar path. However, it is possible that this occurred as the salt structures were first developing and changing shape. This makes the deeper sand much less consistent. They are not as continuous because the salt structures have moved and separated them. Some prospects exist downdip of discovered fields and in between these fields where drilling has not penetrated deeper. The traps are the result of salt diapirism, anticlines, growth faults, normal faults and shale ridges. The sand unit in the following four figures (Figures 8.7, 8.8, 8.9 and 8.10) can also be seen in Figures 7.3 to 7.6. The possible traps in Figures 7.3 to 7.5 lie below the 8500ft sand, at 4000 milliseconds, while figure 7.6 is around 5000ms. The sediment has been trapped in salt bounded interslope basins and transported to unconfined settings downdip.

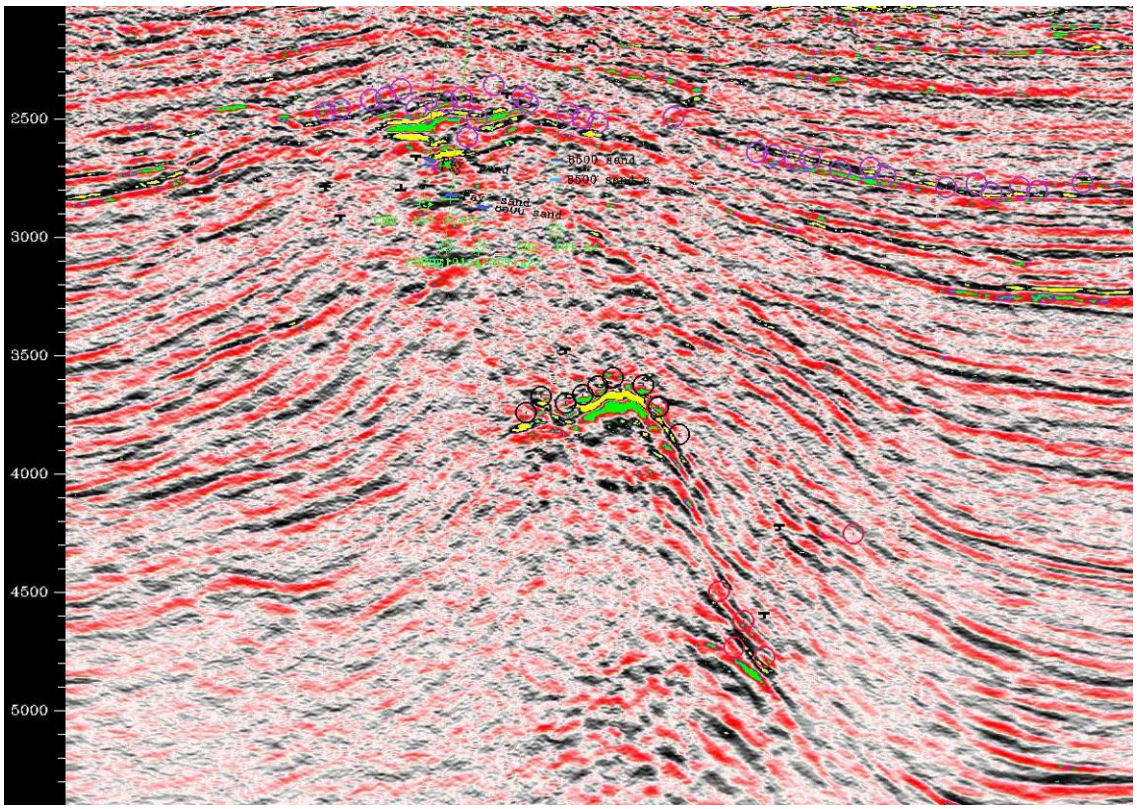

Figure 8.7: Line B: North/South line through Figure 7.3.

The three seimics (Figures 8.9, 8.10 and 8.11) show a possible gas reservoir in the top portion of Block 236 at around 5100-5300 milliseconds, which comes close to the 20,000 feet mark in depth, where 5200 milliseconds is around 19,275 feet (Figure 8.10). This sand is more consistent with Figure 8.6. It lies a little to the south of the pre-drilled areas in 236, while the sand in 8.7-8.9 lies below the areas drilled in 191 and more to the east. They are most likely the same turbidite sheet sand deposited from a westward direction. Everything gets a little distorted at this depth, but we clearly see this zone. It appears to be surrounded by salt structures, and although it has been pushed into a syncline, it may still possess worthwhile pay. It has noticeable amplitude along a fault below a possible salt mass at time around 4000 ms. Block 237 has better entrapment to the right of the mass beginning at time 3500 ms and extends downward to 5500 ms. This is one of the only images where we can see a subsalt event (Figure 8.9, 8.10). There are also two different seismic parameter settings involved.

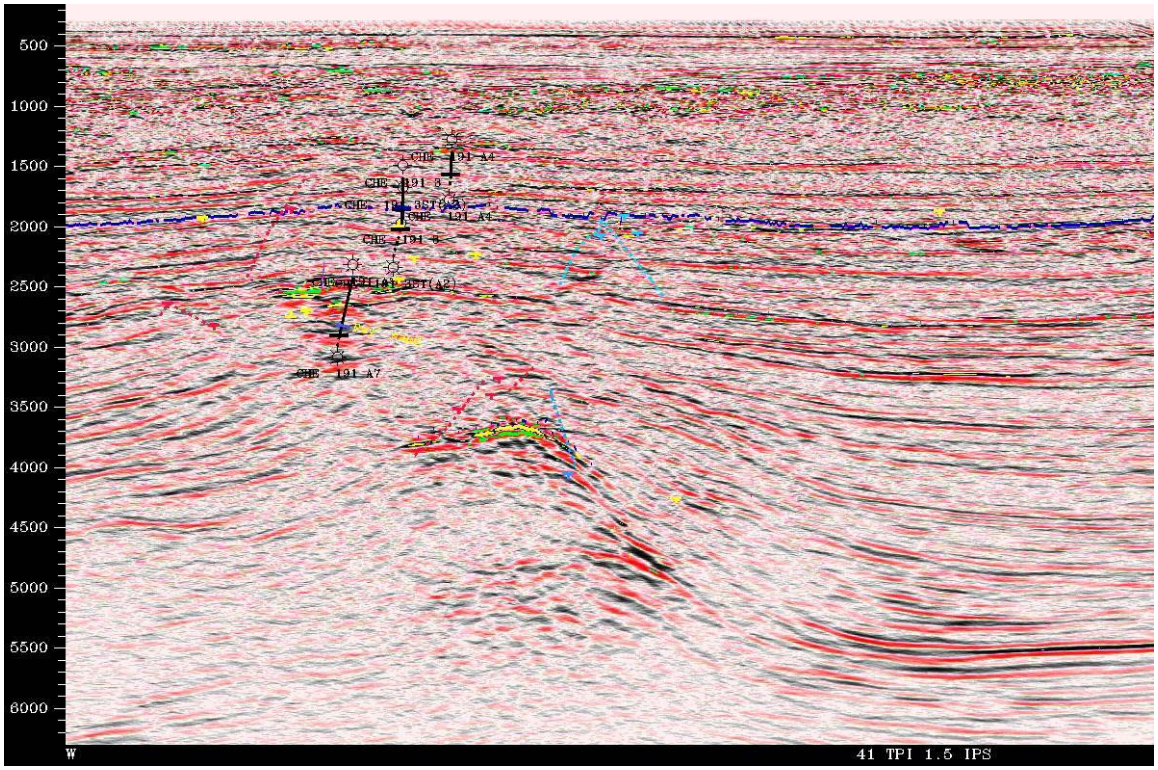

Figure 8.8: Same as figure 8.7 with different time settings.

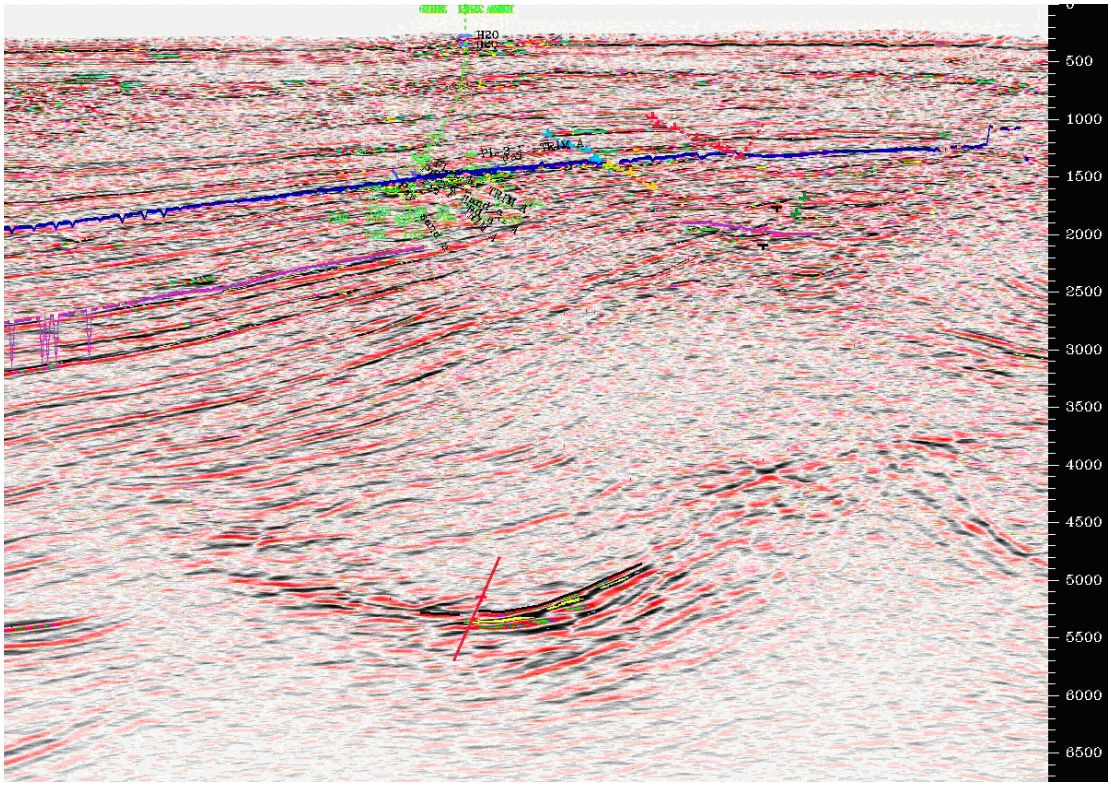

Figure 8.9: Line H from Figure 7.1: Subsalt horizon.

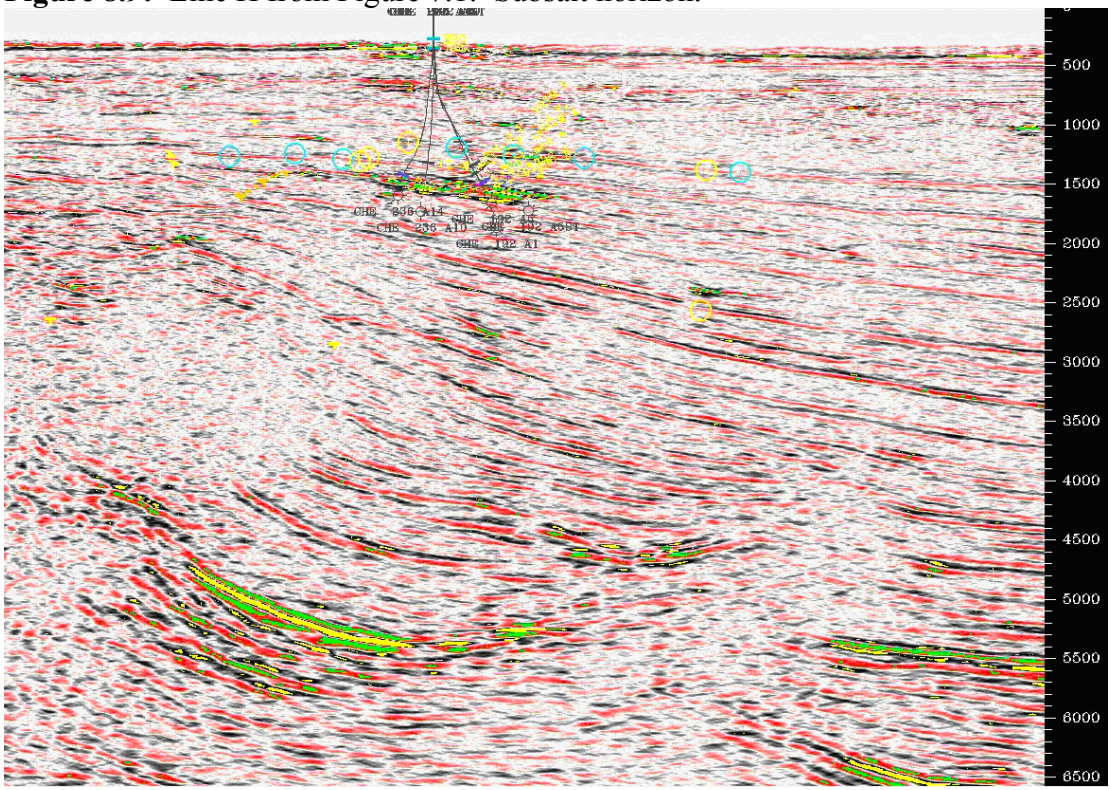

Figure 8.10: Subsalt horizon with different parametric settings and clipping.

Figures 8.9 and 8.10 lie to the south of figure 7.6. Block 236 has upturned sedimentary layers which have encountered uprising salt as they have fed into the lower shelf region. These beds become truncated by salt. This happens because, at depth, surrounding sediments compact and become denser than the salt. The salt offers some resistance and moves upward as the sediments sink further around time 4200 to 5000 ms. Next, moving along trace, a new horizon appears. This was only seen with higher scaled data. It can be seen on the base map, Figure 8.5. This possible pay sand shown in Figures 8.14, 8.15, and 8.16 begins along the north/south trace from Block 192 to 236 at time 3100ms to 4900ms, around 10,000 to 18,000 feet. The images are further north than the four previous images, where salt has come into play and disrupted the sediment flow. This horizon's depth variation is great due to diapirism and reaches depths up to approximately 18,000 feet or 4900 milliseconds. The line intersection of Figure 8.15 is shown is Figure 8.16. The sediment supply is coming from a westward direction. We can see two distinct depositional sequences and much faulting. Moving east, there is less disruption, and a continuous syncline is seen, but only in the northeast region. Continuing south along lines in Block 236 and 237, the deep possibility gets stronger in the north region of 236. Figure 8.11 shows Line F running from the top of block 192 to 236. It intersects Line B at the far right bright spot, Line C at the second bright spot from the right, and Line E at the third bright spot from the right.

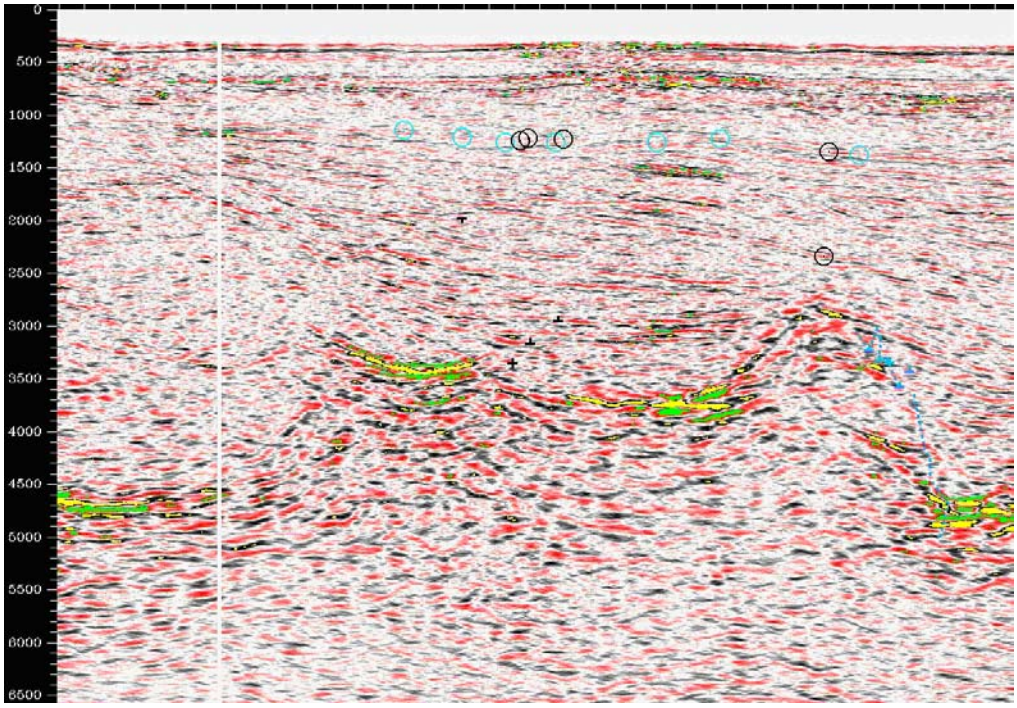

Figure 8.11: Line F from Figure 7.1: Horizon across Block 192 and 236.

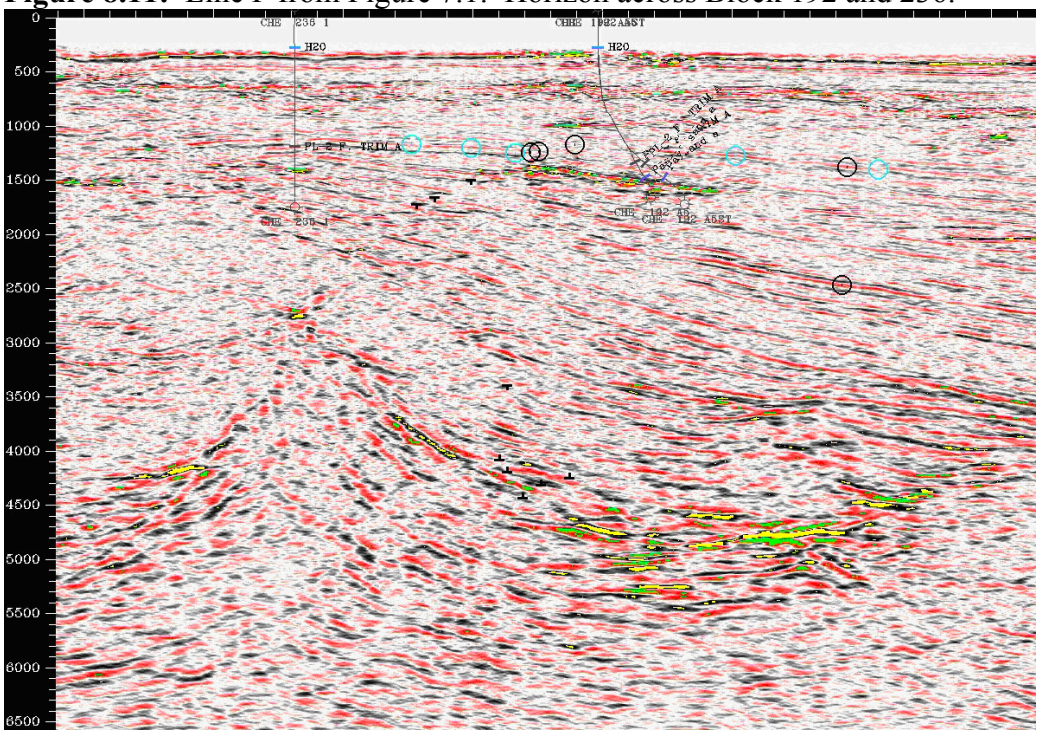

Figure 8.12: Line G from Figure 7.1: Blocks 192/236 moving eastward on trace.

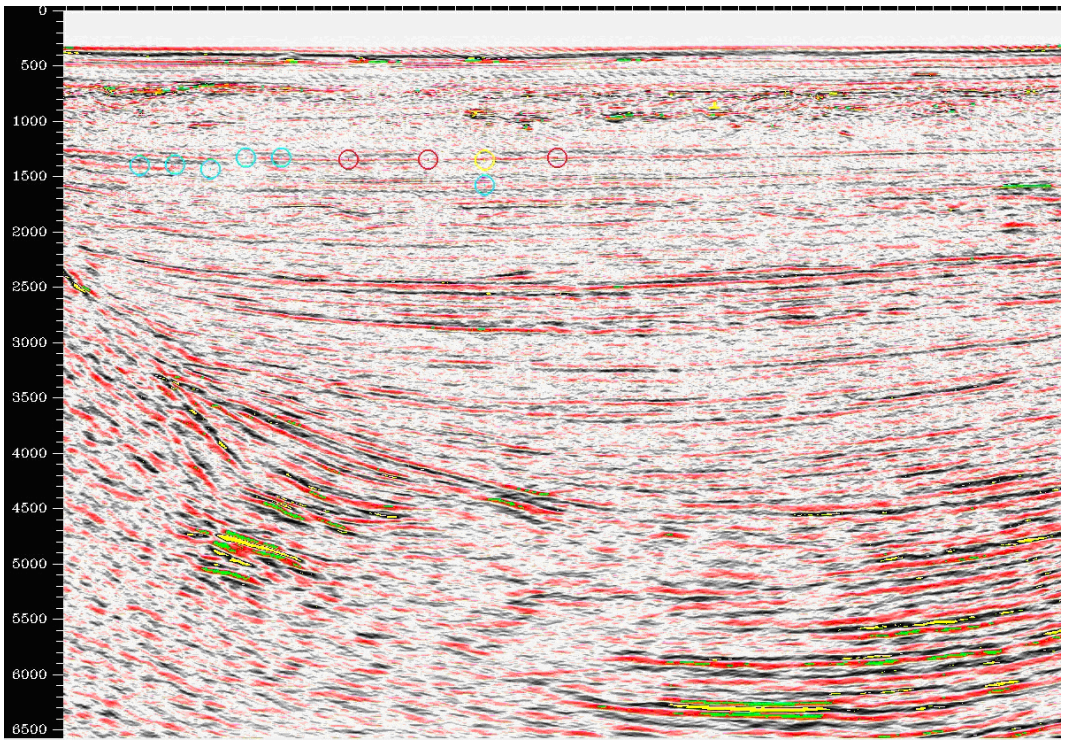

Figure 8.13: Line C from Figure 7.1: Further north than figures 8.11, 8.12 above salt interference-syncline/basin

In block 192, shown below, there is a severely faulted vertical pay beginning at 3100 ms, two-way time. It extends downward varying in depth to almost 5000 ms. Below this on top of a secondary fault system created by a salt diapir there is a large amplitude anomaly at 4250 ms. In order to drill this area a second well should to be employed directed at an opposing angle.

8.3.4: Problems

In Block 193, Well 1locA and 1REV were drilled at 2200 to 3500 ms two way time, and 8000-12,000 feet, true vertical depth (tvd). No logs were run past 8500 tvd. The deeper attempts for 193 were abandoned. This was known as the Copperhead Prospect 193. No deep pay was reached. Block 193 could still have possible deep pay, but it exists in possibly a different area from previous attempts, around 6000ms.

In Block 237, sidewall core analysis from 11,921 to 13,263 feet (tvd) reveals that this area is very shaley. The deepest well drilled is Well 3 at a measured depth of 13,557

feet and a tvd of 13,541 feet. Pay was sought and logged up to around 13,500 feet, time ~4000ms. However, directly below this at ~5000-6000ms are good, high negative amplitude flat spots.

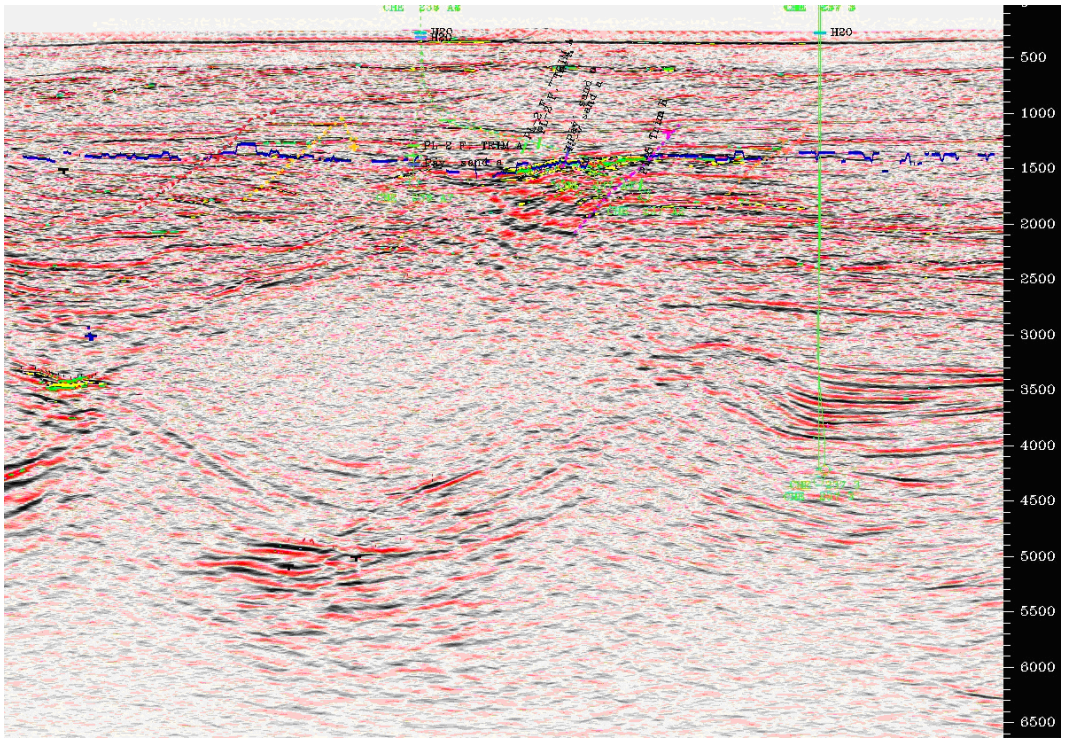

Figure 8.14: Line E from Figure 7.1: Blocks 236/237

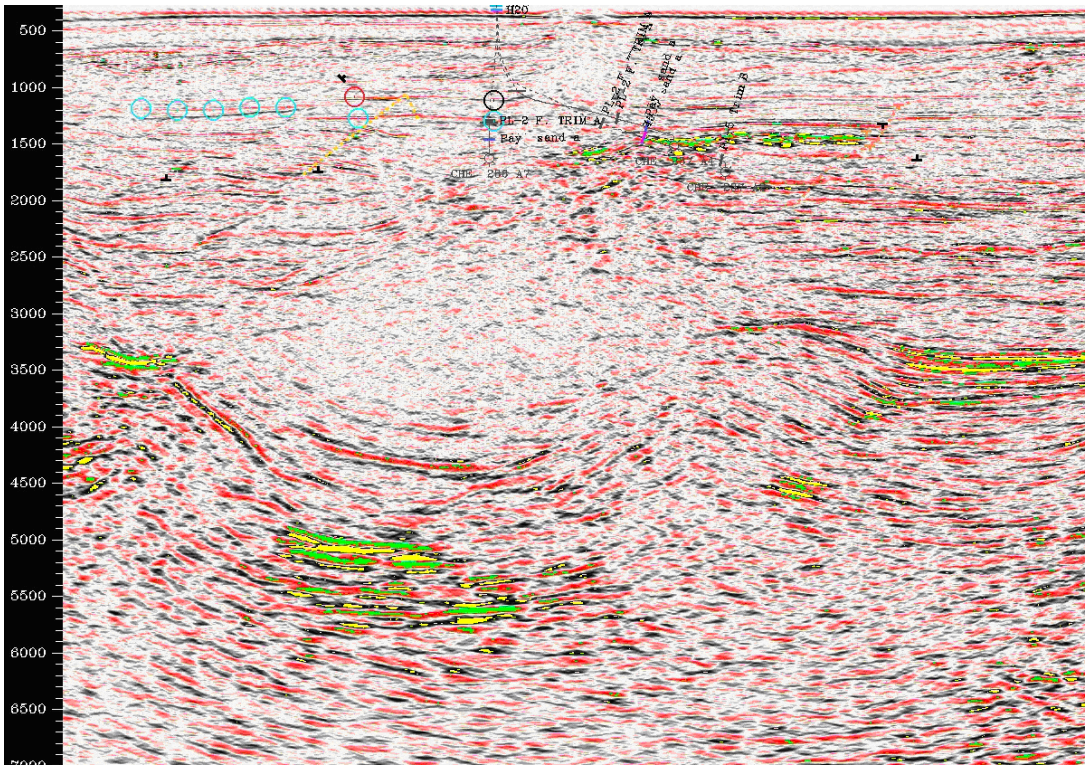

Figure 8.15: Blocks 236/237 at different seimic parameter settings and clipped.

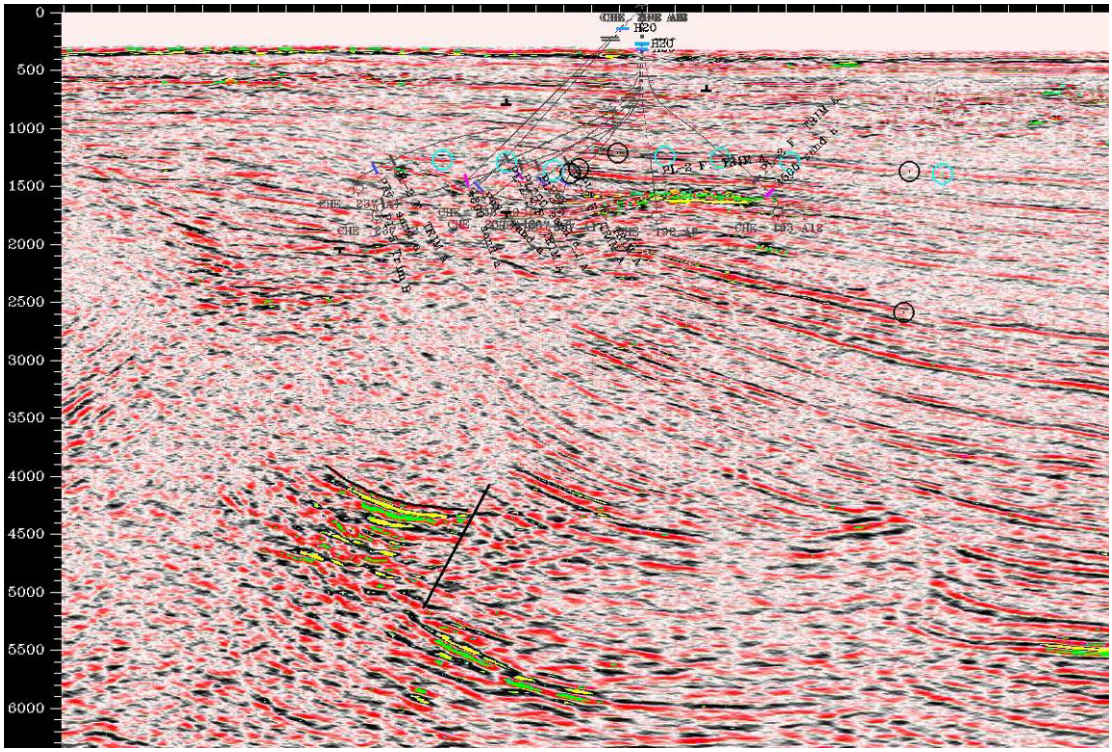

Figure 8.16: Line from Figure 7.1: Intersection of prior image at the fault.

In Block 236, beginning at two way time 4000 ms, to the far left of the seismic image, there seems to be a potential play. The area to the right has been drilled unsuccessfully in Block 237 by Well 3. However, there appears to be high amplitude sand below where they stopped the well (around 4400 time) near the south border of 237. There is noticeable amplitude deeper at a time approximately 6000ms (19,000 feet). This is near the block line under the previous well at a depth of around 12,000ft, time 3600-4100ms. Block 236 has possible pay at tvd: 13,126, md: 16148. Also, there is another large spot at 5000-6000ms. Depth is around 17,000tvd and 19,000md.

8.4: Outside Region

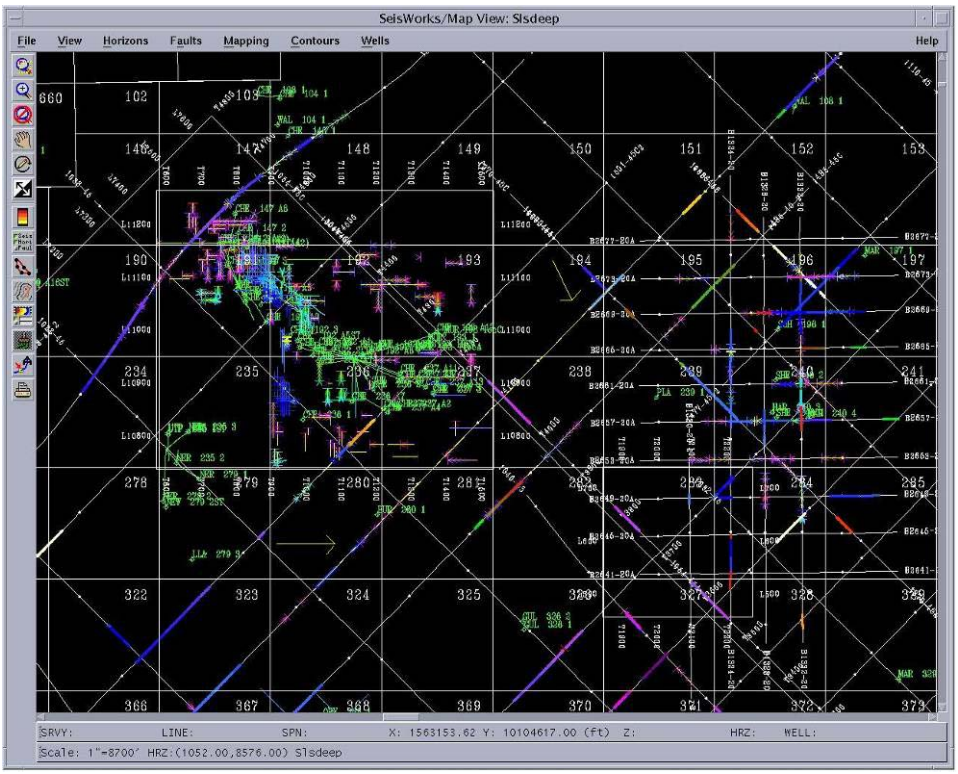

Figure 8.17: 2D base map.

8.4.1: Introduction

2D data is harder to interpret for sequence stratigraphy. It is shown to give a somewhat more inclusive view of the area and to reiterate the basic deposition of the study area. The turbidite system, typically coming from the northerly direction, encounters the east/west running salt. This may create a trap as the salt is pushed over

and between the sediments. Below we see salt diapirs and two channel fill deposits. One is compressed into a synclinal shape, and the other is anticlinal. The anticlinal deposit is better for hydrocarbon trapping. There is also another uprising salt body below.

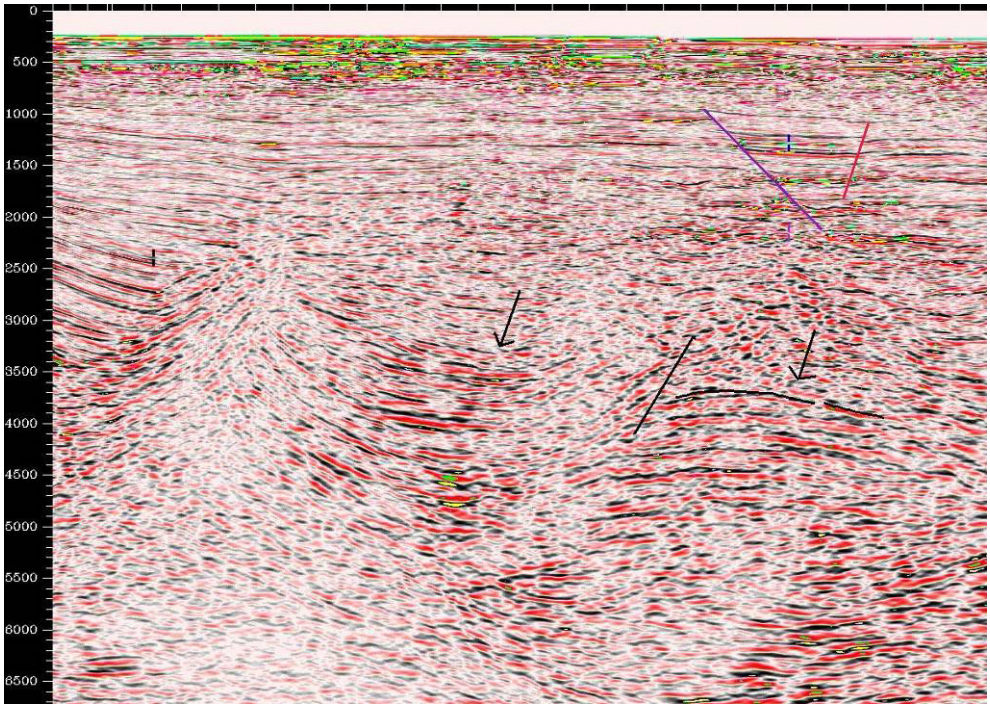

Figure 8.18: Salt diapirs and sediment traps.

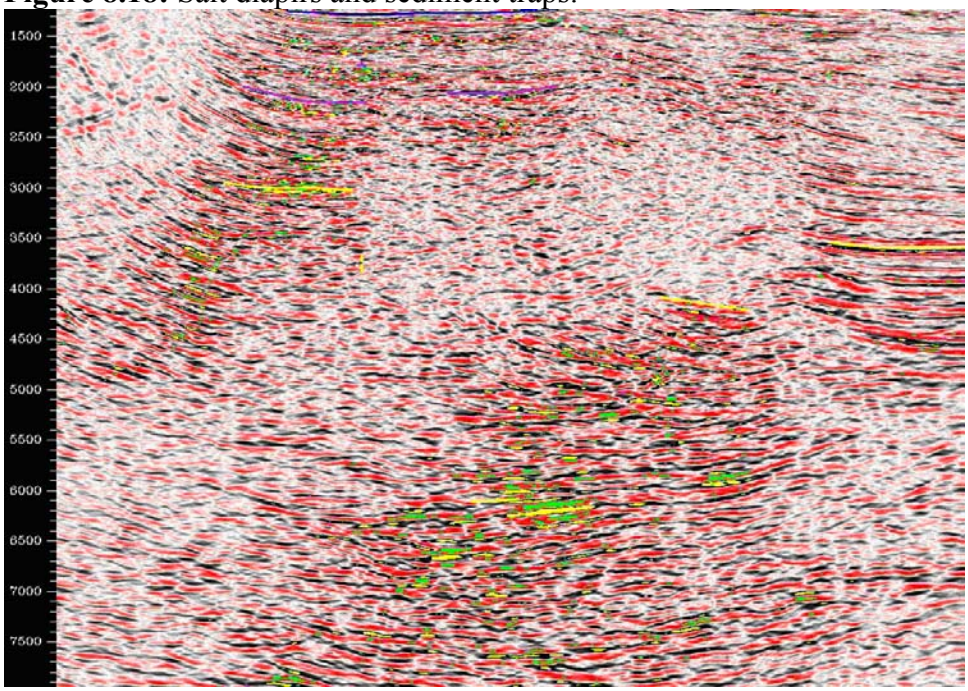

Figure 8.19: Intersection of 8.18.

The two images above show one line running NE/SW, and the intersection running NW/SE. The focus here is placed on the region in the north region of Block 194, shown in Figure 8.18, where possible pay sand may exist. Figures 8.18 and 8.19 cross a turbidite system and encounter a diapir. Figure 8.19 is the intersection line. The salt has caused the strata to be somewhat downwardly flexed and butted up against a salt diapir. This may have good trap possibilities. In Figure 8.20 we see a similar trap possibility in Block 283.

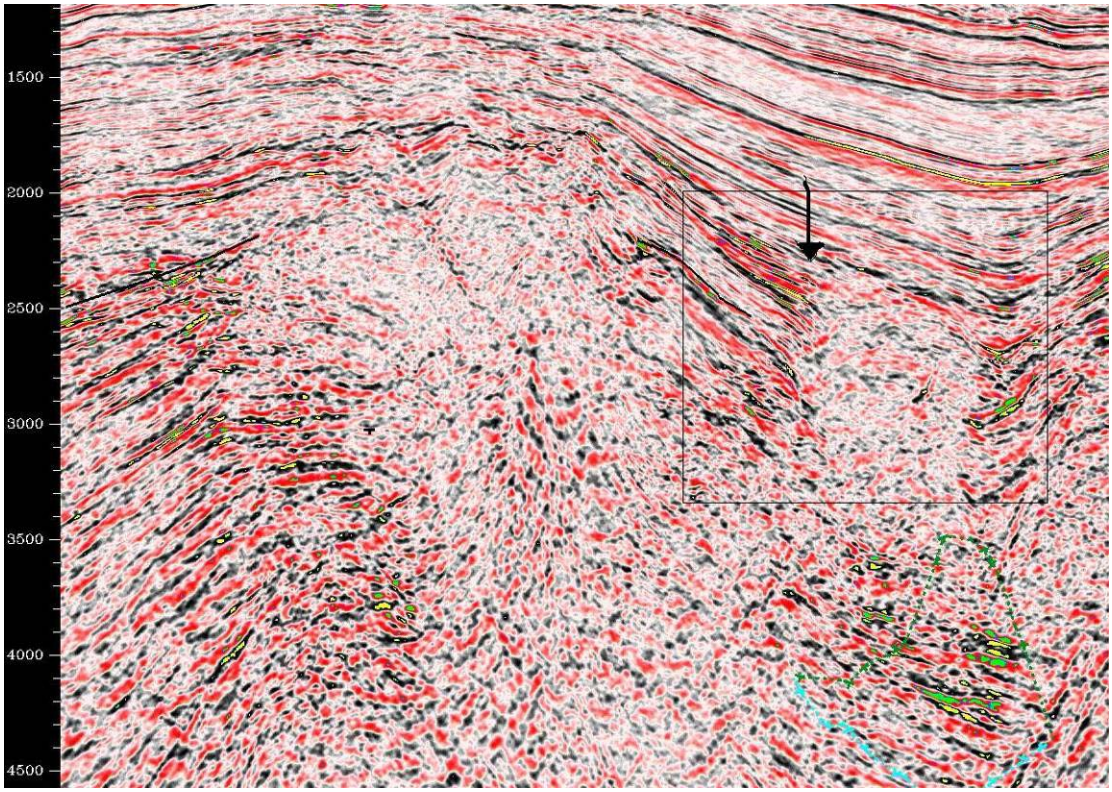

Figure 8.20: 2D image of allochthonous salt diapir with a possible downwardly flexed trap in Block 283.

8.5: Future work

Logs should be run deeper in this area to confirm possible hydrocarbons and have paleontological results taken. Better depth imaging is also needed especially for the depths of importance here. This would require new seimic shootings which as of now have only been done in the northeast section of Garden Banks by Kerr McGee.

References

Alberty, M.W., M.E. Hafle, J.C. Minge, and T.M. Byrd, 1997, Mechanisms of shallow waterflows and drilling practices for intervention: Offshore Technology Conference Proceedings Paper OTC 8301, pp. 241-247.

Baud, R.D., R.H. Peterson, C. Doyle, and G.E. Richardson, 2000, Deepwater Gulf of Mexico: America's emerging frontier: Minerals Management Service Outer Continental Shelf Report 2000-022, p. 89.

Brown, A.R., 2004, Interpretation of Three-Dimensional Seismic Data, AAPG Memoir 42, SEG Investigations in Geophysics. no. 9.

Buffler, R. and Fulthorpe, C., 2005, Sequence Stratigraphy of the Northeastern Gulf of Mexico: An Integrated Seismic, Well Log and Biostratigraphic Approach

Combellas-Bigott, R. and Galloway, W., 2006, Depositional and structural evolution of the Middle Miocene depositional episode, East-Central Gulf of Mexico, AAPG Bulletin Vol 90, No. 3, pp. 335-362.

Chowdhury, A. and Lopez-Mora, S., 2004, Regional Geology of Deep Water Salt Architecture, Offshore Gulf of Mexico, Search and Discovery Articles, TGS-NOPEC, Houston, Texas

Diegel, F.A., J.F. Karlo, D.C. Schuster, R.C. Shoup, and P.R. Tauvers, 2001, The Cenozoic structural evolution and tectono-stratigraphic framework of the northern Gulf Coast continental margin, Search and Discovery Article #30006.

Dutta, N.C., ed., 1987, Geopressure: Society of Exploration Geophysicists Reprint Series 7, p. 365.

Fertl, H.W., 1976, Abnormal formation pressures: Amsterdam, Elsevier, p. 382.

Fillon, R. H., 1999, Biostratigraphic Observations Related to Salt Canopies and Salt Welds in the Deep-Water Gulf of Mexico, Earth Studies Associates, Paleo-Data, Inc.

Hart, W., Albertin, M., 2001, Subsalt Trap Archetype Classification: A Diagnostic Tool for Predicting and Prioritizing Gulf of Mexico Subsalt Traps. GCSSEPM Foudation 21st Annual Research Conference, Petroleum Systems of Deep-Water Basins, Dec. 2-5, pp. 619-637.

Henry, S., 2001, Understanding the Seismic Wavelet, Search and Discovery Article #40028.

Hunt, J. L., Jr., and G. Burgess, 1995, Depositional styles from Miocene through Pleistocene in the north-central Gulf of Mexico: an historical reconstruction: Gulf Coast Association of Geological Societies Transactions, v. 45.

Karlo, J.F. and R.C. Shoup, 1999, Large patterns become predictive tools to define trends, reduce exploration risk: Offshore, v. 59, no. 7, p. 94-95, 156.

Law, B.E., G.F. Ulmishek, and V.I. Slavin, eds., 1998, Abnormal pressures in hydrocarbon environments: AAPG Memoir 70, p. 264.

Lawless, P., Fillon, R., 2000, Lower Miocene - Early Pliocene Deposystems in the Gulf of Mexico: Regional Sequence Relationships, Gulf Coast Association of Geological Societies Gulf Coast Section SEPM

Liro, L., Q., Liao, B., Fontecha, W., Cai, M., Benabentos, 2006, Practical Limitations of the Interpretation of Deepwater Gulf of Mexico Subsalt Seismic Data. AAPG Technical Program.

Lore, G. L. and E. C. Batchelder, 1995, Using production-based plays in the northern Gulf of Mexico as a hydrocarbon exploration tool: Gulf Coast Association of Geological Societies Transactions, v. 45.

Magoon, L.B., M.E., Henry, 2000, Region 5 Assement Summary – North America in U.S. Geological Survey Digital Data Series 60.

McGee, D., Fitzsimmons, R., Haddad, G., 2003, From Fill to Spill: Partially Confined Depositional Systems, Magnolia Field, Garden Banks, Gulf of Mexico. SEG Technical Program Expanded Abstracts, pp. 2297-2299.

Morton, R. A, and Suter J. R., 1996, Sequence Stratigraphy and Composition of Late Quaternary Shelf-Margin Deltas, Northern Gulf of Mexico AAPG Bulletin, v. 80, no. 4.

Pan, J., Barnes, B., Kong, F., Chang, M., Kriechbaum, V., 2006, Depth imaging and regional exploration in Northeast Garden Banks, Gulf of Mexico, The Leading Edge, Volume 25, Issue 4, Kerr-McGee, Houston, USAParallel Data Systems, Houston, USA pp. 468-473

Peel, F., 1999, Structural styles of traps in deepwater fold/thrust belts of the northern Gulf of Mexico (abs.): AAPG International Conference, extended abstracts volume, p. 392.

Peterson, R. H. and D. W. Cooke, 1995, Deep-water northern Gulf of Mexico hydrocarbons plays: Gulf Coast Association of Geological Societies Transactions, v. 45.

Reed, J. C., C. L. Leyendecker, A. S. Khan, C. J. Kinler, P. F. Harrison, and G. P. Pickens, 1987, Correlation of Cenozoic sediments, Gulf of Mexico Outer Continental Shelf: U.S. Department of the Interior, Minerals Management Service, OCS Report MMS 87-0026, variously paginated.

Rowan, M.G., B.D. Trudgill, and J.C. Fiduk, 2000, Deepwater, salt-cored foldbelts: lessons from the Mississippi Fan and Perdido foldbelts, northern Gulf of Mexico: American Geophysical Union Monograph 115, pp. 173-191.

Rowan, M.G., Lawton, T., Giles, K., Ratliff, R., 2003, Near-salt deformation in La Popa basin, Mexico, and the northern Gulf of Mexico: A general model for passive diapirism, AAPG Bulletin, v. 87, no. 5, pp. 733-756

Seni, S.J., B.A. Desselle, and A. Standen, 1994, Scope and construction of a gas and oil atlas series of the Gulf of Mexico: examples from Texas offshore lower Miocene plays: Gulf Coast Association of Geological Societies Transactions, v. 44, pp. 681- 690.

Seni, S. J., B. A. Desselle, and A. Standen, 1994, Scope and construction of a gas and oil atlas series of the Gulf of Mexico: examples from Texas offshore lower Miocene plays: Gulf Coast Association of Geological Societies Transactions, v. 44, pp. 681- 690.

Seni, S.J., 1995, Chronostratigraphic Hydrocarbon Plays and Depositional Styles in the Northern Gulf of Mexico.

Shinol, J.H., Sumner, H., Ford, F., 2000, The Promise of the Best of Both Worlds: Subsalt Exploration in the Gulf of Mexico Deepwater, Spirit Energy Deepwater Exploration, Unocal Corporation.

Shirley, K., 2000, GOM Deepwater +Subsalt Plays: The Promise of the Best of Both Worlds, AAPG Explorer.

Smith, M.A., 1999, MMS regulatory approach to shallow water flow mitigation: Proceedings of the 1999 International Forum on Shallow Water Flows, paper 15.

Smith, K.L., and A.D. Gault, 2002, Subsea mudlift drilling: a new technology for ultradeep-water environments, in A.R. Huffman and G.L. Bowers, eds., Pressure regimes in sedimentary basins and their prediction: AAPG Memoir 76, pp. 171-175.

Stauffer, K.E., A. Ahmed, R.C. Kuzela, and M.A. Smith, 1999, Revised MMS regulations on shallow geohazards in the Gulf of Mexico: Offshore Technology Conference Proceedings Paper OTC 10728, v. 1, pp. 79-81.

Sylvia, D. A., Galloway, W. E. Combelllas, R., 2003, Evolution of the Northern Gulf of Mexico through the Cenozoic. A 3D Visualization Tour, Search and Discovery Article #40093.

Traugott, M., 1997, Pore/fracture pressure determinations in deep water: World Oil, v. 218, no. 8, pp. 68-70.

Wood, L. J., Hentz, T., Zeng, H., DeAngelo, M. and Dutton, S., 2003, Applying Sequence Stratigraphy and Seismic Stratal Slice, Technology in the Gulf of Mexico: *Improved geological understanding of mature gas reservoirs in offshore Gulf of Mexico points towards unrecovered resource.* Bureau of Economic Geology. The University of Texas, pp. 10-21.

Xinxia, W. and Galloway, W., 2004, Deepwater Depostional Style of the Upper Miocene Depositional Episode, East-Central Gulf of Mexico, AAPG Bulletin v. 88, no.13.

Appendix

Copyright Permission Letter:

June 23, 2006

Dear Ms. Sullivan,

I am in receipt of your request for permission to reprint images of PGS Marine Geophysical NSA ("PGS") seismic data over Garden Banks Block 236 ("Data") in future revisions and editions of your Masters thesis entitled "Geomorphologic Evaluation of the Gulf of Mexico, Northwest Garden Banks, and Supra/Subsalt Architectural Influences on Possible Reservoir Characterization from the Miocene to Pleistocene Epochs".

PGS recognizes that scientific studies such as your thesis are subject to revision both during the period of preparation and in future editions subsequent to initial publication. In light of this fact, PGS hereby grants permission for you to use the Data in current and future revisions of your thesis, provided:

- The Data remain in the same form as in the current version submitted to PGS for review, dated August, 2006; and
- The Data are displayed and used only as a part of the thesis for the purpose of earning a Masters Degree in Geology and shall not be copied or distributed separately or apart from the thesis; and
- This edition and all future revisions or editions of the thesis contains an acknowledgement that the Data are proprietary to and are being used with permission granted by PGS Marine Geophysical NSA.

In the event that the Data are required for display or use in any way beyond the scope and provisions specified in this letter, specifically, if the thesis or any part of the thesis containing Data were to be included in other publications not related to the purpose of earning a Masters Degree in Geology, a separate letter of permission from PGS addressing those circumstances will be necessary. We appreciate your diligence in seeking permission for the use of PGS Data and wish you the best of luck with your Masters thesis and in your future career.

Sincerely,

Mark Richardson
Sr. Contracts/Customer Support Representative
PGS Marine Geophysical NSA

PGS Marine Geophysical NSA
15150 Memorial Drive
Houston, Texas 77079
USA
Tel: [illegible]
Fax: [illegible]

Vita

Sheri Sullivan was born in Louisiana, attended Louisiana State University for her undergraduate in Geology where she worked as a laboratory assistant categorizing benthic foraminifera of hydrocarbon seeps. She then went to University of New Orleasns to complete her master's in Geophysics and taught introduction to historical geology for one year. She then began a year long internship with Murphy Exploration and Production.